

**MODIFICATION OF RHEOLOGICAL AND FILTRATION PROPERTIES OF  
WATER-BASED DRILLING MUDS WITH LIGNITE NANOPARTICLES FOR  
OIL WELL DRILLING OPERATION**

**BY**

**EMENIKE, Christian Osita  
MEng/SEET/2017/6987**

**DEPARTMENT OF CHEMICAL ENGINEERING  
FEDERAL UNIVERSITY OF TECHNOLOGY, MINNA.**

**OCTOBER, 2021**

**MODIFICATION OF RHEOLOGICAL AND FILTRATION PROPERTIES OF  
WATER-BASED DRILLING MUDS WITH LIGNITE NANOPARTICLES FOR  
OIL WELL DRILLING OPERATION**

**BY**

**EMENIKE, Christian Osita  
MEng/SEET/2017/6987**

**A THESIS SUBMITTED TO THE POSTGRADUATE SCHOOL  
FEDERAL UNIVERSITY OF TECHNOLOGY, MINNA, NIGERIA  
IN PARTIAL FULFILMENT OF REQUIREMENTS FOR THE AWARD OF  
MASTER OF ENGINEERING (M. ENG) DEGREE IN CHEMICAL  
ENGINEERING**

**OCTOBER, 2021**

## ABSTRACT

Drilling muds are heterogeneous mixture of water or oil, clay materials and chemical, that facilitate drilling operations. Muds are important in successful well drilling as they have common properties that enhanced safe and satisfactory completion of the well by its functions such as removal of rock cuttings to the surface, controlling high pressure zones and cleaning of bottom hole. The importance of drilling muds, cannot be over emphasized as the knowledge on drilling mud is essential in the rotary drilling operation in the petroleum industry and the demand for drilling mud is on increase side as a result of drilling operations ranging from oil wells to ground water bore holes that are being carried out frequently on a daily basis. The aim of this research work is the modification of rheological and filtration properties of water-based drilling muds using Nigerian nano lignite coal. The abundancy of local clay in Nigeria are not exploited in drilling mud because these local clays contains high level of impurities and are mainly calcium-based montmorillonite bentonite with low swelling capacity which results to substandard rheological and filtration properties challenge in their natural form when used for formulation of drilling muds. This necessitates the testing of clays and nano lignite coal used for formulation and modification of mud in this research work via the following method of analysis: TGA, XRD, SEM/EDX, FTIR, and physicochemical analysis. The method employed involved, the formulation of mud, beneficiation of mud using surfactants such as caustic soda (NaOH), soda ash (Na<sub>2</sub>CO<sub>3</sub>) and polyanionic cellulose (PAC) and modification of mud using different Nigerian nano lignite coal concentration at different temperature. The data generated from FANN 35 viscometer at different dia reading of 600,300 200, 100, 6 and 3 rpm respectively, were used for evaluation of rheological and filtration properties of spud, beneficiated and modified drilling mud. The results obtained deduced that the Nigerian nano lignite coal have a thermal stability at the temperature of 570 °C from TGA curve, the XRD, SEM/EDX and FTIR shows that the clays and nano lignite coal were crystalline in nature, contains both metal and nonmetal elements and strong (-OH) functional group. The power law rheological model results obtained deduced that the drilling muds all obeys non-Newtonian fluid with the flow behaviour index of all muds at different concentration of nano lignite coal and temperatures were less than unity ( $n < 1$ ), having the highest value of ( $n$ ) as 0.4653 and 0.4151 for local and commercial bentonite clay respectively. Conclusively, the pretreatment with soda ash, enhanced the swelling capacities of the bentonites and easy dispersion when mixed with water. The characterizations carried out shows that the bentonites were crystalline in nature while lignite nanoparticles were semi crystalline, their internal structure were like spherical in shape. The results of the spud water-based drilling muds obtained shows that the values were below API rheological properties standard ( $\geq 8$  cP for plastic viscosity and  $\geq 15$  cP for apparent viscosity) and above API filtration properties standard ( $\leq 15$  ml for fluid loss). The use of micro size lignite particles is recommended in order to justify the effectiveness of lignite nanoparticles for modification of drilling mud properties. Chemical substance (metallic oxide) such as nano Fe<sub>2</sub>O<sub>3</sub>, TiO<sub>2</sub>, Al<sub>2</sub>O<sub>3</sub>, CuO and SiO extract from plants and solid waste combined with lignite nanoparticles for modification of rheological and filtration properties of drilling muds are recommended

## TABLE OF CONTENTS

<b>Content</b>	<b>Page</b>
Cover Page	i
Title Page	ii
Declaration	iii
Certification	iv
Acknowledgement	v
Abstract	vi
Table of Content	vii
List of Tables	xi
List of Figures	xiii
<b>CHAPTER ONE</b>	<b>1</b>
<b>1.0 INTRODUCTION</b>	<b>1</b>
1.1 Statement of the Research Problem	6
1.2 Aim and Objectives of the Study	6
1.3 Scope of the Study	6
1.4 Justification of Study	6
<b>CHAPTER TWO</b>	<b>8</b>
<b>2.0 LITERATURE REVIEW</b>	<b>8</b>
2.1 Drilling	8
2.2 Drilling Muds	8
2.3 Functions of Drilling Mud	10
2.4 Classification of Drilling Muds	11
2.4.1 Water-based drilling muds	11
2.4.2 Oil-based drilling muds	13

2.5	Drilling Mud Related Challenges	14
2.5.1	Borehole instability	14
2.5.2	Salt section hole enlargement	14
2.5.3	Lost circulation	15
2.6	Mud Properties in Relation to Functions	16
2.6.1	Density	17
2.6.2	Rheological properties	18
2.6.2.1	Plastic viscosity	19
2.6.2.2	Yield point	20
2.6.2.3	Gel strength	21
2.6.3	Rheological models	21
2.6.3.1	Newtonian model	22
2.6.3.2	The Bingham plastic model	23
2.6.3.3	The power law model	23
2.6.3.4	The Herschel-Bulkley law	25
2.7	Bentonite	27
2.8	Coal	29
2.9	Nanoparticles	30
2.10	Nanoparticle Preparation	31
	<b>CHAPTER THREE</b>	<b>33</b>
<b>3.0</b>	<b>METHODOLOGY</b>	<b>33</b>
3.1	Material	33
3.1.1	Equipment and apparatus	33
3.1.2	Preparation of lignite coal nanoparticles	33
3.2	Characterization of Samples	34

3.2.1	Characterization of nano lignite coal	34
3.2.1.1	Physicochemical analyses	34
3.2.1.2	Thermogravimetric analysis	36
3.2.1.3	SEM analysis	36
3.2.1.4	EDX analysis	36
3.2.1.5	XRD analysis	36
3.2.1.6	FTIR analysis	37
3.3	Chemical Treatment of Bentonites	37
3.4	Preparation of Drilling Mud	37
3.5	Mud Weight Measurement	39
3.6	Viscometer Mud Calibration	39
3.7	Filtration loss test	40
3.8	Rheological Test	40
3.9	Rheological Model	41
3.10	Model Parameter Determination and Validation	43
	<b>CHAPTER FOUR</b>	45
<b>4.0</b>	<b>RESULTS AND DISCUSSION</b>	45
4.1	Characterizations	45
4.1.1	Physicochemical analyses of nano lignite coal	45
4.1.2	Thermogravimetric analyses of nano lignite coal	49
4.1.3	SEM analysis	52
4.1.4	EDX analysis	54
4.1.5	XRD analysis	56
4.1.6	FTIR analysis	58
4.2	Rheological and Filtration Properties Analyses	62

4.3	Rheological Model	90
<b>CHAPTER FIVE</b>		102
<b>5.0</b>	<b>CONCLUSION AND RECOMMENDATIONS</b>	102
5.1	Conclusion	102
5.2	Recommendations	102
5.3	Contribution to Knowledge	103
<b>REFERENCES</b>		104
<b>APPENDICES</b>		111

## LIST OF TABLES

<b>Table</b>	<b>Page</b>
3.1 Composition of Drilling Mud at 25 °C	38
3.2 Composition of Drilling Mud at 100 °C	38
3.3 Composition of Drilling Mud at 160 °C	39
4.1A Ultimate Analyses of Lignite Coal	46
4.1B Proximate Analyses on Coal Sample	47
4.1C Comparative Ultimate Analyses Between this and Previous Work	49
4.1D Comparative Proximate Analysis between this and previous works	49
4.1E Elemental Composition of the Local clay, Commercial and Nano Lignite Coal	54
4.2A Rheological and Filtration Properties of Spud Muds at Ambient Temperature	63
4.2B Rheological and Filtration Properties of Beneficiated Muds at Room Temperature	65
4.2C Rheological and Filtration Properties of Modified Muds with Different Nano Lignite Coal Concentration at Room Temperature for 24 Hours	66
4.2D Rheological and Filtration Properties of Modified Muds with Different concentration of Nigerian Nano Lignite Coal Aged at Elevated Temperature (100 °C)	74
4.2E Rheological and Filtration Properties of Modified Drilling Muds with Various concentration of Nigerian Lignite Aged at Elevated Temperature (160 °C)	77
4.2F Comparative Rheological and Filtration Properties of Modified Local Clay Muds at Different Temperature	79

4.2G	Comparative Rheological and Filtration Properties of Modified Commercial Bentonite Clay Muds at Different Temperature	84
4.2H	Comparative Rheological and Filtration Properties between this (Local Clay) and Previous Work	89
4.2I	Comparative Rheological and Filtration Properties between this (Commercial Bentonite Clay) and previous work	90
4.3A	Power Law Model Shear Stress Values of at 25 °C	91
4.3B	Power Law Model Shear Stress Values of at 100 °C	93
4.3C	Power Law Model Shear Stress Values of at 160 °C	95
4.4	Power Law Rheological Model Fitting Parameters	97

## LIST OF FIGURES

Figure		Page
2.1	Shows the Fluid Loss During Drilling (Mohammad, 2013)	16
2.2	Plot of Newtonian Model (Nwaoboli, 2014)	22
2.3	Bingham Plastic Model Plot (Nwaoboli, 2014)	23
2.4	Plot of Power Law Model (Nwaoboli, 2014)	24
2.5	Log-log Plot of Power Law Rheological Model (Nwaoboli, 2014)	25
2.6	Plots of Different Rheological Models (Nwaoboli, 2014)	27
2.7	Crystal Structure and Chemistry of Bentonite Minerals (Omer <i>et al.</i> , 2016)	29
2.8	Pore Throat Sizes in Rocks (adapted from Rezaee <i>et al.</i> , (2012))	31
4.1A	TGA Properties of Lignite Coal	50
4.1B	DTA Properties of Lignite Coal	51
4.1C	SEM Analysis of Nano Lignite Coal	52
4.1D	SEM Analysis of Local Clay	53
4.1E	SEM Analysis of Commercial Bentonite Clay	53
4.1F	EDX Spectra of the Local Clay	55
4.1G	EDX Spectra of Commercial Bentonite	55
4.1H	EDX spectra of nano lignite coal	56
4.1I	XRD Patterns of Local Clay and Commercial Bentonite Clay	57
4.1J	XRD Patterns of the Nano Lignite Coal	57
4.1K	FTIR Spectra of Clay Samples	58
4.1L	FTIR Spectra of beneficiated mud Samples	59
4.1M	FTIR Spectra of Modified Mud Samples Aged at Room Temperature	60
4.1N	FTIR Spectra of Modified Mud Samples Aged at 100 °C Temperature	61
4.1O	FTIR Spectra of Modified Mud Samples Aged at 160 °C Temperature	62

4.2A	The Plastic Viscosity of Modified Local Muds After 10 hours Hot Rolling at Different Temperatures	80
4.2B	The Apparent Viscosity of Modified Local Muds After 10 hours Hot Rolling at Different Temperatures	81
4.2C	The Yield Point of Modified Local Muds After 10 hours Hot Rolling at Different Temperatures	82
4.2D	The Fluid Loss of Modified Local Muds After 10 hours Hot Rolling at Different Temperatures	83
4.2E	The Plastic Viscosity of Modified Commercial Bentonite Clay Muds After 10 hours Hot Rolling at Different Temperatures	87
4.2F	The Apparent Viscosity of Modified Commercial Bentonite Clay Muds After 10 hours Hot Rolling at Different Temperatures	86
4.2G	The Yield Point of Modified Commercial Bentonite Clay Muds After 10 hours Hot Rolling at Different Temperatures	87
4.2H	The Fluid Loss of Modified Commercial Bentonite Clay Muds After 10 hours Hot Rolling at Different Temperatures	88
4.3A	Power Law fitting curves of beneficiated mud at room temperature	91
4.3B	Power Law fitting curves of modified mud at room temperature	92
4.3C	Power Law fitting curves of modified mud at 100 °C temperature	94
4.3D	Power Law Fitting Curves of Modified Mud at 160 °C Temperature	95



## CHAPTER ONE

### 1.0 INTRODUCTION

Drilling muds also referred to as drilling fluids are generally composed of liquid (water or oil or synthetics), clay and surfactant which enhance oil and gas exploration performance for production of petroleum as the major source of energy for industries and domestic purposes. It is also used for machines such as generators and automobiles (Toyese, 2013). The drilling mud is basically charged into the drilling string to the base of the wellbore as it comes out from the nozzles of drilling bit, this action aids the drilling process, thus every drilling mud should have common characteristic features of promoting safety, economy and satisfactory completion of a well. Drilling mud performs the following functions:

- i. Cleans the formation of rock for cutting of rocks
- ii. Transports these rock cuttings through annulus to surface.
- iii. Cools the bit.
- iv. Reducing fluid loss by producing a filter cake on the bore hole's wall,
- v. Reduces the amount of damage done to the reservoir.
- vi. Enhances the drilling string's smooth inter-phase with the hole's sides.
- vii. There will be less of a detrimental impact on the environment (Sedaghatzadeh *et al.*, 2012).

The cost of drilling operations is mainly affected by drilling mud used and difficulties in drilling operation can also be as a result of drilling mud performance. However, for effective drilling operation, it is important to maintain the performance of mud at the pressure and temperature conditions best suited for the well to be drilled by simulating the borehole condition from the surface (Valizadeh and Nasiri, 2012). The drilling safety and economics, and drilling problems (such as borehole instability, shale and drilling mud

interaction, differential pipe sticking and loss of circulation) are majorly as a function of drilling mud used during operation. The proper selection of a drilling mud formulation for a given drilling operation is a critical component of a successful drilling operation (Pavel and Mikhail, 2018). The key factors guiding the choice of drilling muds are as

- i. The kinds of well to be drilled.
- ii. The permeability, strength and opening of muds pressure shown by the well and
- iii. The temperature ranges (Annudeep, 2012).

The behaviour of well formation is a determinant factor in drilling mud effectiveness and selection in drilling operation. However, before drilling operation, the nature and behaviour of well formation would have been analyzed to determine the best mud to be used in the operation. Ebikapaye, (2018) reported that, for adequate performance of drilling muds, the need to apprehend the factors guiding the choice of drilling mud are carefully analyzed for suitable drilling mud to be applied for drilling a well. (Mansoor *et al.*, 2018) revealed that, drilling geothermal wells, deep wells and well associated with high temperature and high-pressure operating conditions, effective drilling mud is extremely needed.

Water-based drilling mud, oil-based drilling mud, and synthetic-based drilling mud are the three types of drilling mud (Ali *et al.*, 2018), and each of these classes is the drilling mud's building base source, depending on the choice and condition of function, which can be either at low operating temperature and pressure (LTLP), high operating temperature and pressure (HTLP), or somewhere in between (Aminu *et al.*, 2013).

Considering the economic and environmental safety, water-based drilling mud is commonly used for oil and gas exploration because it is easily affordable and environmentally friendly. However, it is observed that water-based drilling mud have substandard rheological and filtration performance at high temperature high pressure

operating conditions of the well (Putri *et al.*, 2016). Ali *et al.* (2018) in a study reported that the challenges of water based drilling mud is due to shale swelling during the drilling of shale formation which leads to the devastating problems like unstable well bore, loss of circulation, pipe twig resulting to low penetration rate and increases the cost of drilling operation which makes it ineffective. As a result of these drawbacks, this research intends to modify the rheological and filtration performance of water-based drilling mud using Nigerian lignite nanoparticles for drilling operation in Nigeria.

The oil-based drilling muds were formulated for situation where water-based drilling muds were ineffective which became a solution to problems encountered while using water-based drilling muds for drilling operations. Its higher temperature stability nature, is used for high temperature formation, water sensitive shale, thick salt section and low-pressure well formation (Mohamed *et al.*, 2010). Oil based drilling muds are known for their excellent features such as shale stability, lubricity and temperature stability which enhance their efficiency and reduces difficulties when used as drilling muds during operations. However, oil-based drilling muds have greater lapses such as been more expensive and less environmentally and ecologically friendly than water-based drilling muds (Dantas *et al.*, 2014).

Synthetic based drilling muds are also used when the lubricity of water-based drilling muds is no longer effective during drilling operation. These drilling muds are rich in natural lubricating properties which reduces the frictional coefficient of the drilling process. However, there is need to further enhance the lubricating performance of synthetic based drilling muds in a harsh condition (Dina *et al.*, 2015).

Rheology is an essential property of drilling muds which shows how the flow is been deformed by matter. The rheological performance of muds as a function of plastic viscosity, apparent viscosity, yield point, density and gel strength are specified by

considering the behaviour of flow in the well formation (Ogbeide and Igbidere, 2016). The function of viscosity in drilling muds cannot be under rated because it is the main factor in the performance of the drilling muds, as a matter of fact, it determines the extent of internal resistance of a mud to flow. In drilling operation, muds with relatively high viscosity is suitable but not too high viscous mud which is capable of causing friction thereby decreasing the penetration rate and also hindering the circulation of muds which results to high pump pressure that leads to high velocity of the pump during drilling operation (Nweke *et al.*, 2015). Moreover, viscosity of drilling muds, are affected by particle sizes, molecular sizes, pressure and temperature, but with the aid of low or high viscosity of muds during operation, all weighting material and drill cutting will be suspended and will not be allowed to settle to the bottom of the borehole even when circulation has stopped by the effect of buoyant force (Omole *et al.*, 2013). Plastic viscosity is a measure of the internal resistance to mud movement as a function of the types, quantities, and sizes of fragments present in a given mud. The internal resistance is as a result of interaction between solid fragments and transformation of the liquid fragments under shear stress.

Density is one of the essential parameters used in the evaluation of drilling muds performance. It is defined as weight per unit volume, which is measured in pounds per gallon (lb/gal) or kilograms per cubic meter (kg/m<sup>3</sup>). Density is controllable during drilling operation. According to Nweke *et al.* (2015), the drilling mud density must be greater than the opening pressure of the well formation so as to decrease filter cake permeability, to block the well bore with a thin and to hinder the fluids of the formation from flowing (Ebikapaye, 2018).

All the drilling muds contain different kinds of additives at a specified concentration to enhance drilling mud performance during operation, these additives include a viscosifier

(Bentonite and Xanthan gum), fluid loss reducer (polyanionic cellulose, PAC, carboxymethyl cellulose, CMC), pH controller (sodium hydroxide, NaOH), weight controller agent (Barite) and to improve shale stability, several polymeric swelling inhibitors such as partly hydrolyzed polyacrylamide (PHPA), sodium silicate, and polyalkylene glycols (PAC or glycol) (Mohamed *et al.*, 2010).

Bentonite is the most common viscosifier additive used for drilling mud when mixed with fresh water, it improves hole cleaning qualities and forms a thin, low-permeability filter cake. when drilling deep well or geothermal reservoirs (Ogbeide and Igbinerere, 2016). From the observations made in drilling oil and gas exploring nations, bentonite clay is the major drilling mud raw material because of the excellent colloidal and plastic nature of its suspension. Bentonite is an important clay material formed by in-situ devitrification of volcanic ash and is made up of montmorillonite, bentonites are used for different industrial processes such as, in drilling muds for modification of rheological and enhancement in control of the system stability (Mehaysen and Shakhartreh, 2012). Other chemical compound added to drilling mud to stabilize them include:

- i. Natural organic materials
- ii. Synthetic polymers.

But in this study, Lignite shall be used. Lignite is used as bridging additive for modification of water-based drilling muds rheological and filtration properties. However, lignite is the lowest class of coal mineral, with a heating value of about 9.3034 MJ/kg to 19.304 MJ/kg. It is a very soft coal and brownish in nature, and has the highest moisture content of about 70 % water by weight, it also contains about 25 – 30 % carbon which is low compared with other classes of coal mineral. Lignite is also used to produce electricity (Deepark, 2014).

### **1.1 Statement of the Research Problem**

The abundance of local bentonite in Nigeria are not exploited because these local bentonite contains high level of impurities and are mainly calcium-based montmorillonite with low swelling capacity which results to substandard rheological and filtration performance challenge (such as cleaning of rock formation for rock cuttings, transporting of rock cuttings from wellbore to the surface, suspending of rock cutting when operation is at static condition and control of fluid lost to well bore) in their natural form when used for formulation of water-based drilling muds.

### **1.2 Aim and Objectives of the Study**

The aim of this research work is the modification and evaluation of rheological and filtration properties of water-based drilling muds using Nigerian lignite nanoparticles.

The aim of this research work can be achieved via the following objectives;

- i. Pretreatment and characterization of clays and preparation of Nigerian lignite coal nanoparticles.
- ii. Formulation and characterization of drilling mud.
- iii. Modification of drilling mud using lignite nanoparticle.
- iv. Evaluation of the effects of Nigerian lignite nanoparticles on the rheological and filtration properties of water-based drilling mud for comparative analysis.

### **1.3 Scope of the Study**

This research work will involve the use of Nigerian bentonite clay and coal mineral (lignite) as additives for formulation of water-based drilling muds.

### **1.4 Justification of the Study**

This research is justified based on the following:

- i. To provide an alternative means of enhancing water-based drilling mud to overcome shale swelling.

- ii. To provide an enhanced water-based drilling mud suitable for drilling oil well with operating conditions less than 160 °C temperature, geothermal wells and deep wells formation.
- iii. To provide an enhanced water-based drilling muds which is ecological and environmentally friendly and comparable with oil-based drilling mud.
- iv. To reduce cost of drilling operation by providing cheap and affordable drilling muds in replacement of imported drilling muds.

## CHAPTER TWO

### 2.0 LITERATURE REVIEW

#### 2.1 Drilling

Drilling is the process that enhanced the production of discovered hydrocarbon by creating a passage that allows the flow of hydrocarbon source to the surface. It is done with the use of a drilling bit coupled to a long string of drill pipe, and it entails penetrating the earth's crust for many thousand feet to collect hydrocarbons in a reservoir using the rotary drilling technique. However, from the time of cable tool rig to the use of rotary drilling rigs, many technological advancements have been considered on how best drilling operations can be carried out in the interest of environmental safety and economic possible ways (Francis and Okon, 2012).

#### 2.2 Drilling Muds

Drilling muds are heterogeneous mixture of water or oil, clay materials and chemical, that facilitate drilling operations. They are critical to effective well drilling because they have common qualities that aid in the safe and satisfying completion of the well, such as the removal of cuttings to the surface, the control of high-pressure zones, and the cleaning of the bottom hole. The relevance of drilling muds cannot be overstated, as knowledge of drilling mud is critical in the petroleum industry's rotary drilling operation. Drilling muds are made up of liquids, dispersed and discontinued solids, and treatment chemicals, according to Yao *et al.*, (2013), with the liquid constituting the continuous phase. A filter cake is made from drilling mud to stabilize the wellbore area by bridging the formation face under an overbalanced condition and filtrate moves into the formation.

Bageri *et al.*, (2013), reported that filter cake facilitates the filtration performance of drilling mud which aid the production of hydrocarbon. Drilling mud modification is an important phenomenon for better drilling results. During drilling, solid deposits in the

form of a filter cake improve borehole stability by limiting liquid phase movement from the permeable zone and reducing formation damage (Okorie *et al.*, 2016), this characteristic of drilling mud is controlled by its viscosity which is enhanced by viscosifier.

The drilling muds filtration procedure comprises of three stages:

- i. The spurt loss is the first stage, which occurs as soon as the drill bit penetrates the bottom rock and creates new free surfaces; the spurt loss takes very little time and the filtration rate is relatively high because there is no filter cake on the bottom rock surface.
- ii. The second stage is dynamic filtration, which happens when the drilling mud spreads and deposits cakes soon after the spurt loss. An equilibrium cake thickness is obtained when the forces that maintain colloidal fragments on the cake surface are countered by hydrodynamic shear forces that tend to entrain fragments in the flow stream.
- iii. The static filtration is the third stage, in which the filtration rates slowly reduce during this period because the drilling mud circulation is suspended. (Caenn *et al.*, 2011).

Valizadeh and Nasiri, (2012), reported that drilling mud is the major factor that affects the cost of drilling operation. When the drilling mud properties is not up to the standard, the drilling process is directly affected. Moreover, the efficiency of the drilling operation will increase when the mud properties are maintained under the same pressure and temperature as the hole. Zisis *et al.*, (2016), also stated that due to constant change of downhole conditions across the globe, the mud system should be designed to overcome complex challenges such as High-Pressure/High-Temperature (HPHT) conditions, an effective drilling mud system determines a successful drilling operation, which promote

better productivity with a minimum interference for completion of operations. The formulation and use of exceptional drilling muds is required in drilling new oilfields reservoir environments with high pressure and high temperature (HPHT) reservoir conditions, which maintains their rheological and filtration properties even at such operating conditions, for an optimal performance of the drilling process, effective drilling mud is used (Zisis *et al.*, 2016).

### **2.3 Functions of Drilling Mud**

Formulation of drilling mud is one of the major components of the drilling process, which facilitate drilling operation, while the drilling mud is also referred to as drilling blood. It is a determinant factor that can make the drilling operation either successful or unsuccessful (Okorie *et al.*, 2014). This is due to the useful roles that mud plays and these functions include but are not limited to;

- i. Carrying cuttings below the bit, convey them up through the cylinder, and allow their separation at the surface;
- ii. Cleaning, cooling and lubricating the drilling string and bit as to reduce friction between the drilling string and the side of the wellbore;
- iii. To regulate formation pressure, an overbalanced drilling situation is created;
- iv. supplying hydraulic horsepower to the drill bit in order to achieve optimal penetration rates;
- v. Maintain the stability of the wellbore's uncased parts;
- vi. Reduces the damage caused by the drilling of various horizons;
- vii. Creating an impermeable, rather thin mud coating on the borehole wall of permeable formations to seal them off;

- viii. After the circulation has been stopped, suspend the drill cuttings in the suspension by adding a buoyancy force to gently maintain the weight of the drill string and casing string.
- ix. Assist in the collecting of information from the penetrated well's available drilling cuttings, cores, and electrical logs for interpretation (Apaleke *et al.*, 2012; Jung *et al.*, 2013; Zakaria *et al.*, 2012; Sadeghalvaad and Sabbaghi; 2015 Hossain and Al-Majeed, 2012;).

## **2.4 Classification of Drilling Muds**

Drilling muds are characterized as either water-based or oil-based based on its continuous phase (Putri *et al.*, 2016). Although a new class is introduced which is known as synthetic-based drilling mud because of the environmental challenge of the oil-based drilling muds (Okorie *et al.*, 2016).

### **2.4.1 Water based drilling muds**

Water-based drilling mud is the most popular and commonly used drilling mud in oil and gas exploration, because it is relatively more environmentally friendly and cheaper in cost than oil-based drilling mud. According to Kania *et al.*, (2015), water-based drilling mud deteriorate at HPHT conditions because of its poor rheological and filtration properties and there is a great need to improve their properties to meet the standards and extend their use at extreme downhole conditions. According to Ali *et al.*, (2018), water has become the most prevalent and important fluid for forming drilling muds, which has drawn researchers' attention to modifying the rheological properties of water-based drilling mud to tackle damaging concerns. For water-based drilling mud, instantaneous creation of a filter cake is generated by increased spurt fluid loss, followed by dynamical filtration loss, resulting in thicker filter cakes that screen the fracture tip from the maximum wellbore pressure and allow connection to inhibit further fracture propagation (Hanyi *et al.*, 2018).

In the meantime, the presence of filter cake can obscure fractures, resulting in increased fracture re-opening pressures. In comparison to other forms of drilling mud, water-based mud offers the advantages of high true yield strength, good bit hydraulics, less circulating pressure losses, and higher shear thinning, according to He *et al.*, (2016). Due to environmental challenges, water-based muds remain the preferred drilling muds than the other two types irrespective of their drawback. Moreover, it is necessary to improve the qualities of water-based muds in order to achieve greater success in drilling engineering and water-based drilling muds applications (Ali *et al.*, 2018). The biggest disadvantage of employing water-based muds was noted during the process of accessing a shale formation well, which caused shale swelling, rendering water-based muds ineffective (Liang *et al.*, 2016). Because shale swelling generates other difficulties like pipe twist, an unstable wellbore, and lost circulation, which limits penetration rates and raises drilling expenses (Ewy and Morton, 2009). From the result of experiments conducted on comparative study on drilling muds performance, formulated with geothermal spring and freshwater (Emine and Bayram, 2019). The study concluded that, at constant shear rate and shear thinning behavior, the shear stress values of geothermal water-based muds were found to be lower than those of freshwater prepared muds at both ambient and increased temperatures. When compared to freshwater muds, these muds will have a poorer penetration rate, weaker flow performance, and a reduced capacity to clean holes at both ambient and elevated temperatures. Furthermore, geothermal water muds produce more filtrate volume than freshwater muds, implying that when geothermal water-based muds are employed, the volume of filtrate flowing through the well during drilling increases. Meanwhile, at temperatures exceeding 121 °C, the stability of both muds deteriorates. The cake thickness of muds made with geothermal water was found to be larger than that of muds made with freshwater (Emine and Bayram, 2019).

#### 2.4.2 Oil based drilling muds

Oil is one of the based fluids used in formulating drilling mud which is referred to as oil-based mud. Diesel is one of the petroleum products used in formulating oil-based drilling muds due to its solvency for rubber, viscosity characteristics and low flammability, (Dardira *et al.*, 2014). However, all petroleum-based oils used for formulation of drilling mud were all toxic and harmful to animal and plant life, because they contain large percentage of aromatics and small substantial percentage of n-olefins (Dardira *et al.*, 2014). Meanwhile, the oil-based muds are utilized due of their outstanding lubricating performance, their good rheological performance at high temperatures up to 260 °C, and their efficiency against all sorts of corrosion. Oil-based muds also have the advantage of being able to drill through water-swellable clays in well formations (Okorie *et al.*, 2014). Oil-based mud are commonly used to overcome HPHT conditions problems because of their ability to penetrate formation with the presence of contaminants and a formation in which the temperatures in the bottom hole are exceptionally high (Amani *et al.*, 2012). Oil-Based mud could last for longer periods of time, also offer exceptional corrosion protection. Some things to think about while choosing an oil-based mud are as follows:

- i. Ability to drill low pore pressure formations
- ii. Faster penetration rates.
- iii. Packer fluids that are stable (under high temperature conditions).
- iv. High lubricity, particularly in high deviated and horizontal wells, can help to reduce differential twiggling risk. and
- v. Shale stability.

Oil-based drilling muds generally have better performance in drilling high temperature or low temperature well but, allow drilling of salt zones with minimal dissolving of salt,

which cause some difficulties during the drilling of shale formations well (Adesina *et al.*, 2012).

## **2.5 Drilling Mud Related Challenges**

Some drilling challenges are as result of situations that take place after commencement of drilling in which were not put into consideration when formulating drilling muds. Failure to properly address these challenges can result to unscheduled trouble time, poor performance, excessive drilling costs and high-risk activities that aren't necessary. However, some of these issues can be addressed by modifying the drilling mud's properties with additives (Mohammad, 2013). The major mud related challenges mainly found during drilling operations are as follows:

### **2.5.1 Borehole instability**

Borehole instability challenges are commonly observed in shale formation, when the mud weight is not suitable to shale formation, the formation can collapse as a result of the mud weigh not sustaining the stabilities. Adequate mud properties (mud viscosity, yield point and fluid loss) enhanced the borehole stabilities (Mohammad, 2013).

### **2.5.2 Salt section hole enlargement**

Salt portions may be broken down by the drilling fluid, resulting in hole expansion. The use of saturated salt mud system is best used for drilling through the salt bed in order to prevent the challenges of hole enlargement. Li *et al.*, (2014), used natural vegetable gum for formulation of drilling fluids of high temperature resistance and environmental friendliness, the temperature resistance of the drilling fluid was improved from 100 °C to 140 °C. The potential of the salt-resistant and the shale roll recovery were improved. In addition, the formulated drilling fluid reduced formation damage.

### **2.5.3 Lost circulation**

The non-controlled considerable amount of drilling mud is being pumped into an unexpected formation. during drilling process is referred to as lost circulation. Lost circulation can occur in different ways in the formations, such as in fractured formation, extremely permeable wells, and cavernous layers (Mohammad, 2013). When the mud's hydrostatic pressure exceeds the formation's breaking strength, fractures occur through which the fluid can flow which lead to loss circulation. Fluid will flow in massive fractures more than 100 microns if the pore opening of the shales through which the fluid is lost is in the range of 10 nm-0.1 microns (Sensoy *et al.*,2009). Modifying the mud by adding lost circulation additives to bridge the fractured of the formation and deposition cakes where drilling fluid is lost to the formation in this area, adequate formulation of mud using suitable lost circulation additives will harness the muds weight and also maintain hole cleaning of the formation. The proper size distribution of bridging chemicals helps generate an efficient seal of impermeable filter cake that deposits quickly on the face of the formation, preventing continuous mud losses (Mohammad, 2013).

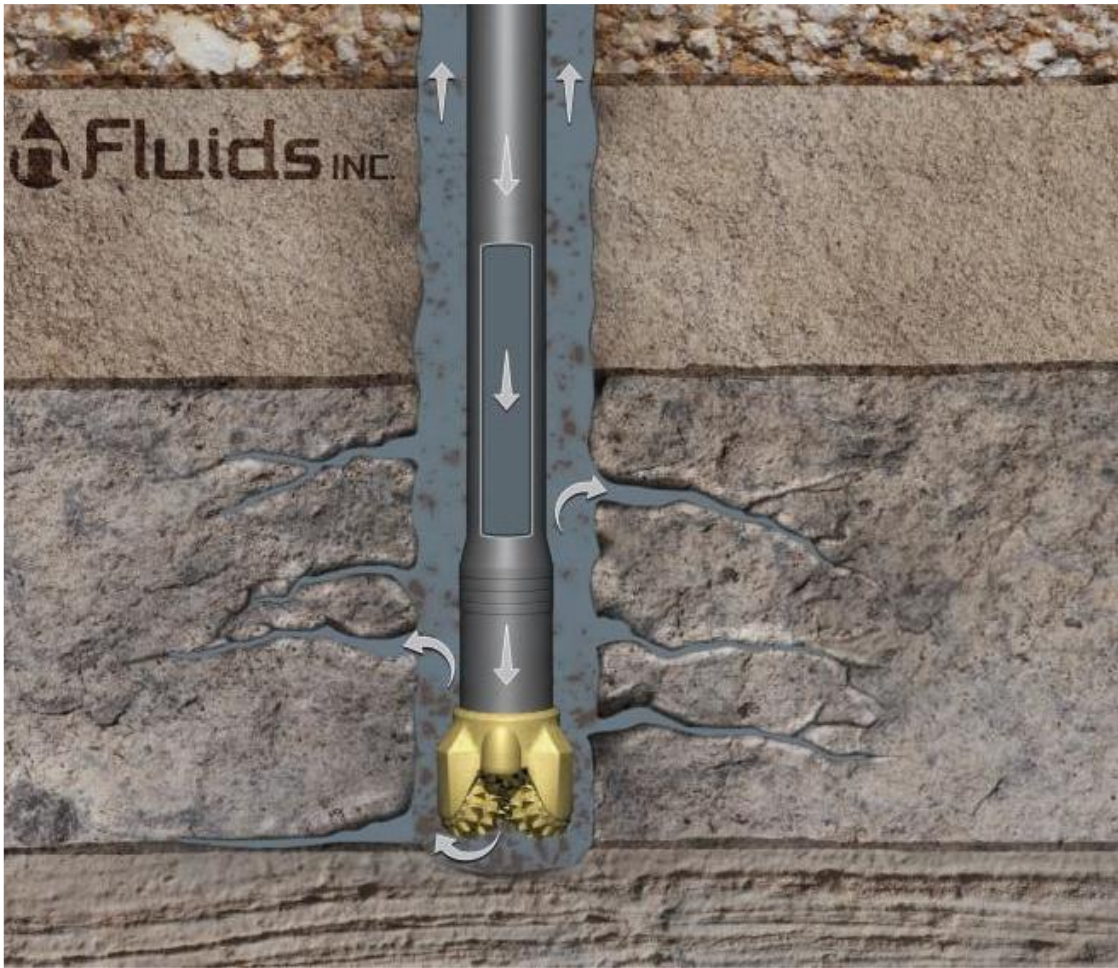


**Figure 2.1:** Shows the Fluid Loss During Drilling (Mohammad, 2013).

## **2.6 Mud Properties in Relation to Functions**

When formulating a drilling mud, it is essential to evaluate the physical, chemical, rheological and filtration properties of the mud system in order to determine and maintain the performance of the mud. There is need to carry out measurement on the properties drilling mud in order to evaluate their performance with standard mud result since there are ranges of standard mud properties values by America Petroleum Institute (API).

### **2.6.1 Density**

In all drilling operation, the density of mud is very important as it helps in controlling the pressure during operation, the weight of mud is a base factor for calculation of all the pressure control in the hole. Increased density reduces mud pit settling rates while increasing the buoyancy force carrying capacity of rock cuttings, which aids in preventing earthhole and flow into the opening (Ebikapaye, 2018). Mud balance is the instrument used for measuring the density of a drilling mud during drilling operation, precaution must be taken during measurement to avoid air bubbles in the mud sample which might lead to error while reading the mud density, especially, for muds having high gel strengths or yield points. There are factors that affect the density of drilling mud, such as temperature and pressure, increase in temperature decreases the density of drilling mud therefore, temperature of mud is inversely proportional to the mud density while increases in pressure increases the density of drilling mud as such pressure is directly proportional to mud density, weighting agents such as barite, hematite, iron oxide, and calcite can be used to increase the density of drilling mud. Barite is the most commonly used weighting agent because of its high specific gravity, low abrasive tendencies, low cost, and inertness. the specific gravity of barite is 4.5. while commercial barite has a specific gravity of 4.25, the difference between the pure barite and commercial barite because impureness are contains in commercial type barite, quality control analysis is recommended to guarantee that the quantity of impureness is largely soluble alkaline earth metals are not above a peak of 250 mg/l expressed as calcium specification range by API standard before using the barite for modification of drilling mud, the impureness in the barite vary as a result of where the barite was sourced from, poor quality control at the grinding plant may also introduce calcium contamination(Ebikapaye, 2018).

### 2.6.2 Rheological properties

The rheological properties of drilling mud describe the mud flow characteristics under different flow conditions, these properties are also known as flow properties. The flow behaviour helps in determining the effects of rheological properties of mud and when the fluid behaviour of a drilling mud is conditioned to an applied force known as shear stress, it also helps to categories the drilling mud (Annudeep, 2012), based on fluid behaviour, it is necessary to know the following:

- i. The point movement started in the fluid, when shear stress is applied and
- ii. The nature of the fluid movement (shear rate), Once movement has been initiated.

The shear stress is the force that a flowing fluid exerts on the surface of a conduit, with the magnitude of shear stress determined by the force between adjacent surfaces of flowing mud flowing at various speeds and the distinct in velocities of adjacent surfaces close to the pipe's wall. The difference in velocities between neighboring strata over a flow route is known as shear rate, note, a driller is interested on the effect of the flow at a maximum shear stress and shear rate on the wall (Annudeep, 2012). Fluids can be categorized into two types based on rheological properties: Newtonian fluids and Non-Newtonian fluids.

Newtonian fluids, such as oil or water, have a constant ratio of shear stress to shear rate, therefore a measurement of shear stress at one shear rate is sufficient to determine the flow behavior at all shear rates. The viscosity is defined as the ratio of shear stress to shear rate (Annudeep, 2012).

The viscosity of a fluid is used to determine its resistance to flow and to examine the flow behavior of Newtonian fluids. Mathematically, it is measured in centipoises

$$\text{Viscosity } (\mu) = \left( \frac{\text{shear stress } (\tau)}{\text{shear rate } (\gamma)} \right) \quad (2.1)$$

When force (shear stress) is applied on Newtonian fluid, the fluid deforms immediately and the degree of movement or flow is proportional to the applied force, **shear thinning** occurs when the effective viscosity is low at high shear rate or high at low shear rates (Annudeep, 2012).

Non-Newtonian fluids are fluids in which the ratio of shear stress to shear rate is not constant (non-linear). These fluids need some amount of shear stress to start movement, as the shear rate increases, there is need to add more stress to keep the fluid flowing, these fluids embody solids that are connected jointly to form a structure that causes flow to stop when there is a pressure drop or reduced shear stress to a spot less than the shear strength of the structure, such as drilling muds and cement slurries.. The yield point or yield stress of a fluid is the point at which shear force is needed to start movement. Allowing non-Newtonian fluids to remain static for an extended period of time will result in the formation of a semi-rigid structure that will necessitate a large shear stress to initiate flow. The gel strength is required high shear stress to commence flow, and the structure becomes highly stiff with time, thereby cause greater gel strength (3) Drilling engineers are interested in three major concerns where shear rate values are of great interest:

- i. With almost no shear rate values, the pits
  - ii. Shear rates are minimal in the annulus.
  - iii. The drill string and collars, which provide hydraulic power from a pump to the bit
- (Annudeep, 2012).

#### **2.6.2.1 Plastic viscosity**

Plastic viscosity is another mud property which determines the internal resistance of fluid flow as result of type size and quantity of solids in the mud. Collisions between solid particles and the mud's liquid phase cause mechanical friction, which causes the fluid to cease moving. The viscosity of the liquid phase and the volume of solids included in a mud determine

the plastic viscosity. Plastic viscosity portrays the outcome behavior of mud at the bit, as it helps to lower high shear rate viscosity, the plastic viscosity has to be reduced. High plastic viscosity is never desirable because high plastic viscosity will only cause more pressure drop down the drill string which will slow the flow rate thereby affect the lifting capacity of the drilling mud (Nwaoboli, 2014).

#### **2.6.2.2 Yield point**

The measure of forces of attraction between particles in a fluid as a result of opposing charges on particle layer, opposing the initial flow of mud motion, the kind of solids contained in the muds and their respective surface charges harness the yield point of the drilling mud.

There are two major mud roles that to yield point does in a drilling mud:

- i. Holes clearing capacity and
- ii. The muds pressure manage capacity (Nwaoboli, 2014).

Based on pressure management, this is typically vital where high mud density is required; in fact, in high density muds, the necessity to achieve a minimum yield point is sometimes more important than the benefits of maintaining a high yield point. Meanwhile, a higher yield point increases mud carrying capacity and circulating pipe pressure drop, which is good for hole cleaning. A higher yield point isn't ideal for problems like lost circulation and swabbing, but it's great for hole cleaning. Increased mud weights increase hole cleaning capabilities, hence higher yield points are usually not necessary in high mud density to ensure good cuttings carrying capacity (Nwaoboli, 2014).

#### **2.6.2.3 Gel strength**

Another essential rheological parameter of drilling mud is gel strength, which is a measure of its thixotropic action and estimates the shear force required to initiate the flow

of a fluid that has been stationary for some time. The ability of a drilling mud to suspend rock cuttings after circulation stops is known as gel strength the suspending capability of a drilling mud is as a result of the group of electrical charges between particles within the structure making the mud to be stiff, the tendency to gelling action of the drilling mud may increase or decrease. The temperature and the quantity, chemical and type of solids in suspension ascertains the stiffness of the mud structure formed (Nwaoboli, 2014).

Viscometer is used to ascertain drilling mud gel strength, by observing the highest dial deflection at 10 seconds and 10 minutes selected time when the gel structure breaks, the difference between the two measured values of gel strength for the two selected time simply portrays the gelation rate of the mud because the two selected set time informs gelation qualities of muds. Gel strength is measured in lb/100ft<sup>2</sup>, and for a mud to be capable of suspending barite, it must have a gel strength of 2 to 4 lb/100ft<sup>2</sup> (Nwaoboli, 2014).

### **2.6.3 Rheological models**

Viscometer (Fann VG meter) is used for measuring rheological properties of drilling muds in the drilling sector and modelling are carried out to a large extent with the interest of evaluating drilling muds rheological properties. Rheological characteristics are often assessed with a 6-speed viscometer with speeds of 600, 300, 200, 100, 6 and 3 rpm.

Three different approaches applied for determining constants of rheology are:

- i. 2 data points oil field approach
- ii. 2 data points standard approach
- iii. 6 data points regression approach

Flow curves also known as rheograms are produced when shear stress values are plotted against shear rate values. Because of the geometry and calibration of the viscometer, a

correction factor of 1.06 is needed to multiply the readings acquired from the Fann to obtain the genuine shear stress values (Skalle 2010).

### 2.6.3.1 Newtonian model.

When a shear stress (force applied) is used on Newtonian fluid, it begins to disfigure and flow; the degree of flow is then the functions of the applied force. The Shear Stress ( $\tau$ ) and the Shear Rate ( $\gamma$ ) in Newtonian fluids have a linear relationship, as shown by the graph in figure 2.2.



**Figure 2.2:** Plot of Newtonian Model (Nwaoboli, 2014).

The mathematical demonstration of Newtonian model is by equation 36.

$$\tau = \mu \gamma \quad (2.2)$$

Where,  $\mu$  is the viscosity.  $\tau$  is the shear stress and  $\gamma$  is the shear rate.

A 300-rpm reading is utilized for Newtonian fluids, and one constant is adequate to characterize Newtonian model using the two data points conventional approach.

$$\mu_{300} = \left( \frac{\tau_{300}}{\gamma_{300}} \right) \quad (2.3)$$

$\mu_{300}$  is the 300 rpm reading viscosity value

$\tau_{300}$  and  $\gamma_{300}$  is the shear stress and shear rate at 300 rpm respectively.

### 2.6.3.2 The Bingham plastic model.

A minimum amount of force is required for a fluid to flow, according to the Bingham plastic model, and this minimum amount of force is known as the fluid's Yield Point (YP), as shown in figure 2.3. Once flow has started, the relationship between  $\tau$  and  $\gamma$  is linear (Newtonian), with PV as the constant. Temperature and pressure have an effect on PV (Nwaoboli, 2014).

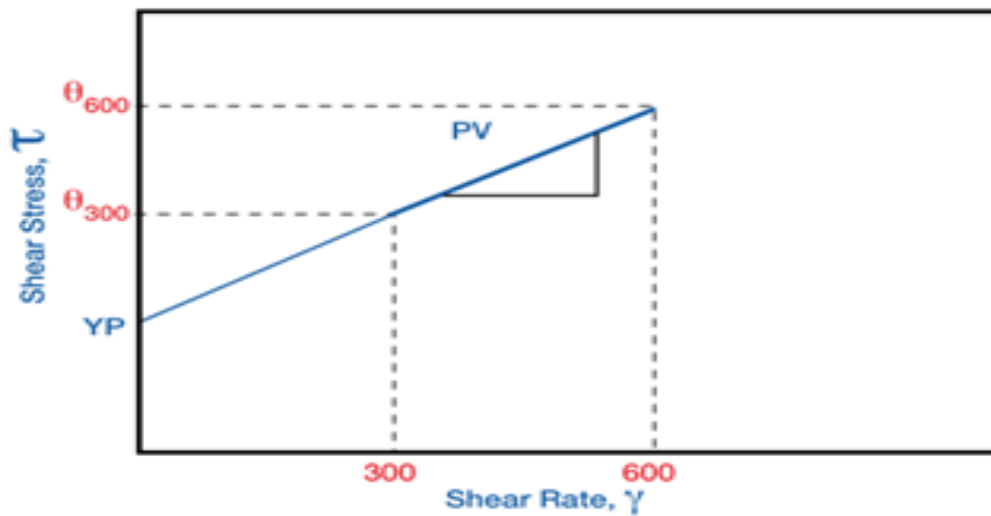


**Figure 2.3:** Bingham Plastic Model Plot (Nwaoboli, 2014).

The Bingham Plastic Model is given mathematically as

$$\tau = PV * \gamma + YP \quad (2.4)$$

### 2.6.3.3 The power law model

The power law rheological model, does not account for yield stress and at high shear rates, the Power Law rheological model accurately predicts the fluid consistency coefficient and flow behavior index, but at lower shear rates, some extent of error was observed (Nwaoboli, 2014). The power law model is more sophisticated than the Bingham Plastic model, because it does not imply a linear relationship between shear stress and shear rate rather, nonlinear relationship between the shear stress and shear. For fluids that obey the Power Law rheological model, there is no shear stress at zero shear rates (Skalle, 2010).

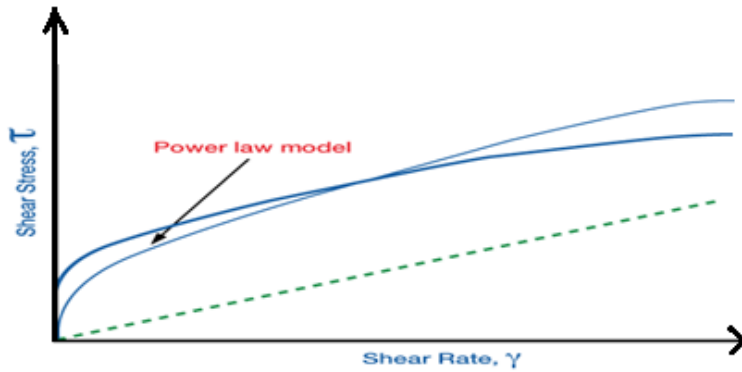


**Figure 2.4:** Plot of Power Law Model (Nwaoboli, 2014).

In Figure 2.4, the Power Law model is depicted. The fluid whose shear stress is proportional to the shear rate to the power of some index is best described by the power Law model. Mathematically demonstration of power law model

$$\tau = k * \gamma^n \quad (2.5)$$

Where

$\tau$  is the Shear stress

$k$  is the Consistency index

$\gamma$  is the Shear rate

$n$  is the Power Law index or flow behavior index (Nwaoboli, 2014).

Figure 2.5 shows a linear relationship of plot for Power Law fluids using log of shear stress against log of shear rate.

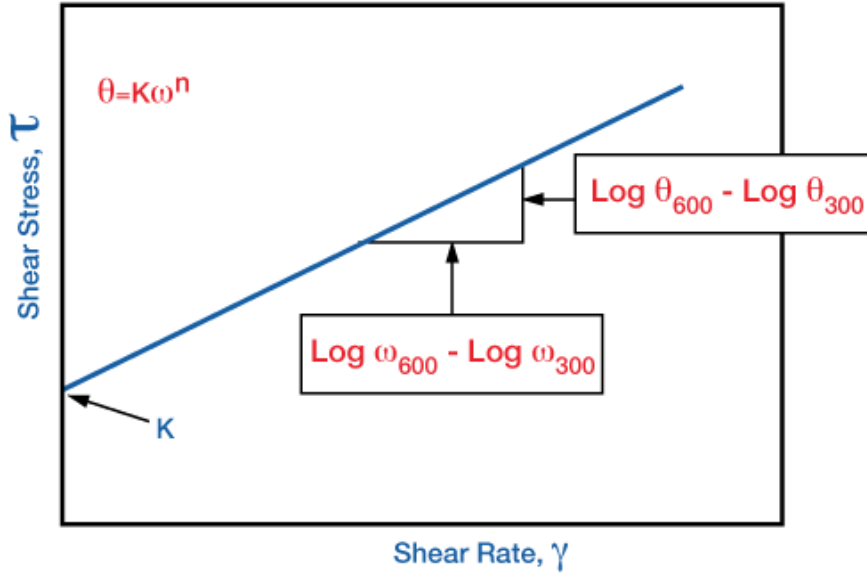


**Figure 2.5:** Log-log Plot of Power Law Rheological Model (Nwaoboli, 2014).

The slope of the line is represented by the (n) value, while the intercept is represented by the (k) value. The (n) number denotes the amount of non-Newtonian behavior of a fluid over a specific shear rate range. Equations 2.6 and 2.7 or 2.8 are used to represent the (n) and (k) values, respectively. Mathematically

$$n = \left( \frac{\log \tau_{600} - \log \tau_{300}}{\log \gamma_{600} - \log \gamma_{300}} \right) \quad (2.6)$$

$$k = \frac{\tau_{300}}{(\gamma_{300})^n} \quad (2.7)$$

$$k = \frac{\tau_{600}}{(\gamma_{600})^n} \quad (2.8)$$

$\tau_{300}$  and  $\gamma_{300}$  is the shear stress at 300 rpm and shear rate at 300 rpm respectively.

$\tau_{600}$  and  $\gamma_{600}$  is the shear stress 600 rpm and shear rate at 600 rpm respectively.

#### **2.6.3.4 The Herschel-Bulkley law**

The Bingham Plastic and Power Law models have been combined to create this model. Generalized Plastic Model is another name for it. The Herschel-Bulkley model has consistency coefficient and flow behavior index (k and n) values that are comparable with that obtained from the Power Law model; however, Herschel-Bulkley model assumes that

a minimum force (yield stress) must be engaged to fluids in order for flow to begin. Mathematically, these ( $\tau$ ,  $\tau_0$ ,  $k_{HB}$  and  $n_{HB}$ ) parameters are expressed by equations 2.9 to 2.12 respectively.

$$\tau = \tau_0 + k_{HB} * \gamma^n \quad (2.9)$$

$$\tau_0 = 2\tau_3 - \tau_6 \quad (2.10)$$

$$k_{HB} = \frac{(\tau_{600} - \tau_0)}{(1022)^{n_{HB}}} \quad (2.11)$$

$$n_{HB} = \left( \frac{\log\left(\frac{\tau_{600} - \tau_0}{\tau_{300} - \tau_0}\right)}{\log(600/300)} \right) \quad (2.12)$$

Where

$k_{HB}$  is the consistency coefficient

$n_{HB}$  is the flow behavior index

$\tau_0$  is the yield point of fluid at zero shear rate

$\tau_3$  and  $\tau_6$  is the shear stress at 3 and 6 rpm respectively

$\tau_{300}$  and  $\tau_{600}$  is the shear stress at 300 and 600 rpm respectively point, though it's calculated value differs.

With  $n = 1$ , the Bingham Plastic Model is formed.

With  $\tau_0 = 0$ , the Power Law Model is derived (Nwaoboli, 2014).

Although it has a shear stress at zero shear rate and is workable for both water and oil-based drilling muds because both reveal shear thinning behavior, the Herschel-Bulkley rheological model is quite complex to estimate the  $n$ ,  $k$ , and  $\tau_0$  values. The combined perspective of the flow curves for the various rheological models is shown in Figure 2.6

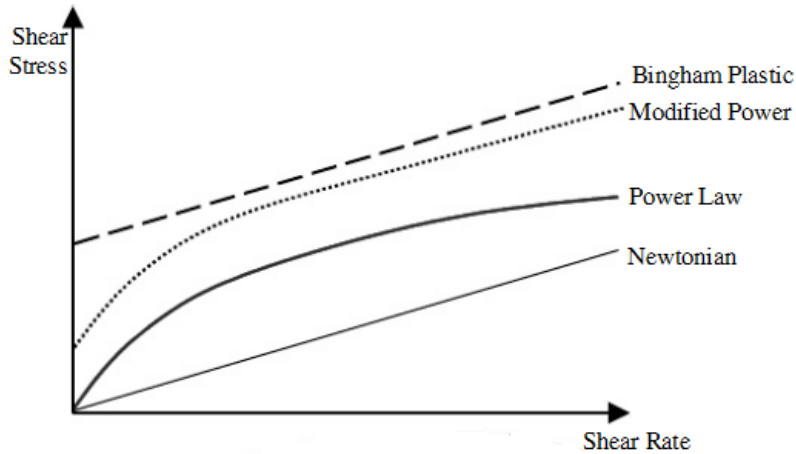


**Figure 2.6:** Plots of Different Rheological Models (Nwaoboli, 2014).

## 2.7 Bentonite

Bentonite have a wide range of industrial usage because it contains minerals of smectite group which have the potential to substitute  $\text{Si}^{+4}$  and  $\text{Al}^{+3}$  by lower valency cations in their crystal structure (Omer *et al.*, 2016). Bentonite may be classified as either sodium-based montmorillonite bentonite and calcium-based montmorillonite bentonite depending on the presence of dominant exchangeable cations, these two types of bentonite display different properties when used for mud formulation, the sodium-based montmorillonite bentonite is the high swelling bentonite while the calcium-based montmorillonite bentonite is the low swelling bentonite (Richard *et al.*, 2016). Generally, when mixed with water, the sodium-based bentonite displays more dispersion and improved rheological properties than calcium-based bentonite. Natural sodium-based bentonites like those in Wyoming, USA are uncommon, the exchangeable cation properties of smectite allows prevalent calcium form to be absolutely changed to sodium-based bentonites by a simple sodium-exchange process. However, calcium-based bentonite is referred to as fuller's earth in some countries particularly in the USA, fuller's earth is related to any clay that has the ability to decolorize oil and may consist of smectite or attapulgite, mineralogically are different but has the same characteristics of adsorption to

calcium-based bentonite. Typically, the physical and chemical properties of bentonites changes between deposits as a result of differences in the nature of the exchangeable cations present, type and amount of impurities present and degree of chemical substitution within the smectite group (Omer *et al.*, 2016). The quantity and type of associated minerals depends on the origin of the bentonite, the use of bentonite as industrial raw materials is not just only to its application in formulation of drilling muds rather, it's also useful raw material in foundry, ceramics refractoriness industries, no bentonite is acceptable for all application because there are different grade and their qualities are naturally part of the physic-chemical properties either in their natural or modified form which depends on industrial application (Omer *et al.*, 2016; Okorie *et al.*, 2016). Furthermore, clays that can swell and gel when dispersed in water are referred to as bentonite, there is no minimum grade of smectite content that determines whether a clay is no longer considered to be a bentonite while commercial bentonites usually contain more than 70% smectite, other associated minerals in clay are quartz, cristobalite, feldspars, zeolites, calcite, volcanic glass and kaolinite (Nweke *et al.*, 2015 and Omer *et al.*, 2016).

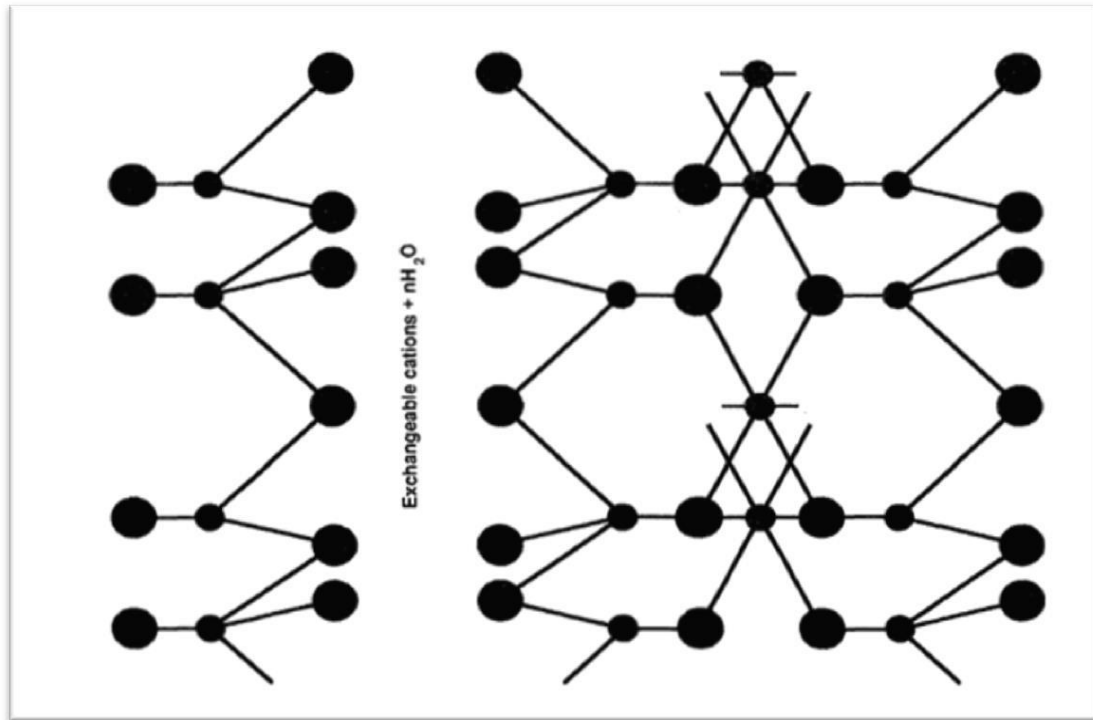


**Figure 2.7:** Crystal Structure and Chemistry of Bentonite Minerals (Omer *et al.*, 2016).

The cost of importing Wyoming bentonite from the USA has brought opportunity for other parts of the world to look within and use their local clays which corresponds to Wyoming bentonite quality when properly harness (Okorie *et al.*, 2016).

## 2.8 Coal

Coal is a combustible form of rock made by the deposition and compression of small particles which contains both compounds of carbon minerals and compounds of non-carbon constituent, coal is highly sufficient and commonly dispensed mineralized energy given substance in the world (Idris and Ahmed, 2019). Power generation, iron and steel manufacture, chemical and pharmaceutical manufacturing, cement production, and paper production are only a few of the applications for coal and its energy-derived substance (Bodude *et al.*, 2018). The layers of dead plants and animals at the bottom of the wetland were enclosed by the surface of water and dirt, trapping the energy of the dead plants and animals over millennia (Bizuallem and Busha, 2017). Coal as a nonrenewable energy

source is formed as a result of transformation of dead plants and animals through the action of heat and pressure acting on their surface.

## **2.9 Nanoparticles**

In most area of research studies, new research trends have revealed a progressive interest to nanotechnology. Nanotechnology is growing rapidly, with respect to technological inventions and innovations and this open space of technology has being the recent way for miniaturization with regard to scientific improvement and has attracted the interest of researchers. The petroleum industry is not immune to this to technology, as various open areas ranging from the starting of exploration to the production stage have seen stepwise investigation for the use of technological advancement of nanoparticles (Hoelscher *et al.*, 2012 and Zakaria *et al.*, 2012). Drilling mud is a key component for drilling operations to exploit the presence of crude beneath the earth's surface (Sehly *et al.*, 2015; Mahmoud *et al.*, 2016). With various amounts of bentonite, the incorporation of nanoparticles in the drilling mud can also improve the mud viscosity to the desired viscosity and fluid loss properties. Due to their ability of modifying rheological and filtration characteristics of the mud, they are good case for drilling mud formulation. The use of nanoparticles for production of water-based drilling muds (WBDMs) to prevents fluid loss in the shale formation drilling process is due to their smaller size, have demonstrated the effectiveness of nanoparticles as additive (Sadeghalvaad and Sabbaghi, 2015; Zakaria *et al.*, 2012; Jung *et al.*, 2013 and Hoelscher *et al.*, 2012;). Rezaee and colleagues claim that (2012). Figure 2.8 depicts the opening size relationship for tight sand, sandstone, and shales.

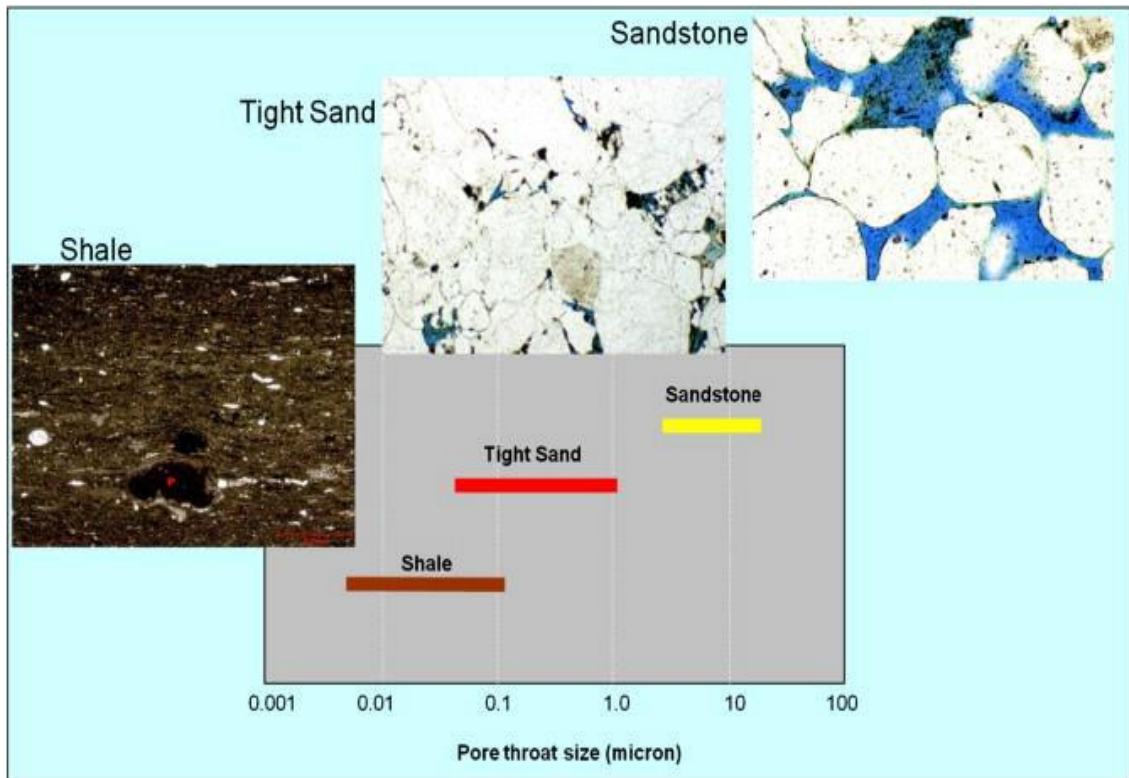


**Figure 2.8:** Pore Throat Sizes in Rock (adapted from Rezaee *et al.*, (2012)).

Fluid leaking into a sensitive formation can benefit from the addition of nanoparticles (Chenevert and Sharma, 2009). Nanoparticles, which are smaller than microparticles and require very low amounts of additives, improve the characteristics of mud at low additive concentrations (Amanullah *et al.*, 2011).

## 2.10 Nanoparticle Preparation

The selection of nanoparticles are function of properties and particle size of a material.

Nanoparticles are prepared using different methods as follows:

- i. Micronizer, jet, and ball milling are examples of dry processes.
- ii. Solvent evaporation, chemical precipitation, spray drying, and the emulsion process are examples of wet methods (Mohammad, 2013).

Husein and Nassar (2008) identified some primary strategies for the synthesis of nanoparticles

- i. sol-gel processing
- ii. chemical co-precipitation
- iii. microemulsions and
- iv. sonochemical (Husein and Nassar, 2008).

## **CHAPTER THREE**

### **3.0 MATERIALS AND METHODS**

#### **3.1 Material**

The local bentonitic clay used for drilling mud preparation were sourced from shabu in Lafiya, Nasarawa State, Nigerian and commercial bentonite clay used for drilling mud preparation was collected from Adex bore hold drilling company in Minna, Niger State, Nigerian while the lignite coal was sourced from Ogwashi Azagba in Aniocha Local Government Area of Delta State, Nigerian. Other surfactants such as caustic soda (NaOH), soda ash (Na<sub>2</sub>CO<sub>3</sub>), polyanionic cellulose (PAC) were purchased. Meanwhile, the based fluid used was distill water and was soured from drilling fluid laboratory from the department of Petroleum Engineering and Geosciences where this experiment was carried out. Bentonite as viscosifer, lignite as the thinner, caustic soda (NaOH) as the pH control agent, soda ash (Na<sub>2</sub>CO<sub>3</sub>) as the hardness control agent and polyanionic cellulose (PAC) as a viscosifer. The water-based drilling muds were formulated with different additives in accordance to American Petroleum Institute (API) recommendation.

All drilling muds samples were prepared by adding certain amounts of additives into the based muds, with specific parameters of muds to be determine the like: plastic viscosity, yield point, gel strength, mud weight, pH, filtrates loss volumes and filter cake thickness.

##### **3.1.1 Equipment and apparatus**

The following equipment were used for the laboratory experiment of this research work: Fann 35A Viscometer, Digital Weighing Balance, 500ml Capacity Measuring Cylinder, Universal pH scale, 704ES Roller Oven, Mud Balance, Digital Stop Watch

##### **3.1.2 Preparation of lignite coal nanoparticles**

The lignite coal was crushed and ground to fine particles, the fine particle size was analyzed via particle size analysis. 5 g of the fine particles was measured and diluted with

distilled water, the diluted sample was allowed to dissolve in water and filter. The filtered sample was put in a sample holder and placed in the analysis chamber and the analysis was run in three stage in order to determine accurate result. After the analysis, the average of the final result was determined by finding the final average of the result.

## **3.2 Characterization of Samples**

### **3.2.1 Characterization of nano lignite coal**

#### **3.2.1.1 Physicochemical analyses**

Ultimate and proximate analyses of physicochemical studies of lignite nanoparticles were performed. The final analysis procedure was gotten from (Bodude *et al.*, 2018).

The calculated moisture content, ash content, volatile matter, and fixed carbon content values was obtained using proximate analysis.

#### **Moisture Content (MC):**

The sample weight of 0.3 g was placed in a plate. The dish containing the sample was weighed and recorded before it was placed in the tray dryer. The drier was then adjusted to 60°C, and the sample was dried to a consistent weight, with the final weight being recorded. The moisture contents were calculated using the following formula:

$$\text{Moisture Content (MC) (\%)} = \left( \frac{\text{Wet Weight} - \text{Dry Weight}}{\text{Wet Weight}} \right) \times 100 \% \quad (3.1)$$

#### **Ash Content (AC):**

The coal sample used in this experiment weighed 0.2 g and was placed in a tarred crucible. The sample was warmed at 600°C for 3 hours. The crucibles were allowed to cool to below 100 °C degrees Celsius in the furnace before being placed in desiccators with a vented lid.

$$\text{AC (\%)} = \left( \frac{\text{Weight of Residue}}{\text{Weight of Sample}} \right) \times 100 \% \quad (3.2)$$

### **Volatile Matter (VM)**

The dry sample was heated in a furnace for 7 minutes at 930 °C to determine the volatile matter (VM). After cooling in a desiccator, the sample was weighed. The VM was calculated using the following equation:

$$\text{VM (\%)} = \left( \frac{Y-Z}{Y} \right) \times 100 \% \quad (3.3)$$

Where Y represents the oven dried sample weight and Z represents sample weight after heating at 930 °C.

### **Fixed Carbon Percentage:**

The percentage fixed carbon (FC) was calculated by subtracting the amount of AC and VM from 100, as shown in equation (3.4).

$$\text{(FC)} = 100 \% - (\text{MC} + \text{AC} + \text{VM}) \quad (3.4)$$

### **Calorific Value Determination**

The coal sample weight of 1.0 g in a nickel-chromium crucible was placed in a Combustion Vessel, which was surrounded by water and had a high-pressure atmosphere. The sample was then set on fire. The fan speed was adjusted to maintain a constant temperature in the calorimeter jacket, while the generated heat of the burnt sample raised the temperature of the bomb and bucket. An electronic thermometer with a resolution of 0.0001 of a degree was used to measure the temperature of the water. During the test, the heat flow between the jacket and the environment was continually monitored and necessary heat leak adjustments were performed automatically. The amount of heat released is proportionate to the sample's gross calorific value (on an air-dried basis) and is presented automatically by the device. The time limit was set at 10 minutes for each run used.

### **3.2.1.2 TGA**

This study was conducted using the combustion in air approach. An SDT Q600 simultaneous DSC/TGA device was used for this investigation. It can do both differential scanning calorimetry (DSC) and thermogravimetric analysis (TGA) at the same time. For this test, coal samples were passed through a test sieve having a 212  $\mu$ m aperture. The amount of coal sample utilized was 25 mg, which was precisely weighed and placed into the instrument's 90-liter lidless alumina crucible. The sample was heated in air at a rate of 10 °C/min from 25 °C to 1000 °C using a 50 ml/min air flow rate. The sample's weight change was automatically recorded until there was no more weight change. The sample's ash content is represented by the residue in the crucible. The test had a run time of around 3.5 hours.

### **3.2.1.3 SEM analysis**

The SEM analysis was carried out using the method adopted from (Gana *et al.*, 2019) to determine the surface morphology of the bentonite clay samples and Nona lignite coal.

### **3.2.1.4 EDX analysis**

The EDX analysis was carried out using the method adopted from (Gana *et al.*, 2019) to determine the elemental composition of the bentonite clay samples and Nona lignite coal.

### **3.2.1.5 XRD analysis**

At a temperature of 25 °C, an X-ray diffraction (XRD) analysis was used to assess the chemical composition of nano lignite coal, local and commercial bentonite clay. Using a Siemens D5000 powder x-ray diffraction instrument, the XRD pattern of the particles was acquired. On samples that passed sieve No. 200 (75  $\mu$ m), XRD tests were done. The powder (2 g) was placed in a 3 mm deep acrylic sample holder. Parallel beam optics with CuK $\alpha$  radiation at 40 kV and 30 mA were used to examine the sample. The sample was

scanned for reflections (2) in steps of  $0.02^\circ$  with a 2 sec count time each step from  $0^\circ$  to  $90^\circ$ . (Ahmed 2016,)

#### **3.2.1.6 FTIR analysis**

The FTIR method analysis was used to evaluate the functional group of the clays and mud samples using the method adopted from (Abdullahi and Audu 2017)

### **3.3 Chemical Treatment of Bentonites**

The method used was adopted from Okorie *et al.*, 2016; and Omole *et al.*, 2013. The bentonite clay sample was pulverized into fine particles. A slurry was formed by dissolving the fine particles into water, the slurry will be wet sieve and then allow the filtrate to settle for about six hours, thereafter decant to obtain clay mud of bentonite clay sample. The bentonite clay sample was sun dry for some days (7 days) to obtain bentonite clay cake which was disaggregated and sieved to obtain fine clay powder. (10) % of soda ash ( $\text{Na}_2\text{CO}_3$ ) was added to the 25 g of clay powder obtained and then dissolved in 350 mL of deionized water for about 24 hours to enable ion exchange to take place, then sample have undergone chemical treatment

### **3.4 Preparation of Drilling Mud**

The method used was adopted from Okorie *et al.*, 2016. Twenty-two (22) types of drilling muds samples were formulated in increasing order of nano lignite coal concentration, (11 from each of the two types of bentonite). Electronic mixer was used to stir each mud for a minimum of 5 minutes when each additives were added to each mud sample, except for the two control samples each from the two types of bentonite, with distill water as the based fluid, in order to increase the solubility and make alkaline the pH of the drilling muds (8 - 11), 7 % of 25 g of caustic soda (NaOH) was added to (20) twenty prepared mud samples. 25 g of bentonite clay was pure into 350 ml deionized water (formula A, base mud) and nano lignite coal (10 - 30) % as (formula  $\beta$ i). Thus, the drilling muds have

the mix of formulas (A +  $\beta$ i), the muds formulated with both local and commercial bentonitic clay were modified with nano lignite coal at three different concentration of (10 - 30 wt%) by weight percent, thereafter, the muds were left for hydration for about 16 hours at room temperature in a sealed container. (12) twelve prepared muds samples undergone the static aging of muds at two different elevated temperatures (100 and 160 °C) for 10 hours in a roller oven in order to simulate the behavior of the static muds in high temperature wells, after which, the aged samples were to allowed to cool to room temperature, removed from the aging cell and stirred for about 5 minutes in order to break down gels formed during the aging process. The composition of drilling muds with varied concentrations of micro lignite coal at various temperatures is shown in Tables 3.1 to 3.3.

**Table 3.1:** Composition of Drilling Mud at 25 °C

Materials	1 <sup>st</sup> Run	2 <sup>nd</sup> Run	3 <sup>rd</sup> Run	4 <sup>th</sup> Run
Water (mL)	350	350	350	350
Bentonite (g)	25	25	25	25
Lignite (g)	-	10 %	20 %	30 %
Polyanionic Cellulose (PAC) (g)	-	10 %	10 %	10 %
Soda Ash (Na <sub>2</sub> CO <sub>3</sub> ) (g)	-	10 %	10 %	10 %
Caustic soda (NaOH) (g)	-	10 %	10 %	10 %

**Table 3.2:** Composition of Drilling Mud at 100 °C

Materials	1 <sup>st</sup> Run	2 <sup>nd</sup> Run	3 <sup>rd</sup> Run	4 <sup>th</sup> Run
Water (mL)	350	350	350	350
Bentonite (g)	25	25	25	25
Lignite (g)	-	10 %	20 %	30 %
Polyanionic Cellulose (PAC) (g)	-	10 %	10 %	10 %
Soda Ash (Na <sub>2</sub> CO <sub>3</sub> ) (g)	-	10 %	10 %	10 %
Caustic soda (NaOH) (g)	-	10 %	10 %	10 %

**Table 3.3:** Composition of Drilling Mud at 160 °C

Materials	1 <sup>st</sup> Run	2 <sup>nd</sup> Run	3 <sup>rd</sup> Run	4 <sup>th</sup> Run
Water (mL)	350	350	350	350
Bentonite (g)	25	25	25	25
Lignite (g)	-	10 %	20 %	30 %
Polyanionic Cellulose (PAC) (g)	-	10 %	10 %	10 %
Soda Ash (Na <sub>2</sub> CO <sub>3</sub> ) (g) (g)	-	10 %	10 %	10 %
Caustic soda (NaOH) (g)	-	10 %	10 %	10 %

### 3.5 Mud Weight Measurement

Drilling fluid density is measured in grams per milliliter or kilograms per cubic meter (pound per gallon, or pounds per cubic foot). The mud balance is a density measuring equipment that is commonly used to determine the density of drilling mud. Before starting, the cup was cleaned and dried, and the calibrations were reviewed (the scale of 8.33 lb/gal or 1.0 S.G for distilled water was calibrated on the mud balance). The mud cup's cover was removed, and the cup was filled with the mud sample. The cup was then taped on the side to ensure that all trapped air bubbles were removed. The cup's cover was reapplied and turned until it was securely in place. A small amount of mud was permitted to pass through the cover's aperture. The mud covering the aperture of the mud cap cover was cleaned and wiped clean of excess mud. With the opening covered, the balance was dried., the balance was put on its base with the edges of the knife on the fulcrum rest. After that, the rider was shifted until the beam was balanced. On the center line, the spirit level bubble was placed. The density of the mud and mud gradient at the knife edge closest to the fulcrum was measured.

### 3.6 Viscometer Mud Calibration

By filling the cup with mud sample to the scribe line and then placing it on the Fann 35 viscometer stage, the sample viscosities was measured using the Newtonian fluids check calibration. The stage was adjusted until the rotor was immersed to the required level as

indicated by the noted line. The instrument was operated at the following speeds of 3 rpm, 6 rpm, 100 rpm, 200 rpm, 300 rpm, and 600 rpm. The dial readings at 600 rpm and 300 rpm were used to find out more about the muds, such as plastic viscosity and yield point, while the dial readings at 3 rpm and 6 rpm were used to find out about the muds' gel strength (10 sec and 10 min).

### 3.7 Filtration Loss Test

Fluid filtration tests were carried out using a medium pressure filtration device in accordance with API requirements (Model SD-3). The mud was put into a stainless-steel container with a bottom opening. The fluid was then exposed to 100 psi (0.69 MPa) pressure at room temperature for 30 minutes, and the volume of fluid lost was measured.

### 3.8 Rheological Test

The Rheological properties test were evaluated by measuring dial reading parameters with the aid of fann 35 viscometer at 3, 6, 100, 200, 300 and 600 revolutions per minute (rpm) respectively for different sample at 25 °C, 100 °C and 160 °C. The dial readings were performed for about three times to ensure consistency in the result, the viscosity values were in cP or mPa.s unit. Equation 3.5 to 3.7 described the plastic viscosity (PV), apparent viscosity (AV) and yield point (YP). The filter press at 100 psi at room temperature was used to determine the filter loss volume (FL). This filter loss volumes were collected every 30 minutes for each sample, and filter cake thickness (Fc) was determined.

$$PV(cP) = (\theta_{600 \text{ rpm}} - \theta_{300 \text{ rpm}}) \quad (3.5)$$

$$AV(cP) = \left( \frac{\theta_{600 \text{ rpm}}}{2} \right) \quad (3.6)$$

$$YP(lb/100 \text{ ft}^2) = (\theta_{300 \text{ rpm}} - PV) \quad (3.7)$$

Where:

PV is the Plastic Viscosity (cP)

AV is the Apparent Viscosity (cP)

YP is Yield Point (lb/100 ft<sup>2</sup> or Pa.s)

$\theta_{600 \text{ rpm}}$  is the dial Reading Value at 600 rpm (cP)

$\theta_{300 \text{ rpm}}$  is the dial Reading Value at 300 rpm (cP).

### 3.9 Rheological Model

The shear stress and shear rate were obtained from the data generated from rheological test and was used for determination of rheological model parameters, When the viscosity of a fluid is not dependent on the shear rate, it is called Newtonian fluid; when the viscosity is dependent on the shear stress, it is called non-Newtonian fluid

**Shear stress ( $\tau$ ):** Force per unit area and is expressed as a function of the velocity gradient of the fluid as:

$$\tau = -\mu \left( \frac{dv}{dr} \right) \text{ (cP)} \quad (3.8)$$

$$\tau = 1.067\theta_i \text{ (lb/100ft}^2\text{s}^n) \quad (3.9)$$

Where:

$\tau$  is Shear stress in (cP) or (lb/100ft<sup>2</sup>s<sup>n</sup>)

$\mu$  is the viscosity of fluid (cP)

$dv/dr$  is the velocity gradient of fluid (s<sup>-1</sup>)

$\theta_i$  is the dial reading values at 600, 300, 200, 100, 6 and 3 rpm

1.067 is Conversion factor from (cP) to (lb/100ft<sup>2</sup>s<sup>n</sup>)

Shear stress is measured in N/m, Pascal, or Dynes/cm. In Equation 3.8, the negative sign appears due to momentum flux flows in the direction of negative velocity gradient. The momentum, in other words, tends to go in the direction of lower velocity. It's also something that can be expressed. The rate of change of velocity when one layer of fluid travels over a neighboring layer divided by the distance between them is known as shear rate ( $\dot{\gamma}$ ). mathematically as:

$$\Upsilon = \left( \frac{dv}{dr} \right) \quad (3.10)$$

The equation 3.11 can be used to convert it to  $\text{sec}^{-1}$ :

$$\Upsilon = 1.703\gamma \quad (3.11)$$

Where:

$\gamma$  is Spera Rate in (rpm)

$\Upsilon$  is Spera Rate in  $\text{s}^{-1}$

Equation 3.8 can also be written as:

$$\tau = \mu \Upsilon \quad (3.12)$$

The rheology of non-Newtonian fluids is described using the mathematical models below:

1. Bingham Plastic model.
2. Power Law model.
3. Hershel Buckley Model.
4. Casson Model

In this research work, the power law model was adopted, because power law model efficiently predicts, at high shear rates, the flow behavior index and consistency coefficient are high, but there is a degree of uncertainty at lower shear rates, and this model does not account for yield stress (Skalle 2010).

The power law model is expressed as:

$$\tau = k * \Upsilon^n \quad (3.13)$$

The shear rates were estimated using equations (3.11).

Where:

$n$  is the fluid flow behavior index, which shows the fluid's tendency to shear thin and is dimensionless, and  $k$  is the fluid consistency coefficient, which acts as the mud system's viscosity index, and the unit is  $\text{lb}/100\text{ft}^2\text{sn}$ , which can be converted to  $\text{Pa}\cdot\text{sn}$  by

multiplying by 0.51. When  $n$  is less than one, the fluid is shear thinning; when  $n$  is greater than one, the fluid is shear thickening. A plot of log shear stress against log shear rate and the resulting straight line's graph parameters  $k$  and  $n$  can be used to derive the parameters  $k$  and  $n$  values. It can also be determined from the following equations

$$n = 3.32 \log\left(\frac{\theta_{600}}{\theta_{300}}\right) \quad (3.14)$$

$$k = \left(\frac{\tau}{\gamma^n}\right) = \left(\frac{\theta_{600}}{1022^n}\right) \quad (3.15)$$

However, a log of shear stress against log shear rate curve fitting or a linear regression will offer the statistically optimal values of  $n$  and  $k$ .

The logarithmic function of Equation (3.13) can be used to get the  $k$  and  $n$  parameters as follows:

$$\log\tau = \log k + n \log \gamma \quad (3.16)$$

### 3.10 Model Parameter Determination and Validation

The nonlinear constitutive rheological model parameters for power law modelling in equation 3.13 to 3.15 were determined using EXCEL SOLVER. Both coefficient of determination ( $R^2$ ) and root mean square error (RMSE) in curve fitting were used to test the accuracy and precision of the predictions of the power law model with experimental data. With 3.17 and 3.18, respectively (Vipulanandan and Mohammed, 2014).

$$R^2 = \left( \frac{\sum_i (X_i - \bar{x})(Y_i - \bar{y})}{\sqrt{\sum_i (X_i - \bar{x})^2} * \sqrt{\sum_i (Y_i - \bar{y})^2}} \right) \quad (3.17)$$

$$RMSE = \sqrt{\frac{\sum_{i=1}^n (Y_i - X_i)^2}{N}} \quad (3.18)$$

Where:

$X_i$  is the power law modelled shears stress values at different speed (Pa)

$\bar{x}$  is he mean of power law modelled shears stress value

$Y_i$  is the experimental shear stress values at different speed (Pa)

$\bar{y}$  is the mean of experimental shear stress values

$N$  is the number of data points.

## CHAPTER FOUR

### 4.0

### RESULTS AND DISCUSSION

The results of this research work on modification of rheological and filtration properties of drilling muds with Nigerian lignite were shown in Table 4.1 to 4.4

#### 4.1 Characterizations

Different methods of analysis were employed so as to ascertain and examine the potentials of the raw materials involved for formulation and modification of rheological and filtration properties analysis carried out in this work.

##### 4.1.1 Physicochemical analyses of nano lignite coal

Deeper Analyses: The information gathered during the final analysis was used to determine the coal grade using elemental criteria (such as carbon, hydrogen, sulphur, oxygen, and nitrogen). According to Table 4.1A, the coal sample has a high carbon content of about 90%, followed by hydrogen content of 8.38 % and lower trace of sulphur, oxygen, and nitrogen content of 0.79 %, 0.67 %, and 0.16 %, respectively. During thermal conversion, the carbon and hydrogen content of coals impacts its maturity (rank), chemical reactivity, and heating value.

The nitrogen and sulphur levels of the lignite coal under investigation were determined using this method. According to this research, the nitrogen and sulphur concentrations of the lignite coal under test were extremely low, implying that little or no NO<sub>x</sub> and SO<sub>y</sub> gases will be discharged into the atmosphere during combustion (Bodude *et al.*, 2018).

However, due of the low percentage of sulphur and nitrogen content found in the analysis, this lignite coal will be environmentally and equipment friendly. The primary components of coal combustion are carbon and hydrogen; and these elements (carbon and hydrogen) are more abundant in this lignite coal when compared to other elements such as sulphur,

oxygen, and nitrogen. Coal's categorization and kind were defined by the quantity of carbon in it, which ranged from lignite to anthracite.

**Table 4.1A:** Ultimate Analyses of Lignite Coal

<b>Parameters</b>	<b>Values (%)</b>
Carbon	90.00
Hydrogen	8.38
Sulphur	0.79
Oxygen	0.67
Nitrogen	0.16

However, coal is classified based on its carbon content; the more the content of carbon, the better the heating value and the better the quality of coal. To determine the area of application in which the coal will be used, hydrogen is usually combined with volatile materials. (Solomon and Aliyu, 2013) also determined that, like in the case of this lignite coal in Table 4.1A, a good coal sample should have a high carbon content when compared to the amount of hydrogen, nitrogen, and oxygen.

Because all coals were excavated wet, the moisture content is a useful property of coal. Groundwater and other unneeded moisture, referred to as external derived moisture, are easily freed, whereas moisture stored inside the coal itself is considered inherent moisture and is quantified. Most coals have some moisture in them due to the fact that they were dug up from the earth. The quantity of moisture content in coal determines its maturity (Idris and Ahmed, 2019). Moisture content influences coal grade because it impacts the heating value; the more the moisture content, the lower the heating value, resulting in a loss in coal capacity; the less the moisture content, the better the heating value. For good coking coal, the moisture content of must be at least 1.5 percent (Solomon and Aliyu, 2013). This lignite coal had a moisture content that was very close to the stated number (1.5 percent) for a good coking coal in Table 4.1A, indicating that it is an excellent coking coal that may be used in a variety of applications that require coking coal.

After volatile matter, moisture content, carbon, oxygen, and sulphur have been removed from coal, the ash content shows the size of mineral matter after the process of dry and devolatilization of coal have been removed during combustion; it also indicates the quality of coals. According to the proximate analysis performed, the ash concentration of the coal used in this study is around 1.77 percent (Table 4.1B).

**Table 4.1B:** Proximate Analyses on Coal Sample

<b>Parameters</b>	<b>Values (%)</b>	<b>MJ/kg</b>
Moisture Content	1.45	
Ash Content	1.77	
Volatile Matter	15.48	
Fixed Carbon	81.30	
HHV		16.113

The mutually sufficient supply of disintegrated materials in wetland is normally indicated by high capitulate ash content of coals, while fusing materials regulate coals with low capitulation ash content, whereas with increased ash capitulate, the proportion of disintegrating materials increases and the concentration of organically attached elements diminishes. However, because lignite largely consists of fusing mineralization, moisture, pyrite, and calcite, with organically bound C and S being prevalent, these findings appear to be appropriate for grading coals (Rasheed *et al.*, 2015).

This finding supports the hypothesis that some coals with low capitulate ash levels (less than 10% ash) contain largely fusing and biogenic inorganic materials, whereas those with greater ash capitulate levels (more than 10% ash) have both disintegrated a lot and fusing inorganic matter (Sahni *et al.*, 2013).

Another property of coal that is liberated in the absence of air is volatile matter; at these temperatures, the moisture content is also entirely liberated. Only the fixed carbon and ash content, which are higher than that temperature, need a higher temperature. A mixture of long and short chain hydrocarbons, aromatic hydrocarbons, and some Sulphur is

referred to as "volatile stuff." A volatile substance having a concentration ranging from 2% to 50%. (Rasheed *et al.*,2015). The volatile matter of the coal sample used in this investigation was estimated to be about 15.48 percent based on proximate analysis (Table 4.1B). Coal with high volatile matter is easily ignited and burns due to the high percentage volatile matter which are flammable composition, coal with high volatile matter is easily ignited, burns easily, and frequently burns with a long smoky fire. High volatile matter of coal indicates low grade coal, whereas low volatile matter content in a coal indicates higher-grade coal (Speight, 2013). The fixed carbon content of coal refers to the carbon that remains after volatile components have been removed.

When the mass of volatiles is subtracted from the original mass of the coal sample, then the fixed carbon is estimated which aids in predicting the quantity of coke that will be created from a coal sample. The fixed carbon contents are obtained from carbon content measured by final analysis because some carbon is freed during devolatilization with the volatiles matters. Coals have a fixed carbon content that ranges from 50 to 98 percent, excluding ash and moisture (Rasheed *et al.*, 2015). However, the carbon content of coal determines its fixed carbon value; utilizing proximate analysis, the fixed carbon of the lignite coal used in this study was calculated to be around 81.30 percent (Table 4.1B). The Calorific Value of this lignite tells how much heat it contains.

The nano lignite coal used in this investigation is compared to prior studies reported in the literature in Table 4.1C. High carbon and hydrogen content are observed in the current study as compared to previous research; the more the carbon content, the better the quality of coal. Meanwhile, when compared to the current work, the prior work has a higher oxygen and nitrogen content, indicating that the low nitrogen and sulphur content of the researched micro lignite coal will cause little or no environmental and equipment harm when used to modify drilling muds.

**Table 4.1C:** Comparative Ultimate Analyses Between this and previous work

Parameters	Carbon (%)	Hydrogen (%)	Sulphur (%)	Oxygen (%)	Nitrogen (%)
W	90.00	8.38	0.79	0.67	0.16
X	70.42	5.42	0.88	10.48	1.09
Y	68.24	6.48	0.97	10.43	1.67
Z	60.21	5.89	0.58	9.46	1.07

W (present study); X, Y and Z-(Idris and Ahmed., 2019)

**Table 4.1D:** Comparative Proximate Analysis between this and previous works

Parameters	Moisture Content (%)	Ash Content (%)	Volatile Matter (%)	Fixed Carbon (%)	HHV (MJ/kg)
X	1.45	1.78	15.84	81.30	16.113
Y	12.78	19.83	41.24	26.15	16.02

X (present study) and Y-(Mehran *et al.*, 2015).

Table 4.1D shows the comparisons between this work and other published work. The HHV, on the other hand, were similar; the previous experiment contained more volatile materials, ash, and moisture than the current study.

#### 4.1.2 Thermogravimetric analyses of nano lignite coal

Figures 4.1B and 4.1C demonstrate the TG and DTA decomposition curves of lignite nanoparticles generated from locally supplied lignite coal from Ogwashi Azagba in nitrogen environment, as determined at a heating rate of 10.00 °C /min.

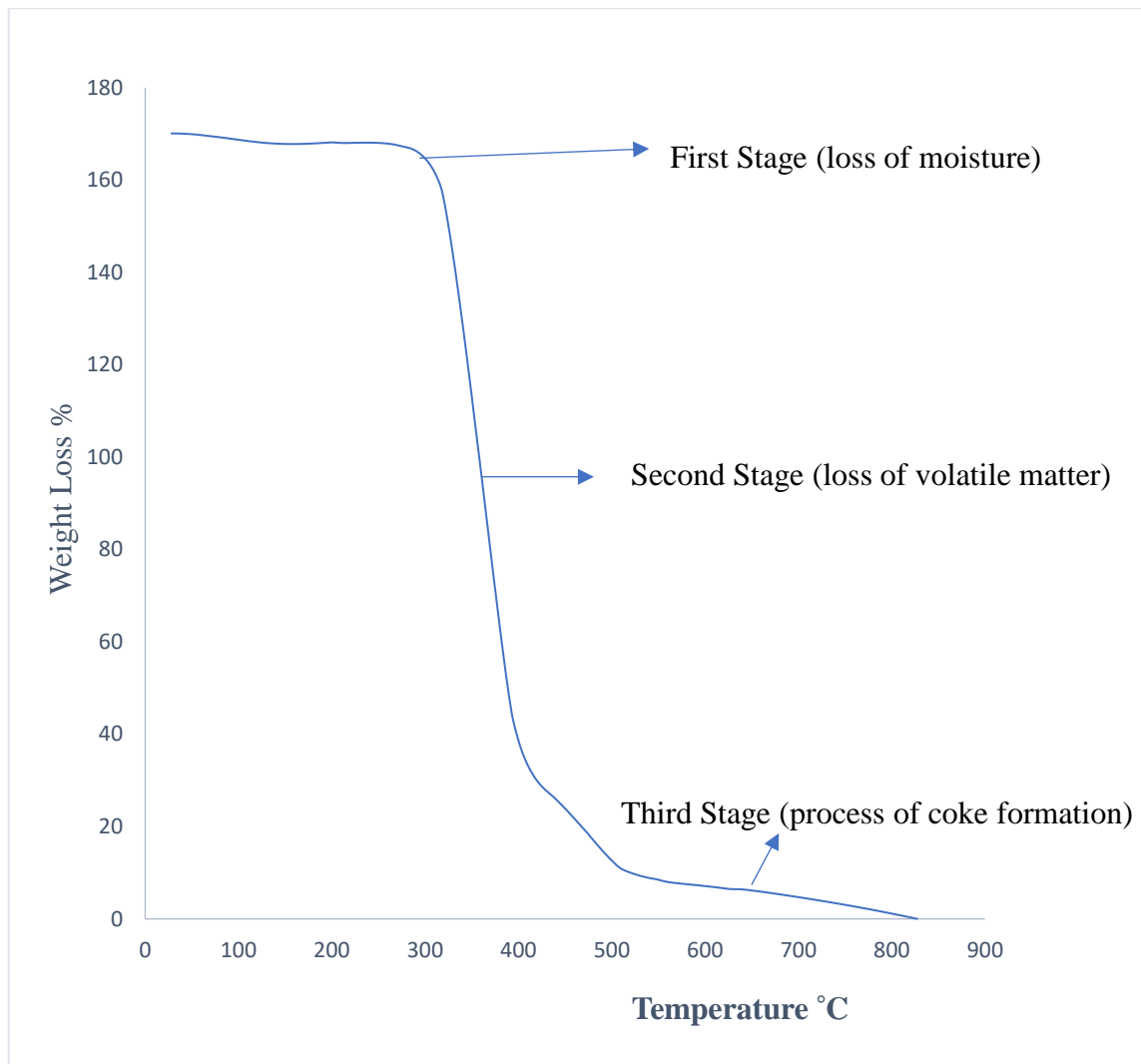


**Figure 4.1A:** TGA Properties of Lignite Coal

The TG curve depicts a coal sample's percent weight loss over a temperature range of 27.00 °C to 950 °C. Temperature has an effect on weight loss: the higher the temperature, the more weight is shed because the pyrolysis process starts slowly at lower temperatures. The TG curve illustrated in Figure 4.1A included three stages: the first stage, which showed weight loss at temperatures between 27 and 266, was referred to as the drying process or loss of water vapor or moisture. Weight loss was seen in the second stage at temperatures ranging from 266 to 580 degrees Celsius, which was attributed to the loss of the devolatilization process or volatile materials. The last stage showed a temperature range of (580 - 820) °C deterioration, which was attributable to the sluggish coke production process.

Figure 4.1B, shows the DTA curve of a nano lignite coal sample heated at a rate of 10 °C/min. the DTA curve shows two peaks, one for moisture evaporation and the other for primary and secondary breakdown

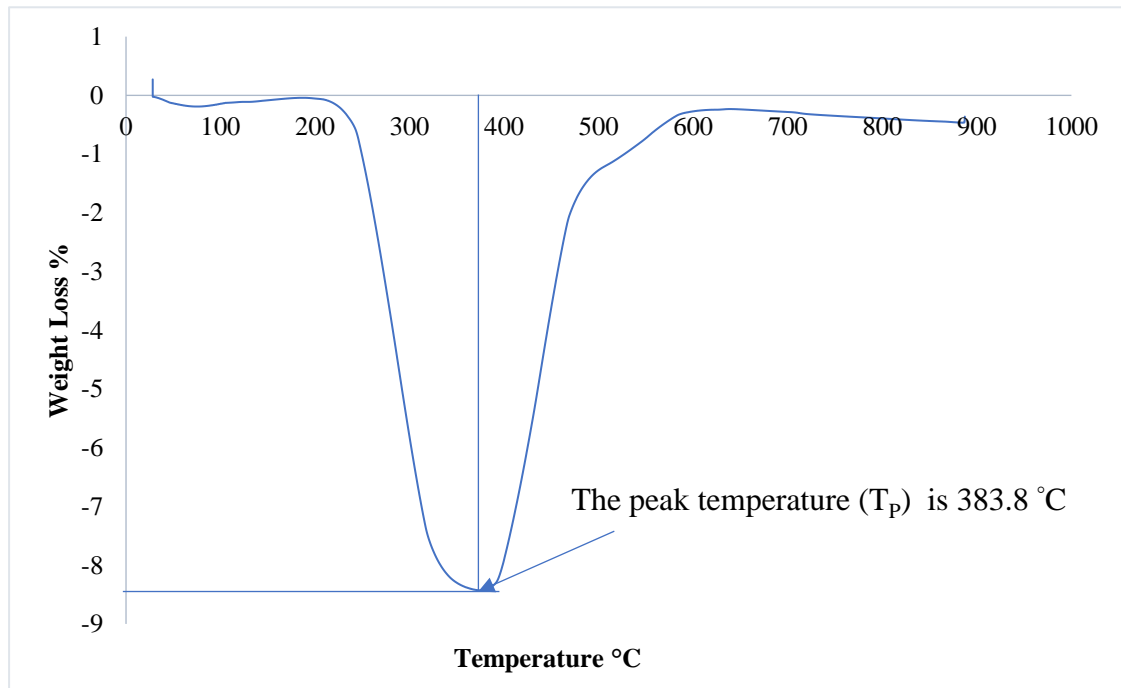


**Figure 4.1B:** DTA Properties of Lignite Coal

The little peak reflects moisture content evaporation, which occurs at temperatures ranging from 30 - 183.92 °C. The second peak in this coal sample was found between 183.92 and 576.02 °C, indicating that a devolatilization process involving the liberation of volatile matter content as well as the thermal breakdown of certain covalent connections, such as ether bonds and the methylene group, will result in the production of gases such as hydrogen, carbon monoxide, and lighter hydrocarbons (Aboyade *et al.*, 2013). The TG curve depicts a coal sample's percent weight loss over a temperature range of 27.00 °C to 950 °C. Temperature has an effect on weight loss: the higher the temperature, the more weight is shed because the pyrolysis process starts slowly at lower temperatures. The second peak in this coal sample was found between 183.92 and 576.02 °C, indicating that a devolatilization process involving the liberation of volatile matter

content as well as the thermal breakdown of certain covalent connections, such as ether bonds and the methylene group, will result in the production of gases such as hydrogen, carbon monoxide, and lighter hydrocarbons.

#### 4.1.3 SEM analysis

The SEM images of nano lignite coal, local and commercial bentonite clay samples in figure 4.1C to 4.1E at of 50,000; magnification shows massive plates like a spherical shape structures with some phase separations which are different surface morphology, a rough surface where big thin plate like set to form big mass with a surface disposition as a result of grain size of the sample observed.

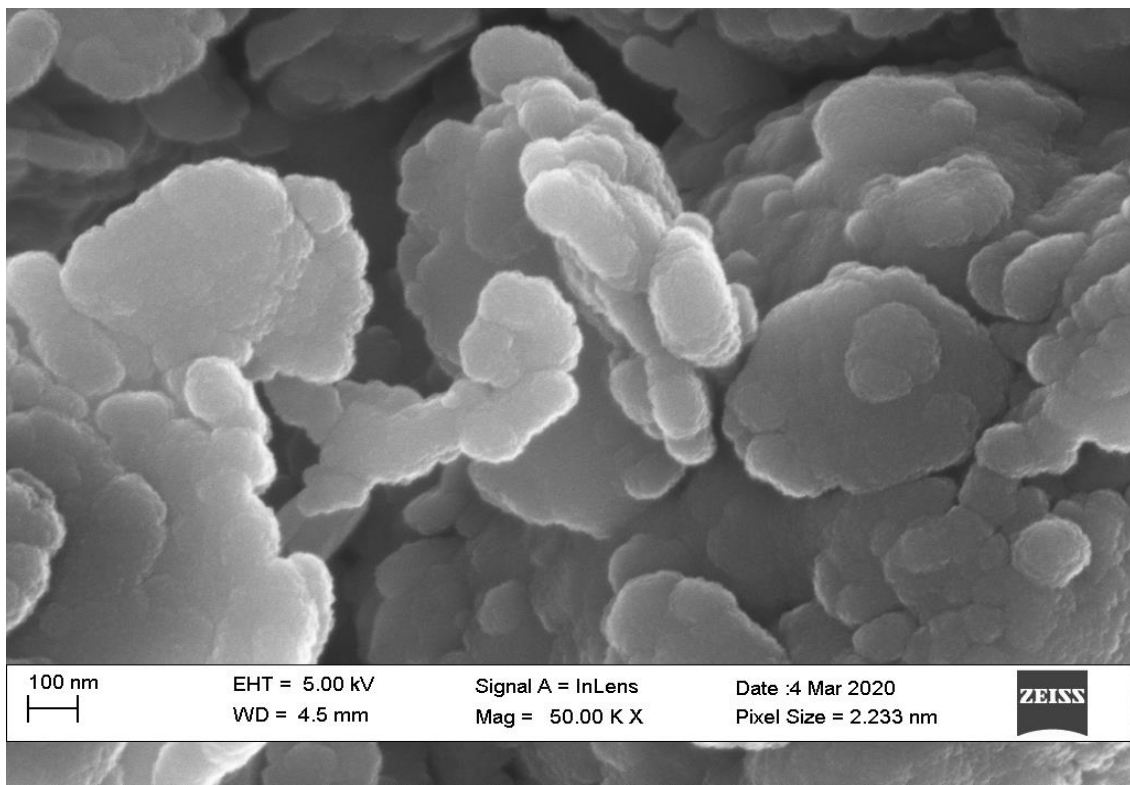


**Figure 4.1C:** SEM Analysis of Nano Lignite Coal.

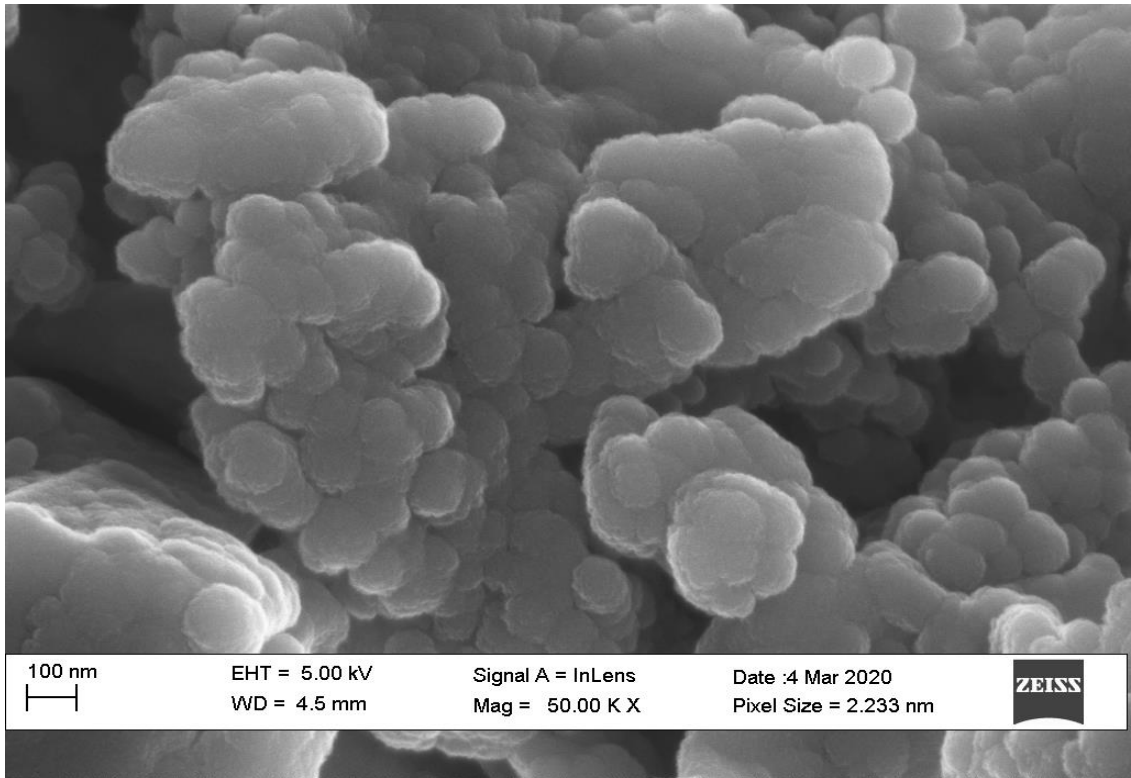


**Figure 4.1D:** SEM Analysis of Local Clay.

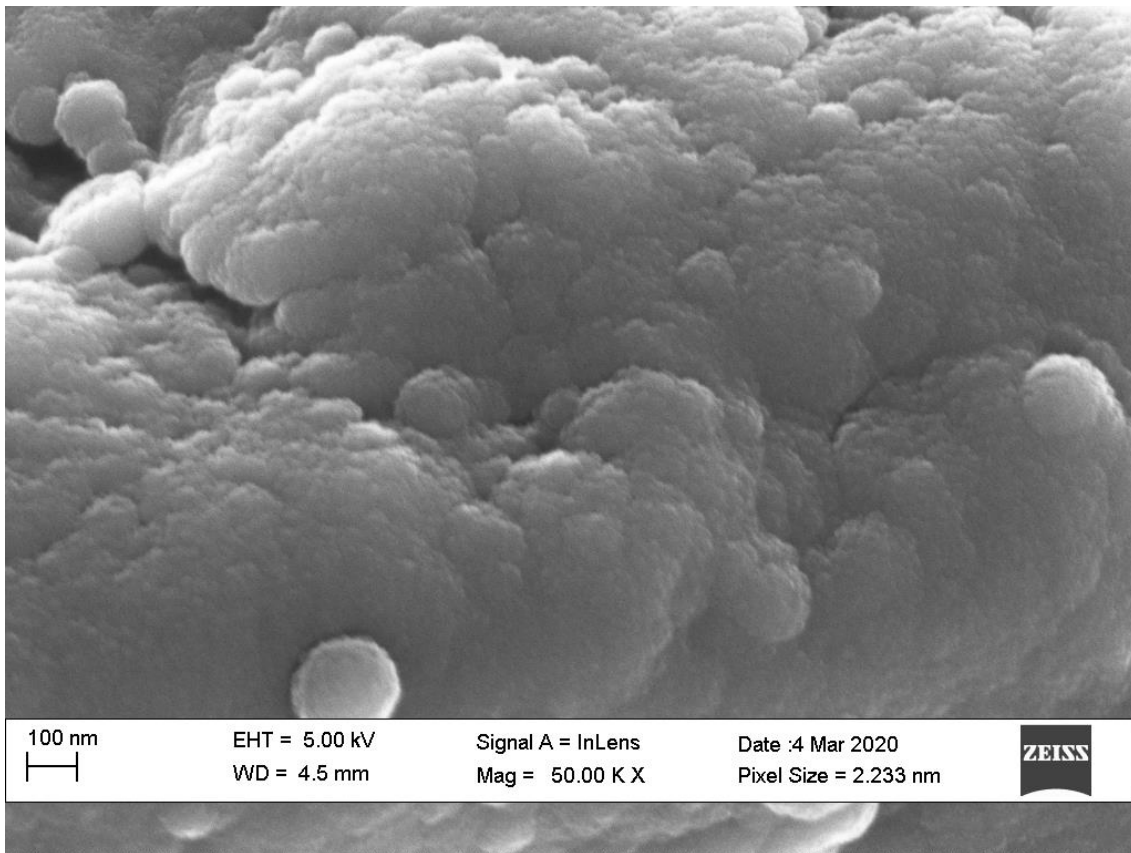


**Figure 4.1E:** SEM Analysis of Commercial Bentonite Clay.

#### 4.1.4 EDX analysis

The EDX analysis was carried out to determine the elemental composition of local clay, commercial bentonite and nano lignite coal samples, this analysis shows that all the samples contain both metals and nonmetal as shown in table 4.1E. The local clay is composed of oxygen (O), silica (Si), aluminum (Al), calcium (Ca) and iron (Fe); with trace of potassium (K), magnesium (Mg), phosphorus (P) and sulphur (S). Theoretically, expected stoichiometric weight percent of the element are 49.03 %, 10.66 %, 6.54 %, 27.64 % and 3.93 %; 0.78 %, 0.79 %, 0.33 % and 0.30 % respectively. The EDX spectra of the local clay in Figure 4.1F also indicated the presence of these element (O, Si, Al, Ca, Fe, K, Mg, P and S). The commercial bentonite is composed of O, Si, Al, Fe and Mg; with trace of Na, K Ti and Ca.

**Table 4.1E:** Elemental Composition of the Local, Commercial Bentonite and Nano Lignite Coal

Element	LOCAL (Wt%)	CLAY COMMERCIAL BENTONITE (Wt%)	NANO LIGNITE COAL (Wt%)
O	49.03	36.12	42.52
Si	10.66	24.7	26.26
P	0.33	0	0
S	0.30	0	6.97
Al	6.54	11.46	14.05
Fe	3.93	23.21	8.03
Ca	27.64	0.18	0.69
K	0.78	0.72	0.51
Mg	0.79	2.29	0
Ti	0	0.53	0.97
Na	0	0.79	0

The expected theoretical stoichiometric weight percent of the element are 36.12 %, 24.7%, 11.46 %, 23.21 % and 2.29 %; 0.79 %, 0.72 %, 0.53 % and 0.18 % respectively.

The EDX spectra of the commercial bentonite in Figure 4.1G also indicated the presence of these element (O, Si, Al, Fe, Mg, Na, K, Ti and Ca). The nano lignite coal is composed of O, Si, Al, Fe and S; with trace of Ti, Ca and K. The expected theoretical stoichiometric weight percent of the element are 42.52 %, 26.26 %, 14.05 % and 6.97 %; 0.97 %, 0.69 %

and 0.51 % respectively. The EDX spectra of the local clay in Figure 4.1H also indicated the presence of these element (O, Si, Al, Fe, S, Ti, Ca and K.). However, the local clay has the biggest content of oxygen and calcium, the commercial bentonite has the biggest content of iron and magnesium while the nano lignite coal has the biggest content of silicon, aluminum and Sulphur.

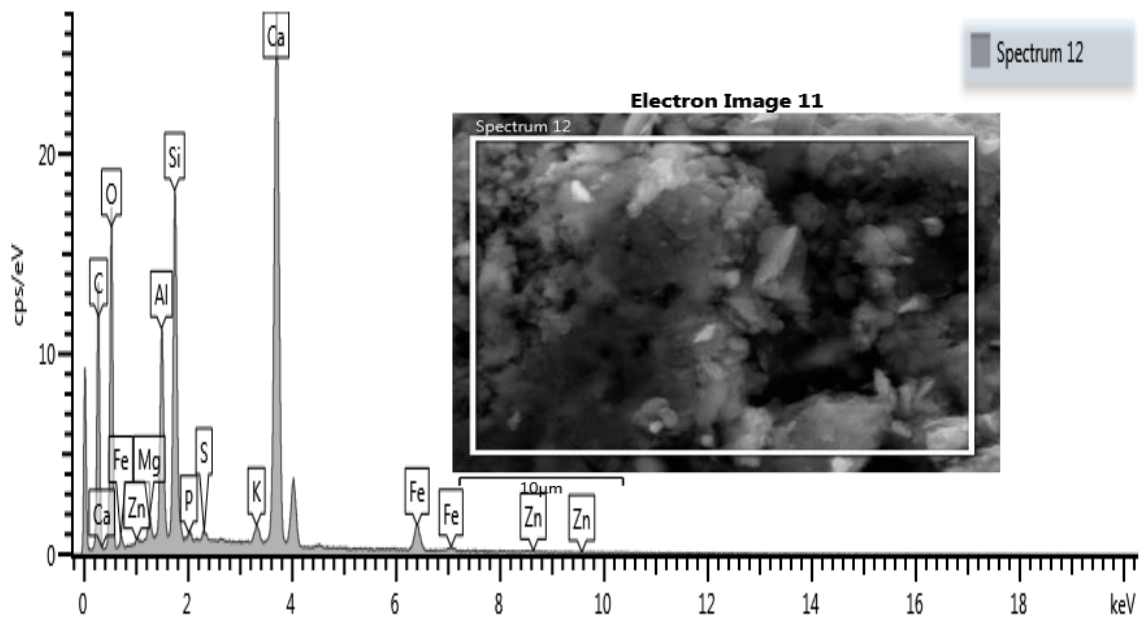


**Figure 4.1F:** EDX Spectra of the Local Clay

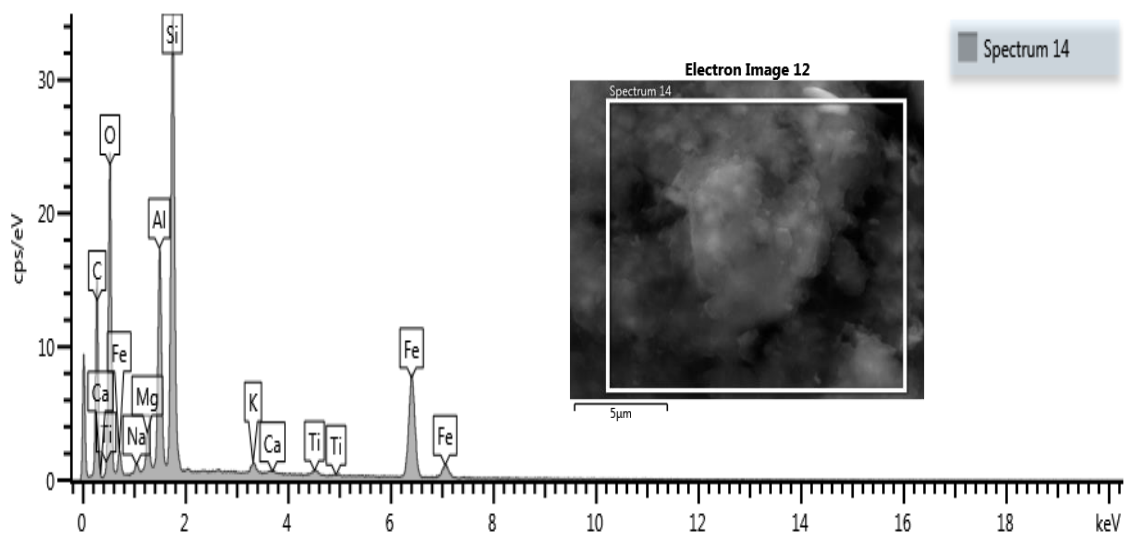


**Figure 4.1G:** EDX Spectra of Commercial Bentonite

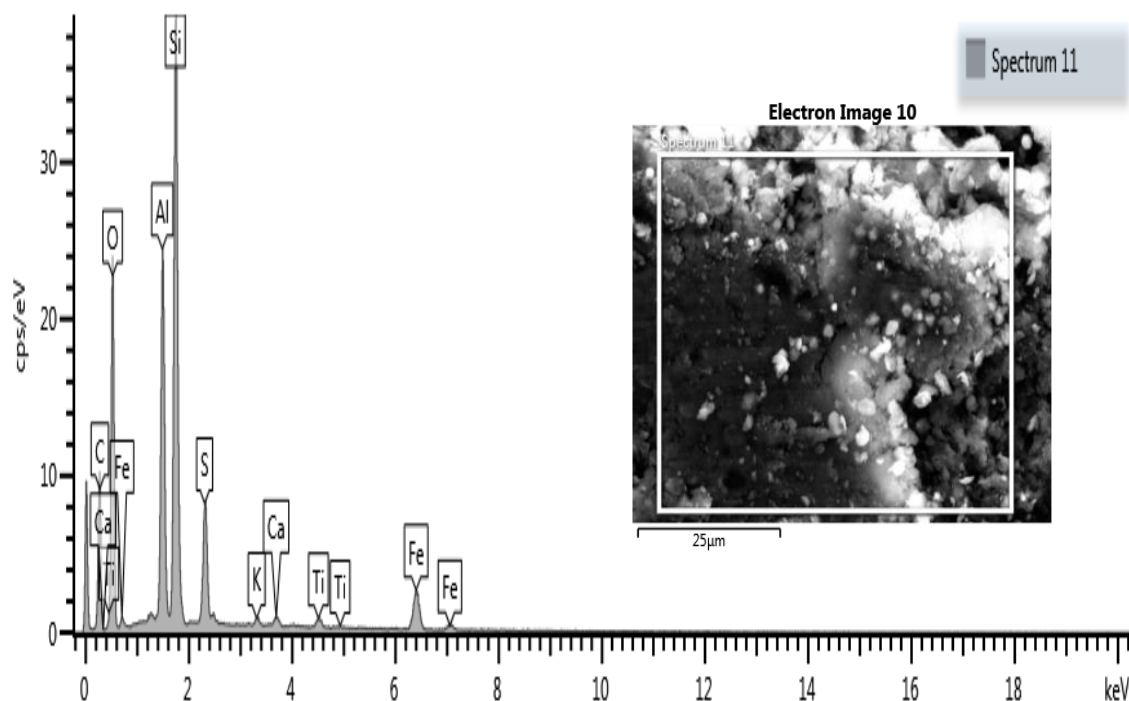


**Figure 4.1H:** EDX Spectra of Nano Lignite Coal

#### 4.1.5 XRD analysis

XRD analysis (Figure 4.1I and 4.1J) was performed to investigate the crystal structure of the nano lignite coal, local and commercial bentonite clay. The XRD patterns of the samples were recorded in the diffraction angle range  $5^{\circ}$  to  $80^{\circ}$ . The sharp and strong diffraction peaks in the XRD patterns of the local clay, commercial bentonite clay and nano lignite coal confirms the crystalline nature of the samples, with sharpest and strongest peak at diffraction angle,  $2\theta$  of  $26.61^{\circ}$  for commercial bentonite clay,  $26.54^{\circ}$  for local clay and  $26.54^{\circ}$  for nano lignite coal. The presence of quartz and mica was due to silicate minerals present in the nano lignite coal, local and commercial bentonite clay, the XRD study confirmed that the major component present in the clay samples were predominantly quartz constituting about 79.35 % and 87.21 % of the particles for commercial bentonite clay and local clay. While for nano lignite coal was also predominantly quartz constituting about 46.75 %.

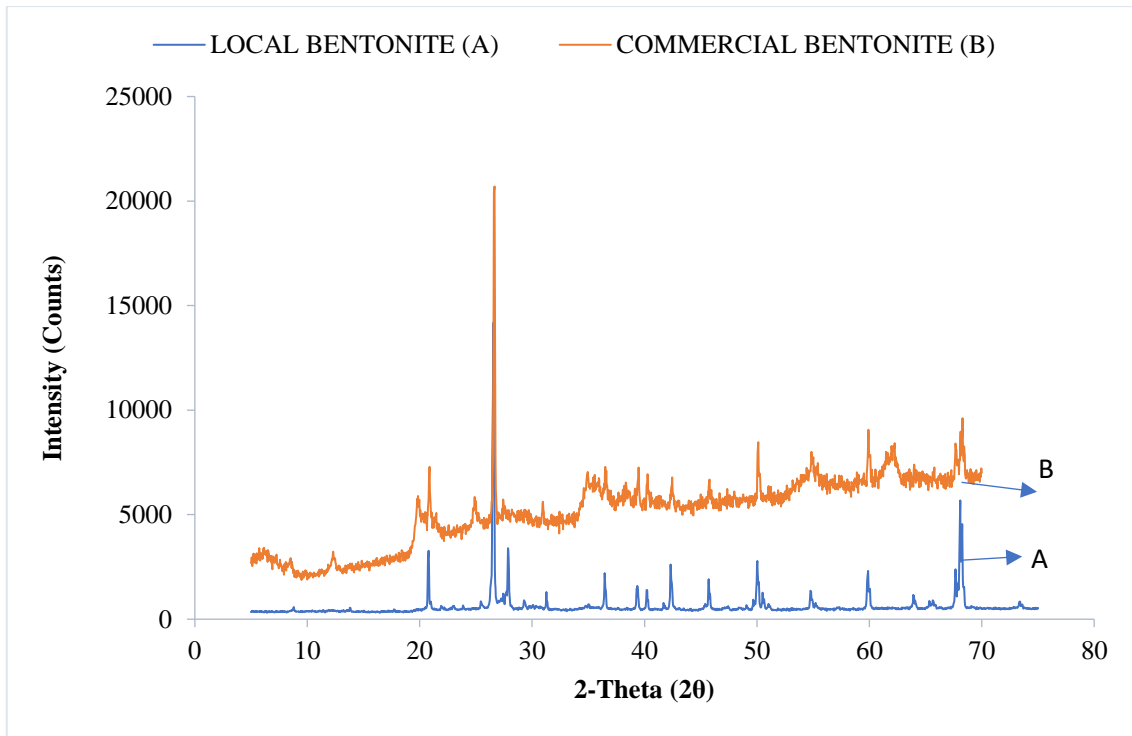


**Figure 4.1I:** XRD Patterns of Local and Commercial Bentonite.

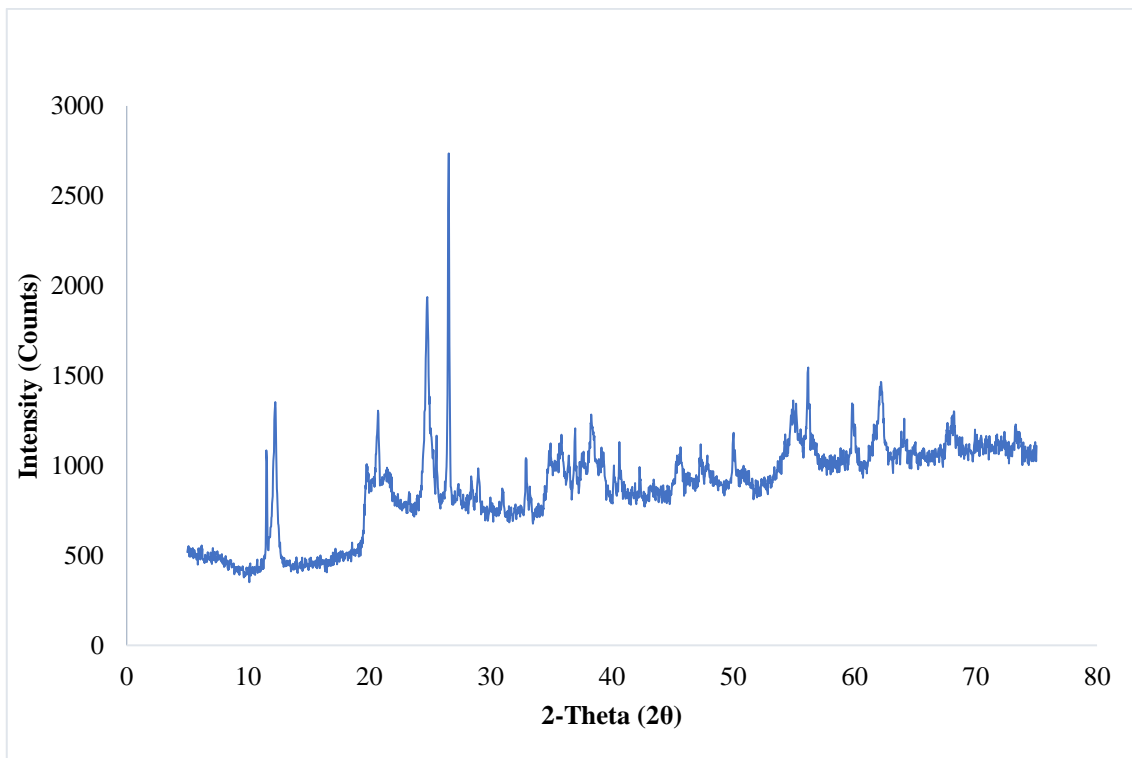


**Figure 4.1J:** XRD Patterns of the Nano Lignite Coal.

#### 4.1.6 FTIR analysis

The FTIR results obtained in this research work for the clays, beneficiated muds and modified muds with 7.5 g of nano lignite coal at different temperatures were compared. The band of strong intensity located at higher frequencies at  $3693\text{ cm}^{-1}$ ,  $3693\text{ cm}^{-1}$  and  $3623\text{ cm}^{-1}$ ,  $3623\text{ cm}^{-1}$  in the FTIR spectra of the local clay and commercial bentonite clay samples in figure 4.1K was attributed to OH groups stretching vibrations in the Si-OH and Al-OH of the tetrahedral and octahedral sheets, and the results showed that the FTIR spectrum for both clay samples were similar.

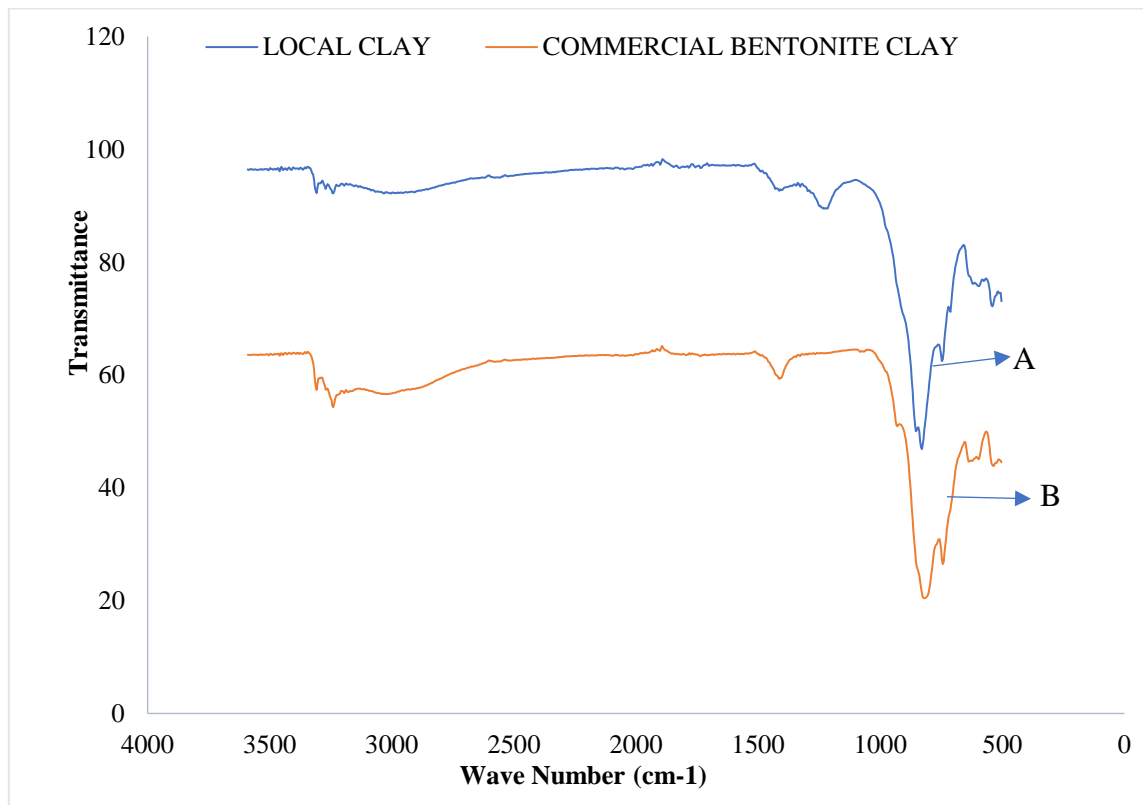


**Figure 4.1K:** FTIR Spectra of Clay Samples.

Aroke *et al.*, (2013) obtained values of  $3698\text{ cm}^{-1}$  and  $3620\text{ cm}^{-1}$ ;  $3693\text{ cm}^{-1}$  and  $3620\text{ cm}^{-1}$ ;  $3698\text{ cm}^{-1}$  and  $3620\text{ cm}^{-1}$ ;  $3693\text{ cm}^{-1}$  and  $3622\text{ cm}^{-1}$  and  $3693\text{ cm}^{-1}$  and  $3622\text{ cm}^{-1}$  for the OH group stretching vibrations in the Si-OH and Al-OH groups, respectively; (Dutta and Singh, 2014); (Bhattacharya and Mandot, 2014). Local and commercial bentonite clay samples of low intensity band located at lower frequencies region produced the

bending vibration mode of adsorbed water at  $1625\text{ cm}^{-1}$  and  $1639\text{ cm}^{-1}$ , which was similar to the values  $1639\text{ cm}^{-1}$ ;  $1630\text{ cm}^{-1}$ ;  $1636\text{ cm}^{-1}$  obtained by Dutta and Singh (2014); Angaji *et al.*, (2013) and Ezquerro *et al.*, (2015), and was attributed to the O-H deformation mode of water. The most intense bands were produced by the stretching mode of Si–O (out-of-plane) and Si–O stretching (in-plane) vibration for octahedral clay at  $1002\text{ cm}^{-1}$  and  $913\text{ cm}^{-1}$ ;  $991\text{ cm}^{-1}$  and  $909\text{ cm}^{-1}$  for local clay and commercial bentonite clay, respectively.

For the beneficiated muds at room temperature, the FTIR spectra of both muds from local clay and commercial bentonite clay samples in figure 4.1L, the band of strong intensity located at higher frequencies at  $3339\text{ cm}^{-1}$  and  $3306\text{ cm}^{-1}$  are assigned to O-H stretching vibrations in the functional group with H-bonded which is broad, this O-H stretching is the band of absorbed inter-water layer.

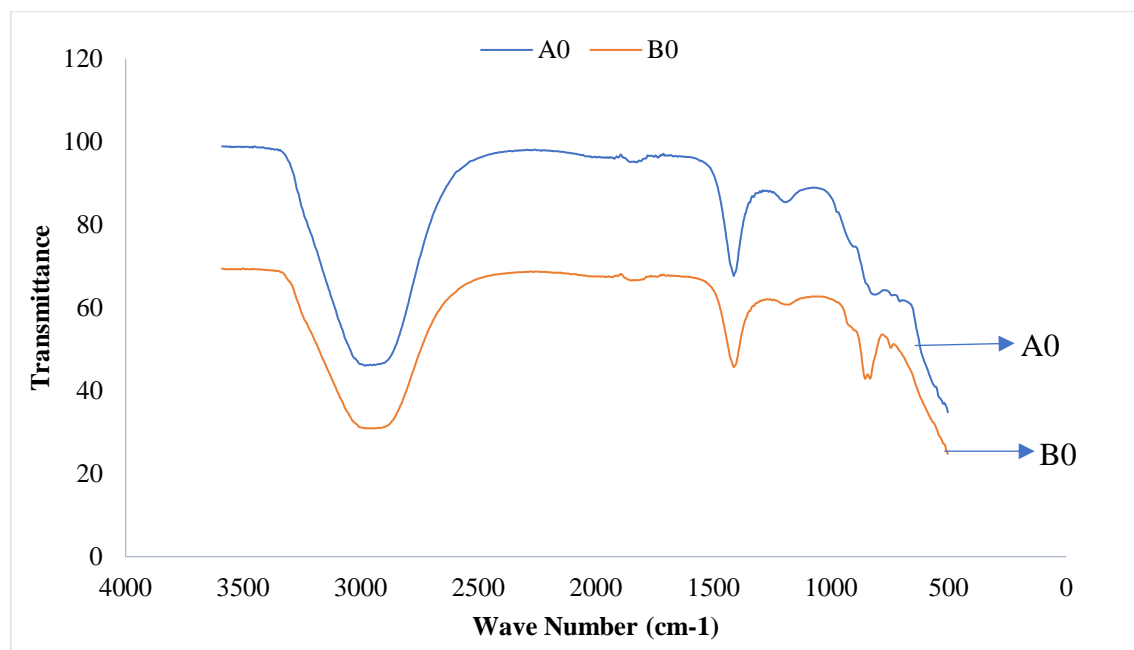


**Figure 4.1L:** FTIR Spectra of Beneficiated Mud Samples

Both muds have the absorption peaks of  $1639\text{ cm}^{-1}$  which was attributed to the O-H deformation mode of water. In the lower frequency region, montmorillonite had a

strong band at  $984\text{ cm}^{-1}$  and  $1028.09\text{ cm}^{-1}$  for Si-O stretching vibration of layered silicates.

For the modified muds with 7.5g of nano lignite coal at room temperature, the FTIR spectra of both muds from local clay and commercial bentonite clay samples showed that the presence of absorption bands at  $3697\text{ cm}^{-1}$  and  $3339.5\text{ cm}^{-1}$ ;  $3693.8\text{ cm}^{-1}$  and  $3339.7\text{ cm}^{-1}$  which can be assigned to the asymmetric and symmetric stretching of structural hydroxyl groups, respectively.

An absorption band at  $1638\text{ cm}^{-1}$ , assigned to the angular vibration of the OH group and related to region  $1002.7$ ;  $1028.7\text{ cm}^{-1}$  and  $1006.4\text{ cm}^{-1}$ , assigned to the Si-O bond, the bands at  $909.7\text{ cm}^{-1}$  for both muds were assigned to the stretching mode of Si-O vibration for octahedral sheet.

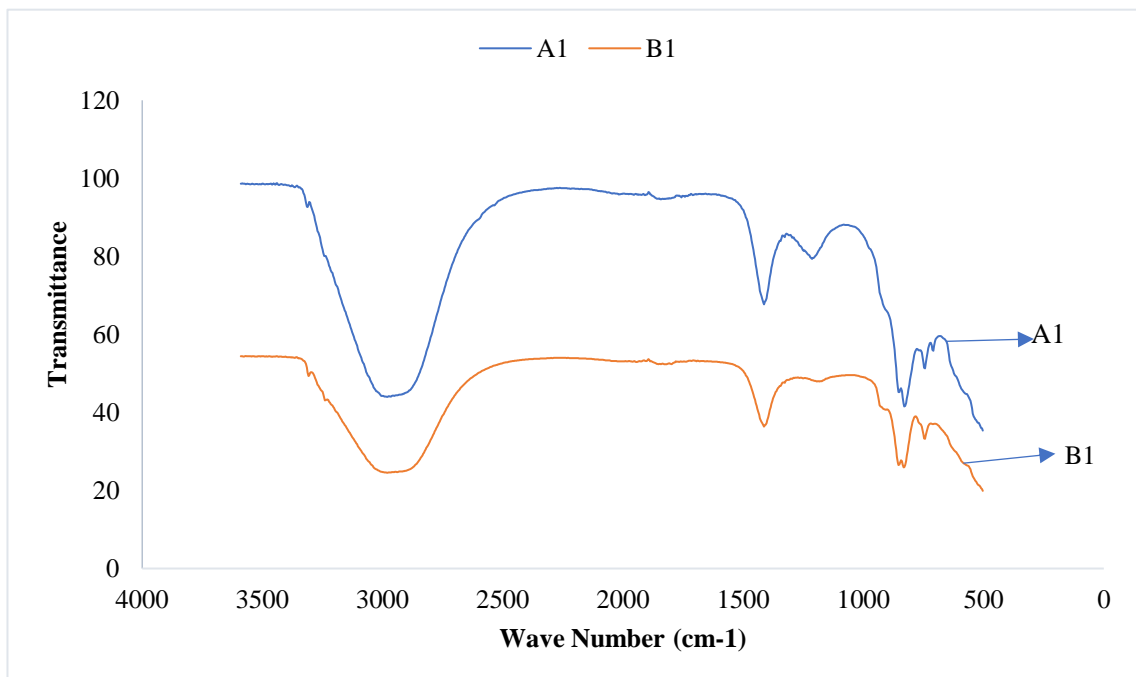


**Figure 4.1M:** FTIR Spectra of Modified Mud Samples Aged at Room Temperature

The characteristic absorption of local clay and commercial bentonite clay can be observed for the modified muds with 7.5g of nano lignite coal at 100 °C temperature, from figure 4.1M, the FTIR spectra of both muds from local clay and commercial bentonite clay samples showed that the presence of absorption bands at 3291.2 cm<sup>-1</sup> and 3336.0 cm<sup>-1</sup> can be assigned to the symmetric stretching of structural hydroxyl groups, both muds have the absorption peaks of 1636.3 cm<sup>-1</sup> which was attributed to the O-H deformation mode of water,

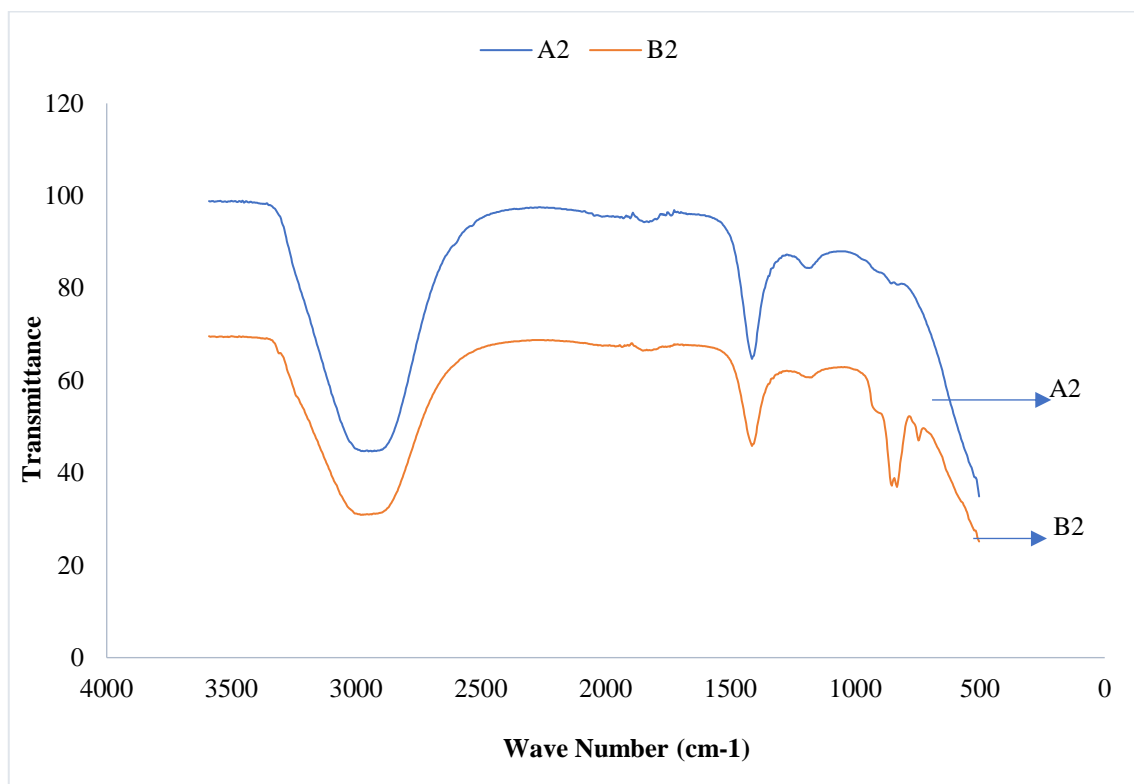


**Figure 4.1N:** FTIR Spectra of Modified Mud Samples Aged at 100 °C Temperature

But mud from commercial bentonite clay have characteristic absorption in the region 1028.7 cm<sup>-1</sup> which is assigned to the Si-O bond and the bands at 913.2 cm<sup>-1</sup> assigned to the stretching mode of Si-O vibration for octahedral sheet.

For the modified muds with 7.5g of nano lignite coal at 100 °C temperature, from figure 4.1N, the FTIR spectra of both muds from local clay and commercial bentonite clay samples showed that the presence of absorption bands at 3306.1 cm<sup>-1</sup> and 3339.7 cm<sup>-1</sup>

can be assigned to the symmetric stretching of structural hydroxyl groups, an absorption band at  $1638\text{cm}^{-1}$ , assigned to the angular vibration of the OH group.

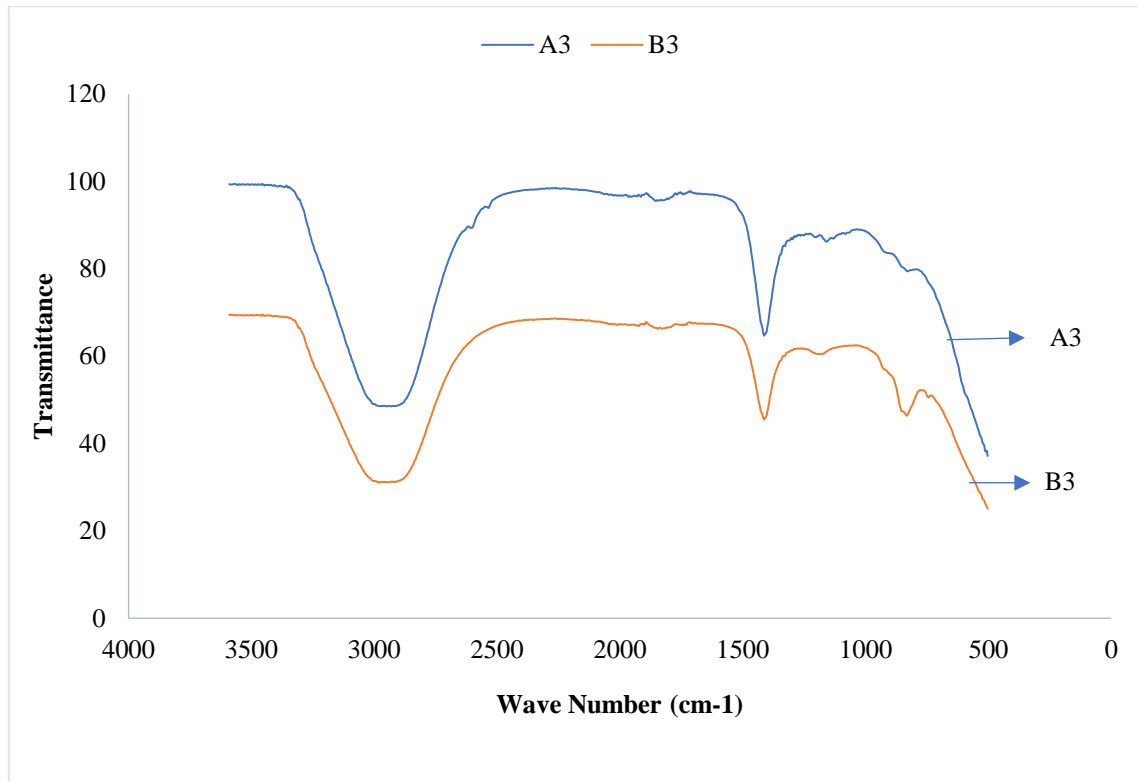


**Figure 4.10:** FTIR Spectra of Modified Mud Samples Aged at 160 °C Temperature

Characteristic absorption of local clay and commercial bentonite clay can be observed in the region  $1002.7$ ; and  $1006.4\text{ cm}^{-1}$ , assigned to the Si-O bond.

The results showed that the FTIR spectrum for the clays sample did not correspond with beneficiated muds and modified muds the, which be as a result of presence of excess free silica that serves as impurities in the raw sample since it has not been beneficiated. However, the effect of temperature on the samples was also observed as modified muds aged at elevated temperatures were not similar with mud modified at room temperature.

## 4.2 Rheological and Filtration Properties Analyses

Drilling mud properties were either directly or indirectly related to most challenges encountered during drilling operation, because a slight change in the drilling mud properties can cause unpredictable problems. Meanwhile, in this research work, the

modification of rheological and filtration properties of drilling muds with Nigerian lignite nanoparticles were carried out using different concentrations of lignite nanoparticles at different temperatures. Muds samples were prepared with varying concentration of Nigerian lignite nanoparticles, examined and compared at varying temperatures.

The properties of rheology and filtration of Spud muds formulated with both local bentonite (A) and commercial bentonite (B) at Ambient Temperature are shown in table 4.2A. From table 4.2A, both the local and commercial bentonite used for mud preparation, indicated the need for beneficiation as a result of substandard values of rheological and filtration properties of the mud samples obtained. However, this is likely due to the calcium-based nature of both bentonites, which causes their low performance potential (Okorie *et al.*, 2016).

**Table 4.2A:** Rheological and Filtration Properties of Spud Muds at Ambient Temperature.

Sample	A	B
θ600 (cP)	3.0	10.0
θ300 (cP)	2.0	5.0
PV (cP)	1.0	5.0
AV (cP)	1.5	0
YP(Ib/100ft <sup>2</sup> )	1	5.0
10 sec. Gel (Ib/100ft <sup>2</sup> )	0	0
10 min. Gel (Ib/100ft <sup>2</sup> )	0	0
Fluid loss (mL)	248.0	20.0
Cake thickness (mm)	0.1	0.2
Density (ppg)	8.3	8.45
pH	8.0	9.0

For sample A, the rheological and filtration properties such as plastic viscosity, apparent viscosity, yield point, fluid loss, and filter cake were 1.0 cP, 1.5 cP, 1.0 Ib/100ft<sup>2</sup>, 248 mL and 0.1 mm respectively. While sample B, the rheological and filtration properties such as plastic viscosity, apparent viscosity, yield point, fluid loss, and filter cake were 5.0 cP, 0 cP, 5.0 Ib/100ft<sup>2</sup>, 20.0 mL and 0.2 mm respectively. These parameters for both clays were below the API required standard for drilling mud (Okorie *et al.*, 2016). As a result

of substandard values of the plastic viscosity, apparent viscosity, yield point and gel strengths of the mud samples, these will result to difficulties of transporting cuttings to surface through annulus, suspending of rock cuttings, cleaning the rock formation for rock cuttings, while the low quality of filter cakes causes excess fluid loss on the well bore thereby result to shale swelling causing instability of the well, pipe sticking, low penetration rate, loss of circulation and easy damage of the reservoir during drilling operations of shale formation (Toka and Toka, 2015). Table 4.2A shows that there was significant difference in the rheological, filtration and physical properties of the formulated drilling muds from both local and commercial bentonites when compared.

Table 4.2B shows the results obtained for beneficiated drilling muds samples rheological and filtration properties formulated from both the local and commercial bentonites at room temperature, the results obtained indicated drastic improvement of rheological and filtration properties which were up to required standard in the drilling operations. After the beneficiation process, there is an indication that the beneficiation process increases the performance of both bentonites as a result of the increased in sodium content of both bentonites (Okorie *et al.*, 2016). However, the need for this beneficiation process is to enhance the performance of rheological and filtration properties of drilling muds from clays which were in calcium-based nature to sodium-based nature by increasing sodium content and swelling tendency of clays with the aid of chemical additives as a viscosifier. This drastic improvement of rheological and filtration properties of both clays were as a result of introduction of polyanionic cellulose which was used as a viscosifier and soda ash ( $\text{Na}_2\text{CO}_3$ ), the soda ash ( $\text{Na}_2\text{CO}_3$ ) improved the properties of both clays as some of the sodium cations ( $\text{Na}^{++}$ ) occupied the surface area and increased the swelling tendency of the bentonites. Thus, the higher the concentration of sodium ion, the more the attraction

between bentonites and water increased during the beneficiation process (Francis and Okon, 2012).

**Table 4.2B:** Rheological and Filtration Properties of Beneficiated Muds at Room Temperature.

Sample	A	B
θ600 (cP)	145	112
θ300 (cP)	112	84
PV (cP)	33	28
AV (cP)	72.5	56
YP (Ib/100 ft <sup>2</sup> )	79	56
10 sec. Gel (Ib/100 ft <sup>2</sup> )	7	6
10 min. Gel (Ib/100 ft <sup>2</sup> )	10	9
Fluid loss (mL)	12.4	14.2
Cake thickness (mm)	0.35	0.45
Density (ppg)	8.3	8.2
pH	11.0	12.0

Also, introduction of chemical additives into the clays influence the particles shape, size distribution of particles and the filter cake compressibility of the drilling muds filtration properties by causing flocculation resulting to random positions and forming different clay associations with each other, these randomly arrangement of various particles formed an effective seal when they are being compressed by pressure during filtration (Omole *et al.*, 2013).

From Table 4.2B, for sample A, the plastic viscosity, apparent viscosity, yield point, gel strength (10 sec./10 min.), fluid loss, and filter cake were 33.0 cP, 72.5 cP, 79.0 Ib/100ft<sup>2</sup>, (7 and 10) Ib/100ft<sup>2</sup>, 12.4 mL and 0.35 mm respectively. While sample B, the plastic viscosity, apparent viscosity, yield point, gel strength (10 sec./10 min.), fluid loss, and filter cake were 28.0 cP, 56.0 cP, 56.0 Ib/100ft<sup>2</sup>, (6 and 9) Ib/100ft<sup>2</sup>, 14.2 mL and 0.45 mm respectively. Interestingly the beneficiated muds rheological and filtration properties: plastic viscosities, apparent viscosities, yield point, gel strength (10 sec./10 min.), fluid loss and cake thickness were more satisfactory to the API standard test for mud parameters as summarized in Table 4.2B. However, it can be deduced, that the beneficiation process has enhanced the performance of rheological and filtration

properties of both drilling muds to overcome shale swelling and improve stability of the well, reduced pipe sticking and loss of circulation, improve penetration rate for drilling operation of shale formation and deep well.

Table 4.2C shows the results of rheological and filtration properties of modified drilling muds samples formulated with both the local and commercial bentonite clay with different concentration of nano lignite coal at room temperature, the results obtained also indicated drastic improvement of rheological and filtration properties which were up to required standard in the drilling operations just as seen in Table 4.2B. However, the results obtained show that the muds containing Nigerian nano lignite coal have higher rheological and filtration properties, indicating that Nigerian lignite have the trace of viscosifier and fluid loss control potentials for drilling muds.

**Table 4.2C:** Rheological and Filtration Properties of Modified Mud with Different Nano Lignite Coal Concentration at Room Temperature for 24 hours.

Sample	A1	A2	A3	B1	B2	B3
θ600 (cP)	160	170	175	160	173	176
θ300 (cP)	120	131	135	123	133	139
PV (cP)	40	39	40	37	40	37
AV (cP)	80	85	87.5	80	86.5	88
YP (Ib/100 ft <sup>2</sup> )	80	92	95	86	93	102
10 sec. Gel (Ib/100 ft <sup>2</sup> )	6	9	9	12	20	24
10 min. Gel (Ib/100 ft <sup>2</sup> )	6	10	10	15	24	25
Fluid loss (mL)	9.6	9.4	9.2	9.2	10	10
Cake thickness (mm)	0.8	0.4	0.5	0.4	0.9	0.6
Density (ppg)	8.4	8.3	8.3	8.2	8.2	8.2
pH	12.0	12.0	12.0	13	13	13

Generally, drilling mud with high Plastic Viscosity is difficult to pump, as such may require high hydrostatic pressure which is therefore not economically favorable for drilling operations. As a result, mud with a lower viscosity has a lower hydrostatic pressure, which isn't always a desirable performance. meanwhile, a drilling mud should

have a proper viscosity to streamline the hydrostatic pressure thereby, improve safety and economically drilling operations, all the conditions of operation of the well and the required properties of the mud should be considered (Piroozian, *et al.*, 2012). The plastic viscosity of local bentonite (based mud) was estimated to be 33 cP. The plastic viscosity of both muds was typically raised by the addition of Nigerian micro lignite coal, which was calculated to be 28 cP as reported in Table 4.2B. Meanwhile, the quantity of plastic viscosity in each form of mud was different at different concentrations of Nigerian nano lignite coal (from 10 to 30 wt percent). For sample A, the amount of local clay mud plastic viscosity increased to 40 cP by adding 10 wt% Nigerian nano lignite coal, 39 cP by adding 20 wt% Nigerian nano lignite coal and at the addition of 30 wt% Nigerian nano lignite coal, the plastic viscosity increased to 40 cP. For sample B, the amount of commercial bentonite clay mud plastic viscosity increased to 37cP by adding 10 wt% Nigerian nano lignite coal, 40 cP by adding 20 wt% Nigerian nano lignite coal and upon 30 wt% addition of Nigerian nano lignite coal, the plastic viscosity was observed to be 37 cP. But it was observed that at 10 wt% addition of Nigerian nano lignite coal, the sample A, have a plastic viscosity of 40 cP while sample B have a plastic viscosity of 37 cP., at 20 wt% addition of Nigerian nano lignite coal, the sample A, have a plastic viscosity of 39 cP while sample B, have a plastic viscosity of 40 cP., and at 30 wt % addition of Nigerian nano lignite coal, the sample A, have a plastic viscosity of 40 cP while sample B, have a Plastic Viscosity of 37 cP. as shown in Table 4.2C. The addition of Nigerian nano lignite nano coal enhanced the plastic viscosity of both muds. The apparent viscosity of both muds were 72.5 cP and 56 cP as summarized in Table 4.2B while in the Table 4.2C the amount of apparent viscosity for the two type of muds at different concentrations (from 10 to 30 wt%) of Nigerian nano lignite coal were different, but increases as the concentration of Nigerian lignite nano-particles increases, for sample A, apparent

viscosity were 80 cP, 85 cP and 87.5 cP respectively while sample B, apparent viscosity were 80 cP, 86.5 cP and 88 cP respectively. The yield point is also a barrier to fluid flow induced by electrochemical forces inside the fluid, which are caused by electrical charges on the surfaces of particles in the fluid. High yield point values help the drilling cuttings faster and transported toward the ground surface (Naoh *et al.*, 2017). The yield point must be high enough to convey cuttings out of the hole, but not so high that it causes excessive pump pressure when mud flow begins (Agarwal *et al.*, 2011). The yield points of both muds were calculated to be 79 lb/100ft<sup>2</sup> and 56 lb/100ft<sup>2</sup>, respectively, according to Table 4.2B. In Table 4.2C, the yield point of both muds exhibits varied performances at varying concentrations of Nigerian lignite nano-particles (from 10 to 30 wt percent). For sample A, the yield point of the mud increases as the amount of Nigerian nano lignite coal increases. The maximum value of yield point for mud sample A was 95 lb/100ft<sup>2</sup> at a concentration of 30 wt % of Nigerian lignite nano-particles while minimum value of yield point for mud sample A was 80 lb/100ft<sup>2</sup> at a concentration of 10 wt % of Nigerian nano lignite coal. For sample B the yield point of the mud also increases as the amount of Nigerian lignite nano-particles increases and the maximum value of yield point for mud sample B was 106 lb/100ft<sup>2</sup> at a concentration of 30 wt % of Nigerian nano lignite coal while minimum value of yield point for mud sample B was 86 lb/100ft<sup>2</sup> at a concentration of 10 wt% of Nigerian lignite nano-particles. Surprisingly, both mud samples have an increasing tendency at all concentrations tested.

One of the most essential drilling mud features is gel strength, which refers to a drilling mud's capacity to suspend drilling fluid. (Toka and Toka, 2015) The gel strength is a measurement of electrochemical forces within a fluid when it is in a static state (Naoh *et al.*, 2017). The initial gel strength measurements for both muds show that the gel strength values for 10 s and 10 min for mud sample A were 7 lb/100ft<sup>2</sup> and 10 lb/100ft<sup>2</sup> for mud

sample A, respectively and 6 lb/100ft<sup>2</sup> and 9 lb/100ft<sup>2</sup> for mud sample B respectively as shown in Table 4.2B, The gel strength values for both tests (10 s and 10 min) for mud sample A were the same. 6 lb/100ft<sup>2</sup> at the addition of 10 wt% concentration of Nigerian nano lignite coal and upon addition of 20 wt% concentration of Nigerian nano lignite coal to mud sample A, the gel strength was 9 lb/100ft<sup>2</sup> for both tests (10 s and 10 min). and 10 lb/100ft<sup>2</sup> while upon addition of 30 wt% concentration of Nigerian nano lignite coal to mud sample A, the gel strength for both tests (10 s and 10 min) were also 9 lb/100ft<sup>2</sup> and 10 lb/100ft<sup>2</sup>. In mud sample A, there was a similar trend in gel strength values at concentrations of Nigerian nano lignite coal of 20 wt percent and 30 wt percent. However, considering mud sample B, the values of gel strength for both tests (10 s and 10 min) were 12 lb/100ft<sup>2</sup> and 15 lb/100ft<sup>2</sup> When 10 wt percent Nigerian nano lignite coal was added to mud sample B, the gel strength for both tests (10 s and 10 min) was 20 lb/100ft<sup>2</sup> and 24 lb/100ft<sup>2</sup>, respectively, while when 30 wt percent Nigerian nano lignite coal was added to mud sample B, the gel strength for both tests (10 s and 10 min) was 30 lb/100ft<sup>2</sup>. In mud sample B, there was an increasing trend in gel strength values at concentrations of Nigerian micro lignite coal ranging from 10 wt percent to 30 wt percent, indicating that mud sample B had a stronger suspending potential for drilling mud solids and cuttings. Because of the mud's high gelling qualities, a large beginning torque may be required, which must be justified by looking at the fluid shear thinning behavior. Furthermore, high gel strength isn't required to avoid serious drilling issues (Ghosn *et al.*, 2017).

The ability of solid material in a mud to produce a thinner mud cake with limited permeability is measured by fluid loss. The performance of the components that make up the drilling fluid determines the volume of fluid loss (Jeffrey *et al.*, 2018). In a filtration property test, the volume of fluid loss and mud cake thickness are the two measured

parameters; a large volume of fluid loss is not desired for drilling a well because it may result to formation damage and formation instability problems (Deng *et al.*, 2015).

The result of fluid loss of both muds obtained are shown in Table 4.2B. The amount of fluid loss for both muds after 30 min were 12.4 mL and 14.2 mL respectively. While Table 4.2C shows the results of muds containing different concentrations (from 10 to 30 wt%) of Nigerian nano lignite coal, for sample A, by adding 10 wt% of Nigerian nano lignite coal to sample A, 9.6 mL of fluid loss was obtained, upon the addition of 20 wt% of Nigerian nano lignite coal, 9.4 mL of fluid loss was obtained and upon the addition of 30 wt% of Nigerian nano lignite coal, 9.2 mL of fluid loss was obtained. It was observed that increased in concentrations of Nigerian nano lignite coal in the mud sample A starts to improve the fluid loss volume reduction which shows a reduction trend of fluid loss at all examined concentrations of Nigerian nano lignite coal. For sample B, at 10 wt% of Nigerian nano lignite coal addition, the fluid loss volume was 9.2 mL, upon the addition of 20 wt% of Nigerian nano lignite coal, 10.0 mL of fluid loss volume was obtained and upon the addition of 30 wt% of Nigerian nano lignite coal, 10.0 mL of fluid loss was obtained. It was also observed that increased in concentrations of Nigerian nano lignite coal in the mud sample B improved the fluid loss volume reduction but shows an increasing trend of fluid loss at all examined concentrations of Nigerian nano lignite coal. However, because lignite contains humic acid, which makes it soluble in water, it functions as a clay deflocculant, improving the quality of filter cake by limiting fluid loss into the formation (Jeffrey *et al.*, 2018). Based on the fluid loss results in Tables 4.2B and 4.2C, muds containing Nigerian nano lignite coal can be considered to have good filtration control properties when compared to muds without Nigerian nano lignite coal, and this property is suitable for drilling purposes because it can prevent stuck pipe incidents.

The quality of filter cake is one of the factors that should be considered in drilling operation, and it can be evaluated via slickness, hardness and toughness of mud cake which determines the amount of fluid loss and guarantee the stability of the wellbore during operation (Ali *et al.*, 2018). Table 4.2B shows the results of both muds without Nigerian nano lignite coal, it was observed that both muds have light filter cake thickness and low quality which resulted to high fluid loss. While Table 4.2C shows the results of muds containing different concentrations (from 10 to 30 wt%) of Nigerian nano lignite coal. For mud sample A, the mud with 20 wt% concentration of Nigerian nano lignite coal has the heavy filter cake thickness of 0.8 mm while mud with 30 wt% concentration of Nigerian nano lignite coal has the light filter cake thickness of 0.5 mm. For mud sample B, the mud 20 wt% concentration of Nigerian nano lignite coal has the heavy filter cake thickness of 0.9 mm. while mud with 10 wt% concentration of Nigerian nano lignite coal has the light filter cake thickness of 0.45 mm. However, the presence of Nigerian nano lignite coal in the muds enhanced the muds by forming effective seal for controlling fluid loss.

For sample A, the rheological properties: plastic viscosity, apparent viscosity, and yield point increase by 21.21 percent, 10.34 percent, and 1.27 percent, respectively, the gel strength (10 sec./10 min.) decreases by 14.29 percent and 40.00 percent, and the filtration increases by 14.29 percent and 40.00 percent. The pH of the mud rises by 9.09 percent, respectively. While sample B, the rheological properties: plastic viscosity, apparent viscosity and yield point increase by 32.14 %, 42.86 % and 53.57 %, the gel strength (10 sec./10 min.) increases by 100.00 % and 66 67 %., the filtration properties: fluid loss reduces by 35.21 % and cake thickness remain the same and the mud pH increases by 8,33 % respectively. Meanwhile, the 10 wt% concentration Nigerian lignite nano-particles of 25 g of clay in 350 mL of deionized water, was more effective on mud sample

B than mud sample A. Furthermore, the rheological parameters of sample A, which contained 20 wt percent Nigerian nano lignite coal and 25 g of clay in 350 mL of deionized water, were as follows: plastic viscosity, apparent viscosity and yield point increase by 18.18 %, 17.24 %, 16.46 %, the gel strength (10 sec./10 min.) increases by 28.57 and 0.0 %., the filtration properties: fluid loss reduces by 24.19 % and cake thickness also increases by 128.57 %, the pH increases by 9.09 % respectively. While sample B, the rheological properties: plastic viscosity, apparent viscosity and yield point increase by 42.86 %, 54.46 %, 66.07 %, the gel strength (10 sec./10 min.) increases by 233.33% and 166.67 %., the filtration properties: fluid loss reduces by 29.58 % and cake thickness increases by 100 %, the mud pH increases by 8.33 % just as mud sample B containing 10 % concentration of Nigerian lignite nanoparticles. It was observed that the 20 wt% concentration Nigerian lignite nanoparticles of 25 g of clay in 350 mL of deionized water, was also more effective on mud sample B than mud sample A when compared. In addition, considering the mud samples containing 30 wt% concentration Nigerian lignite nano-particles of 25 g of clay in 350 mL of deionized water, for sample A, the rheological properties: plastic viscosity, apparent viscosity and yield point increase by 21.21 %, 20.69 %, 20.25 %, gel strength (10 sec./10 min.) increases by 28.57 % and 0.0 %., the filtration properties: fluid loss reduces by 25.81 % and cake thickness increases by 42.86 % while the mud pH increases by 9.09 % respectively. While sample B, the rheological properties: plastic viscosity, apparent viscosity and yield point increase by 32.14 %, 57.14 %, 82.14 %, gel strength (10 sec./10 min.) increases by 300 % and 177.78 %., the filtration properties: fluid loss reduces 29.58 % and cake thickness increases by 33.33 %, the mud pH increases by 8.33 % respectively.

The rheological and filtration properties of modified drilling muds with Nigerian nano lignite coal formulated with both local clay and commercial bentonite clay aged at elevated temperatures were shown in Table 4.2D and Table 4.2E below. The drilling muds formulated with local clay was sample A while sample B was drilling mud formulated with commercial bentonite clay. However, each of the mud samples were modified with Nigerian nano lignite coal at different concentration (from 10 to 30 wt%) and aged at different elevated temperatures of 100 °C and 160 °C respectively. Both muds were evaluated, examined and compared based on the concentration at each temperature point of view.

Table 4.2D shows the results obtained for rheological and filtration properties of modified drilling muds with different concentration of Nigerian nano lignite coal (from 10 to 30 wt%) aged at 100 °C. When the mud formulated with both local and bentonite clays were modified using 10 wt% Nigerian nano lignite coal (by total weight of clay in the mud) and aged at 100 °C temperature, the plastic viscosities were 8 cP and 9 cP respectively, when modified using 20 wt% Nigerian nano lignite coal, the plastic viscosities were 8 cP and 11 cP, and using 30 wt% Nigerian nano lignite coal, the plastic viscosities were 9 cP and 11 cP respectively, it was observed that as the concentration of Nigerian nano lignite coal increases, the plastic viscosity of both mud also increases significantly, the mud formulated with bentonite clay have more better plastic viscosities than mud formulated with local clay.

The apparent viscosity for both drilling muds modified using 10 wt% Nigerian nano lignite coal were 18 cP and 20 cP respectively, when both muds were modified using 20 wt% Nigerian nano lignite coal, the apparent viscosity were 20.5 cP and 23 cP, and when both muds were modified using 30 wt% Nigerian nano lignite coal, the apparent viscosity were 22 cP and 24 cP, as the concentration of Nigerian nano lignite coal increases, the

apparent viscosity of both mud also increases proportional, the mud formulated with bentonite clay have more better apparent viscosities than mud formulated with local clay.

**Table 4.2D:** Rheological and Filtration Properties of Modified Muds with Different concentration of Nigerian Nano Lignite Coal Aged at Elevated Temperature (100 °C)

Sample	A <sub>1</sub>	A <sub>2</sub>	A <sub>3</sub>	B <sub>1</sub>	B <sub>2</sub>	B <sub>3</sub>
θ600 (cP)	36	41	44	40	46	48
θ300 (cP)	28	33	35	31	35	37
PV (cP)	8	8	9	9	11	11
AV (cP)	18	20.5	22	20	23	24
YP (Ib/100 ft <sup>2</sup> )	20	25	26	22	24	26
10 sec. Gel (Ib/100 ft <sup>2</sup> )	0	0	0	3	3	4
10 min. Gel (Ib/100 ft <sup>2</sup> )	1	1	1	4	4	6
Fluid loss (mL)	7.6	7.2	6.8	10	9.6	9.2
Cake thickness (mm)	1.3	0.8	0.5	1.0	1.0	0.8
Density (ppg)	8.2	8.2	8.2	8.2	8.2	8.2
pH	12.0	12.0	12.0	13	13	13

The yield point for both drilling muds modified using 10 wt% Nigerian nano lignite coal were 20 Ib/100 ft<sup>2</sup> and 22 Ib/100 ft<sup>2</sup> respectively, when both muds were modified using 20 wt% Nigerian nano lignite coal, the yield point were 25 Ib/100 ft<sup>2</sup> and 24 Ib/100 ft<sup>2</sup> and when both muds were modified using 30 wt% Nigerian lignite nanoparticles, the yield point were 26 Ib/100 ft<sup>2</sup> and 26 Ib/100 ft<sup>2</sup>. As the concentration of Nigerian nano lignite coal increases, the yield point of both muds also increases proportional, with both muds having the highest yield point of 26 Ib/100 ft<sup>2</sup> Upon the addition of 30 wt% Nigerian nano lignite coal for modification as shown in Table 4.2D. The 10 sec Gel strength of mud formulated with local clay were constantly zero while that of bentonite clay increases significantly at different concentration of Nigerian nano lignite coal and also, the 10 min Gel strength have the same trend as shown in Table 4.2D. Based gel strength at 100 °C temperature, bentonite clay shows better potential of suspending rock cutting than local clay.

The fluid loss obtained were 7.6 mL and 10.0 mL, when both drilling muds were modified using 10 wt% Nigerian nano lignite coal, when both muds were modified using 20 wt% Nigerian nano lignite coal, fluid loss obtained were 7.2 mL and 9.6 mL, and when both muds were modified using 30 wt% Nigerian nano lignite coal, fluid loss obtained were 6.8 mL and 9.2 mL respectively. It was observed that, as the concentration of Nigerian nano lignite coal increases, fluid loss of both muds obtained also decreases proportional, the mud formulated with local clay have more better fluid loss than mud formulated with bentonite clay. However, the drilling muds modified with various concentration Nigerian nano lignite coal (from 10 wt% to 30 wt%) with both local clay and commercial bentonite clay aged at 100 °C temperature have exhibited the potential of cleaning rock formation for rock cuttings, transporting these rock cuttings to surface through annulus, cooling the bit during operation, minimizing the fluid loss by forming a fitter cake on the wall of the well bore and reduces the reservoir damage which were primary functions of drilling mud. Based on the aging temperature (100 °C) of both modified drilling muds, from the rheological properties point of view, the drilling muds formulated with commercial bentonite clay, will perform better in rocking cutting and suspending drilling cutting at static conditions during operation than drilling muds formulated with local clay, as a result of their plastic viscosity and gel strength for both test ( 10 sec and 10 min), otherwise, there is no much different in their other rheological property such as yield point, therefore both muds may likely have equal performance in transporting of drill cutting to the ground surface through annulus. Furthermore, from the filtration properties point of view, the drilling muds formulated with local clay have shown better fluid loss reduction and quality filter cake performance by reducing the reservoir damage and minimizing the fluid loss by forming a filter cake on the wall of the well bore than the muds formulated with commercial bentonite clay. It can be deduced that with the modifying additive (Nigerian

nano lignite coal), local clay muds can be used to drill high temperature well of 100 °C, geothermal well and deeper well within 100 °C of operating condition and water-based muds is comparable with oil-based muds because Nigerian nano lignite coal offers thermal resistance to the drilling muds which could be degraded at high temperature of 100 °C.

Table 4.2E summarized the results of rheological and filtration properties of modified drilling muds formulated from both local clay and commercial bentonite clay with different concentration of Nigerian nano lignite coal (from 10 wt% to 30 wt%) aged at 160 °C temperature in a hot roller oven. When the mud formulated with both local and commercial bentonite clays were modified using 10 wt% Nigerian nano lignite coal, the plastic viscosity of both muds were the same as 8 cP, similar results were obtained in the case when both muds were modified using 20 wt% Nigerian lignite nanoparticles and when modified using 30 wt% Nigerian nano lignite coal, the plastic viscosity obtained were 11 cP and 9 cP respectively, it was observed that as the concentration of Nigerian nano lignite coal increases from 10 wt% to 20 wt%, the plastic viscosity of both muds were constant and at 30 wt% of Nigerian lignite nanoparticles in both muds, the plastic viscosity of both muds increases, with the local clay mud having the highest value. The apparent viscosity obtained for both drilling muds, when modified using 10 wt% Nigerian nano lignite coal were 14.5 cP and 18.5 cP respectively, when both muds were modified using 20 wt% Nigerian nano lignite coal, the apparent viscosity obtained were 18 cP and 21 cP, when both muds were modified using 30 wt% Nigerian nano lignite coal, the apparent viscosity obtained were 20 cP and 22.5 cP, as the concentration of Nigerian nano lignite coal increases, the apparent viscosity of both mud also increases proportionally, the mud formulated with commercial bentonite clay have more better apparent viscosity than mud formulated with local clay.

**Table 4.2E:** Rheological and Filtration Properties of Modified Drilling Muds with Various concentration of Nigerian Lignite Aged at Elevated Temperature (160 °C)

Sample	A <sub>1</sub>	A <sub>2</sub>	A <sub>3</sub>	B <sub>1</sub>	B <sub>2</sub>	B <sub>3</sub>
θ600 (cP)	29	36	40	37	42	45
θ300 (cP)	21	28	29	29	34	36
PV (cP)	8	8	11	8	8	9
AV (cP)	14.5	18	20	18.5	21	22.5
YP(Ib/100ft <sup>2</sup> )	13	20	18	21	26	27
10 sec. Gel (Ib/100 ft <sup>2</sup> )	0	2	0	2	2	2
10 min. Gel (Ib/100 ft <sup>2</sup> )	0	2	2	3	3	4
Fluid loss (mL)	10	9.6	9.2	10	9.6	9.2
Cake thickness (mm)	0.7	0.7	0.5	0.9	0.9	0.8
Density (ppg)	8.2	8.2	8.2	8.2	8.2	8.2
pH	12.0	12.0	12.0	13.0	13.0	13.0

The yield point obtained for both drilling muds, when modified using 10 wt% Nigerian nano lignite coal were 13 Ib/100ft<sup>2</sup> and 21 Ib/100ft<sup>2</sup> respectively, when both muds were modified using 20 wt% Nigerian nano lignite coal, the yield point obtained were 20 Ib/100ft<sup>2</sup> and 26 Ib/100ft<sup>2</sup>., and when both muds were modified using 30 wt% Nigerian nano lignite coal, the yield point obtained were 18 Ib/100ft<sup>2</sup> and 27 Ib/100ft<sup>2</sup>. As the concentration of Nigerian nano lignite coal increases, the yield point of mud sample B, increases proportionally, with mud sample A, having it highest yield point of 20 Ib/100ft<sup>2</sup>. Upon the addition of 20 wt% Nigerian nano lignite coal for modification while mud sample B, having it highest yield point of 27 Ib/100ft<sup>2</sup>. Upon the addition of 30 wt% Nigerian nano lignite coal for modification as shown in Table 4.2E.

The 10 sec Gel strength of mud formulated with local clay obtained were zero upon the addition of 10 wt% and 30 wt% of Nigerian nano lignite coal, while upon the addition of 20 wt% of Nigerian nano lignite coal, the 10 sec Gel strength obtained was 2 Ib/100ft<sup>2</sup>. But the 10 sec Gel strength of mud formulated with commercial bentonite clay obtained was 2 Ib/100ft<sup>2</sup> at all examined concentration of Nigerian nano lignite coal (from 10 wt% to 30 wt%). For the 10 min Gel strength of muds, upon the addition of 10 wt% of Nigerian

nano lignite coal in sample A, 0 Ib/100ft<sup>2</sup> was obtained and upon the addition of 20 wt% and 30 wt% of Nigerian nano lignite coal in sample A, 2 Ib/100ft<sup>2</sup> was obtained. While for sample B, the 10 min Gel strength obtained was 3 Ib/100ft<sup>2</sup> upon the addition of 10 wt% and 20 wt% of Nigerian nano lignite coal, but upon the addition of 30 wt% of Nigerian nano lignite coal, the 10 min Gel strength obtained was 4 Ib/100ft<sup>2</sup>., as shown in Table 4.2e. When both drilling muds were modified using 10 wt% Nigerian lignite nanoparticles, the fluid loss obtained were 10.0 mL and 10.0 mL, when both muds were modified using 20 wt% Nigerian nano lignite coal, fluid loss obtained were 9.6 mL and 9.6 mL and when both muds were modified using 30 wt% Nigerian nano lignite coal, fluid loss obtained were 9.2 mL and 9.2 mL respectively. It was observed that, as the concentration of Nigerian nano lignite coal increases, fluid loss of both muds obtained also decreases proportionally.

Generally, similar observation was made for the drilling muds modified with different concentration Nigerian nano lignite coal (from 10 wt% to 30 wt%) with both local clay and commercial bentonite clay aged at 160 °C temperature in a hot roller oven, in this case, these modified muds have also exhibited the potential of cleaning rock formation for rock cuttings, transporting these rock cuttings to surface through annulus, cooling the bit during operation, minimizing the fluid loss by forming a fitter cake on the wall of the well bore and reduces the reservoir damage which were primary functions of drilling mud. Based on the aging temperature (160 °C) of both modified drilling muds, from the rheological properties point of view, the drilling muds formulated with commercial bentonite clay, will perform better in rock cutting and transporting of drill cutting to the ground surface through annulus than drilling muds formulated with local clay, as a result of their plastic viscosity and yield point, but observed poor gel strength for both test (10 sec and 10 min), in all the mud samples. Furthermore, from the filtration properties point

of view, the drilling muds formulated with both local clay and commercial bentonite clay have shown better fluid loss reduction and quality filter cake performance by reducing the reservoir damage and minimizing the fluid loss by forming a fitter cake on the wall of the well bore. It can be deduced that further investigation is required for another modifying additive to be combined with Nigerian nano lignite coal for use in modifying drilling muds used in drilling high temperature wells, geothermal wells and deeper wells within 160 °C and above. However, the Nigerian nano lignite coal still offers thermal resistance to the drilling muds at high temperature of 160 °C and seen to be more effective in terms of filtration properties than rheological properties at high operating conditions.

From concentration point of view, at different temperatures, the mud samples modified with different concentration (from 10 wt% to 30 wt%) Nigerian nano lignite coal of 25 g of clay in 350 mL of deionized water were examined and compared.

**Table 4.2F:** Comparative Rheological and Filtration Properties of Modified Local Clay Muds at Different Temperatures. (API- Okorie *et al.*, 2016)

Samples	Room Temperature (25 °C)			Elevated Temperature (100 °C)			Elevated Temperature (160 °C)			API
	A1	A2	A3	A1	A2	A3	A1	A2	A3	
PV (cP)	40	39	40	8	8	9	8	8	11	≥ 8
AV (cP)	80	85	87.5	18	20.5	22	14.5	18	20	≥ 15
YP	80	92	95	18	25	26	13	20	18	-
GS Ib/100ft <sup>2</sup>	6	9	9	0	0	0	0	0	0	-
GS Ib/100ft <sup>2</sup>	6	10	10	1	1	1	0	2	2	
FL (ml)	9.6	9.4	9.2	7.6	7.2	6.8	10	9.6	9.2	≤ 15
CT (mm)	0.8	0.4	0.5	1.3	0.8	0.5	0.7	0.7	0.5	

For sample A, the plastic viscosity obtained after beneficiation was 33 cP as seen in table 4.2B, and when modified with various concentration of Nigerian nano lignite coal at room temperature, the plastic viscosity obtained were 40 cP, 37 cP and 40 cP respectively. At elevated temperature of 100 °C, the plastic viscosity obtained were 8 cP, 8 cP and 9 cP respectively, and at elevated temperature of 160 °C, the plastic viscosity obtained were 8 cP, 8 cP and 11 cP respectively, as shown in figure 4.2A. However, as the temperature

increases from room temperature to 100 °C, the plastic viscosity decreased by 80 %, 78.38 % and 77.5 % respectively, and as the temperature was increased to 160 °C, the plastic viscosity decreased by 80 %, 78.38 % and 72.5 % respectively with respect to different concentration of Nigerian nano lignite coal used for modification. It was observed that at 30 wt% of Nigerian nano lignite coal used for modification, about 22.5 % and 27.5 % of its original values were retained at elevated temperatures examined

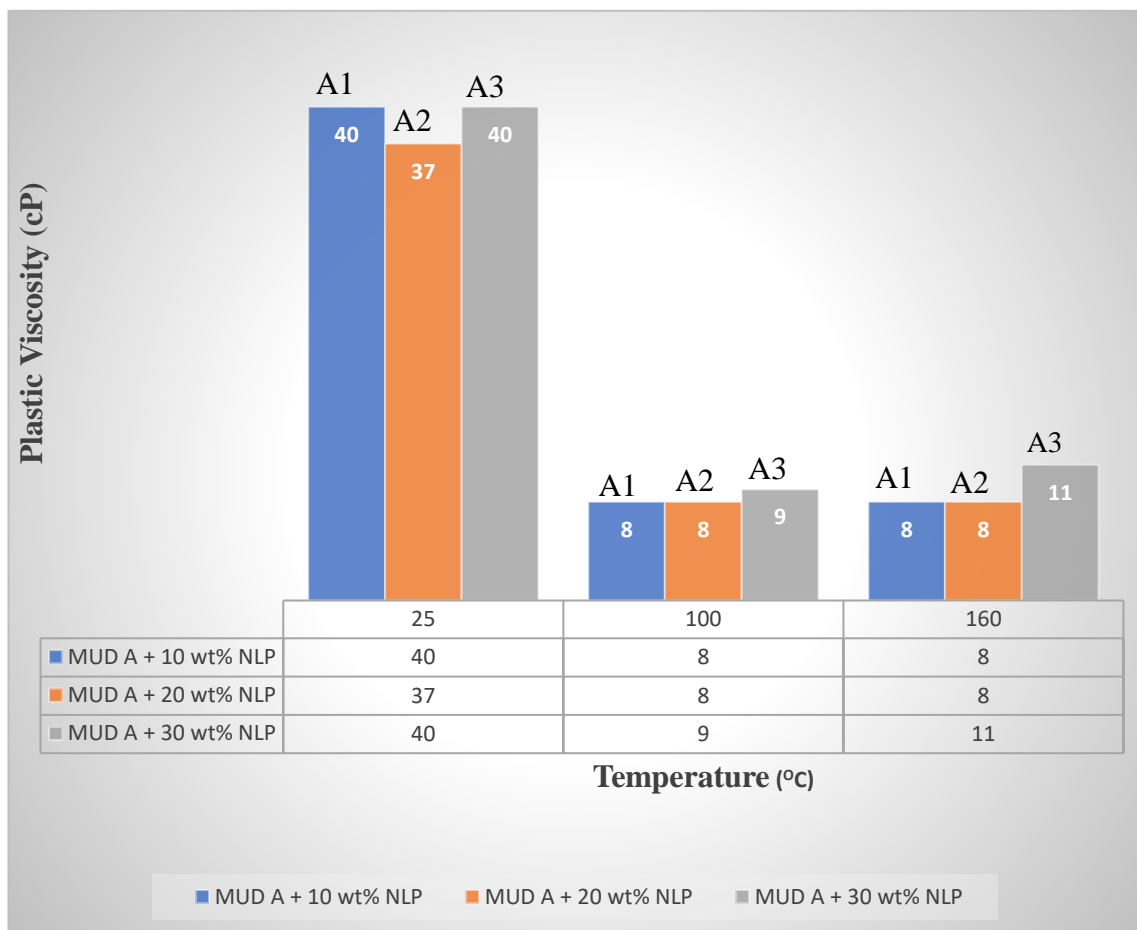


**Figure 4.2A:** The Plastic Viscosity of Modified Local Muds After 10 hours Hot Rolling at Different Temperatures.

Figure 4.2B, shows the apparent viscosity of muds modified with various concentration of Nigerian nano lignite coal at different temperatures, it was observed that the apparent viscosity decreases as a result of increasing aging temperature but there were more decrease in the apparent viscosity of mud modified with 10 wt% of Nigerian nano lignite

coal at different elevated temperatures than the drop in the apparent viscosity of mud modified with other concentrations.

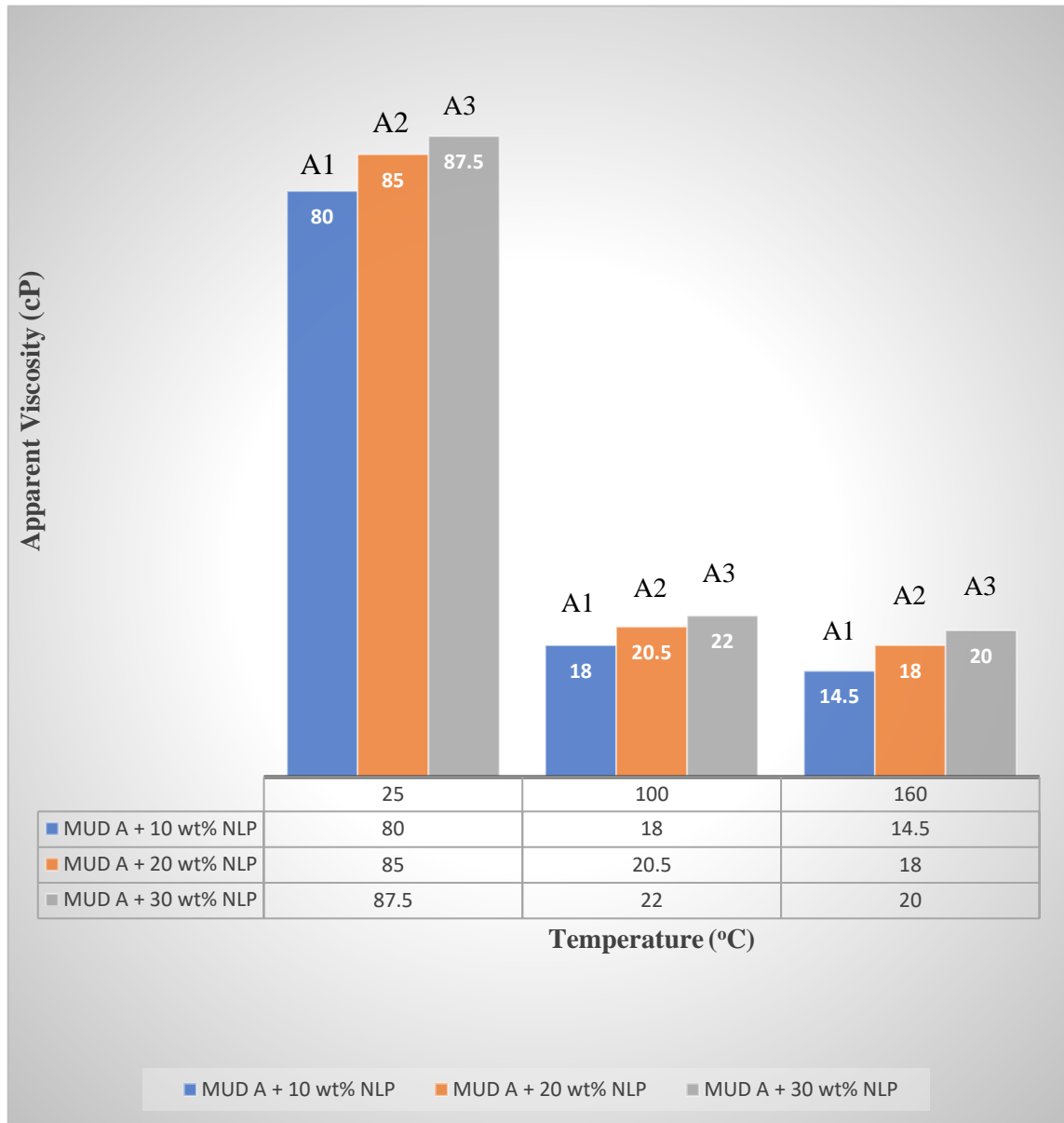


**Figure 4.2B:** The Apparent Viscosity of Modified Local Muds After 10 hours Hot Rolling at Different Temperatures.

However, as the temperature increases from room temperature to 100 °C, the apparent viscosity decreased by 77.50 %, 75.88 % and 74.86 % respectively, and as the temperature was increased to 160 °C, the apparent viscosity decreased by 81.88 %, 78.82 % and 77.14 % respectively with respect to different concentration of Nigerian nano lignite coal used for modification. More than 18.0 % of their original values were retained at various

concentration (from 10 wt% to 30 wt%) of Nigerian nano lignite coal used for modification at elevated temperatures examined.

Figure 4.2C shows the yield point of muds modified with various concentration of Nigerian nano lignite coal at different temperatures. As the concentration of Nigerian nano lignite coal increases, the yield point also increases at 100 °C temperature, except at 160 °C temperature which did not have similar case.

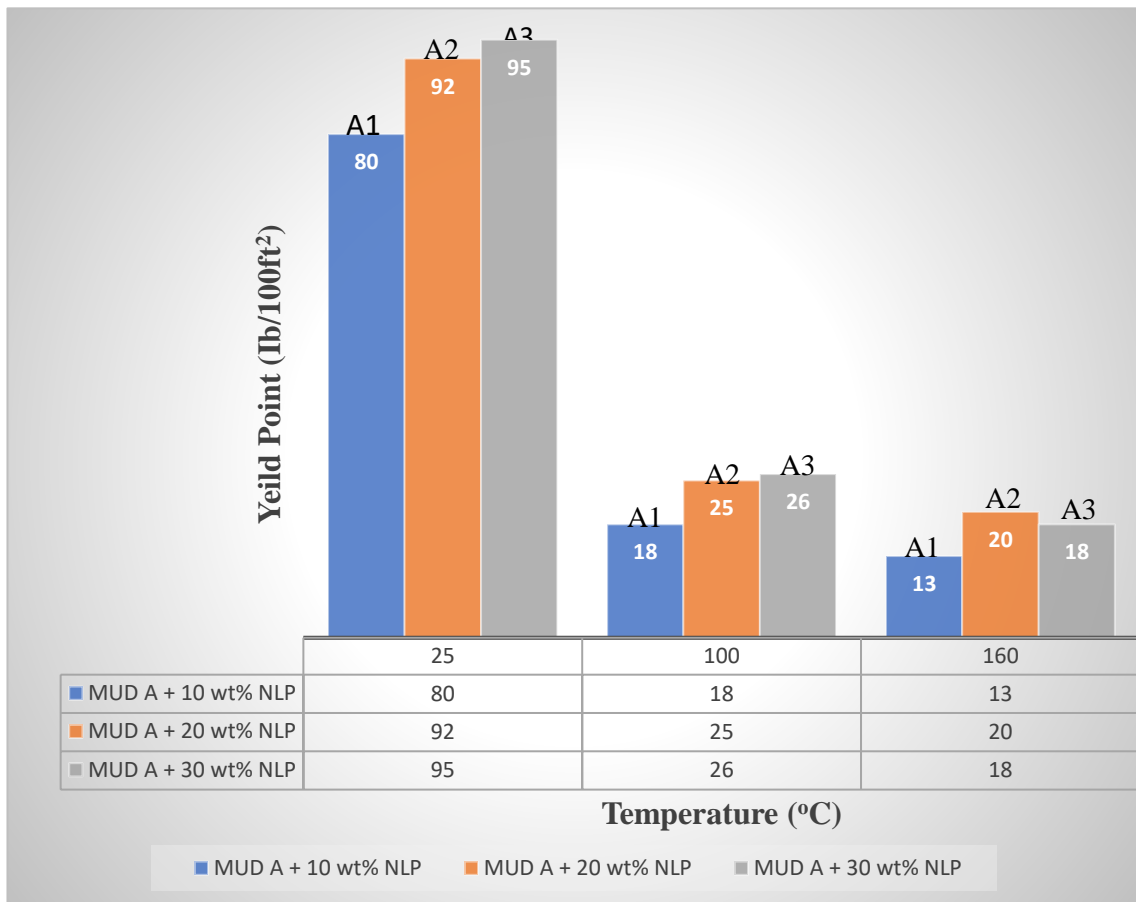


**Figure 4.2C:** The Yield Point of Modified Local Muds After 10 hours Hot Rolling at Different Temperatures.

However, as the temperature increases to 100 °C, yield point decreased by 77.50 %, 72.83 % and 72.63 % respectively, and as the temperature was increased to 160 °C, the yield point decreased by 83.75 %, 78.26 % and 81.05 % respectively. It was observed that at 30 wt% and 20 wt% of Nigerian nano lignite coal used for modification, about 27.37 % and 18.95 % of its original values were retained at elevated temperatures examined.

The amount of API fluid loss is one of the important parameters used in evaluating the efficiency of mud (Valizadeh and Nasiri, 2012). Figure 4.2D shows the fluid loss of muds modified with different concentration of Nigerian lignite nanoparticles at different temperatures.

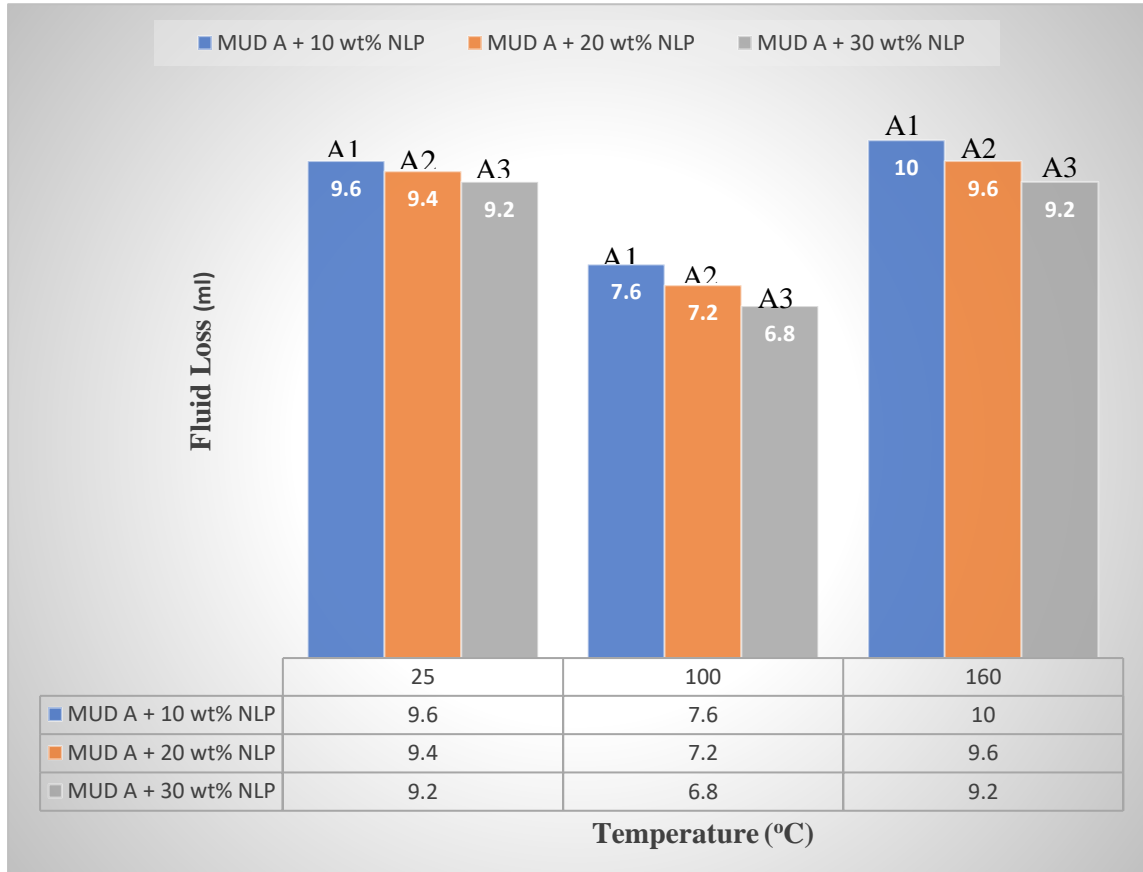


**Figure 4.2D:** The Fluid Loss of Modified Local Mud After 10 hours Hot Rolling at Different Temperatures.

As the concentration of Nigerian lignite nanoparticles increases, fluid loss decreases at each temperature in similar reduction trend. However, as the temperature increases to 100 °C, fluid loss decreased by 20.83 %, 23.40 % and 26.08 % respectively, and as the temperature was increased to 160 °C, the fluid loss increased by 4.17 %, 2.13 % and 0.00 % respectively. It was observed that at 100 °C temperature, the fluid loss of muds was all decreased from their original values with various concentration of Nigerian nano lignite

coal and at 160 °C temperature, the fluid loss of muds increased significantly except for mud modified with 30 wt% of Nigerian nano lignite coal.

**Table 4.2G:** Comparative Rheological and Filtration Properties of Modified Commercial Bentonite Clay Muds at Different Temperature.

sample	Room Temperature (25 °C)			Elevated Temperature (100 °C)			Elevated Temperature (160 °C)			API
	B1	B2	B3	B1	B2	B3	B1	B2	B3	
PV (cP)	37	40	37	9	11	11	8	8	9	≥ 8
AV (cP)	80	86.6	88	20	23	24	18.5	21	23	≥ 15
YP Ib/100ft <sup>2</sup>	86	93	102	22	24	26	21	26	28	
GS Ib/100ft <sup>2</sup>	12	20	24	3	3	4	2	2	2	
GS Ib/100ft <sup>2</sup>	15	24	25	4	4	6	4	2	3	
FL (ml)	9.8	9.6	9.4	10	9.6	9.2	10	9.6	9.2	≤ 15
CT (mm)	0.4	0.9	0.9	1.0	1.0	0.8	0.9	0.9	0.8	

Similarly, for sample B, the plastic viscosity obtained after beneficiation was 28 cP and when modified with different concentration of Nigerian nano lignite coal at room temperature, the plastic viscosity obtained were 37 cP, 40 cP and 37 cP respectively. At elevated temperature of 100 °C, the plastic viscosity obtained were 9 cP, 11 cP and 11 cP respectively, and at elevated temperature of 160 °C, the plastic viscosity obtained were 8 cP, 8 cP and 9 cP respectively, as shown in fig 4.2e. However, as the temperature increases from room temperature to 100 °C, the plastic viscosity decreased by 75.68 %, 72.5 % and 70.27 % respectively, and as the temperature was increased to 160 °C, the plastic viscosity decreased by 78.38 %, 80.0 % and 75.68 % respectively with respect to different concentration of Nigerian nano lignite coal used for modification, more than 20.0 % of its original values were retained at different concentration (from 10 wt% to 30 wt%) of Nigerian nano lignite coal used for modification at elevated temperatures examined.

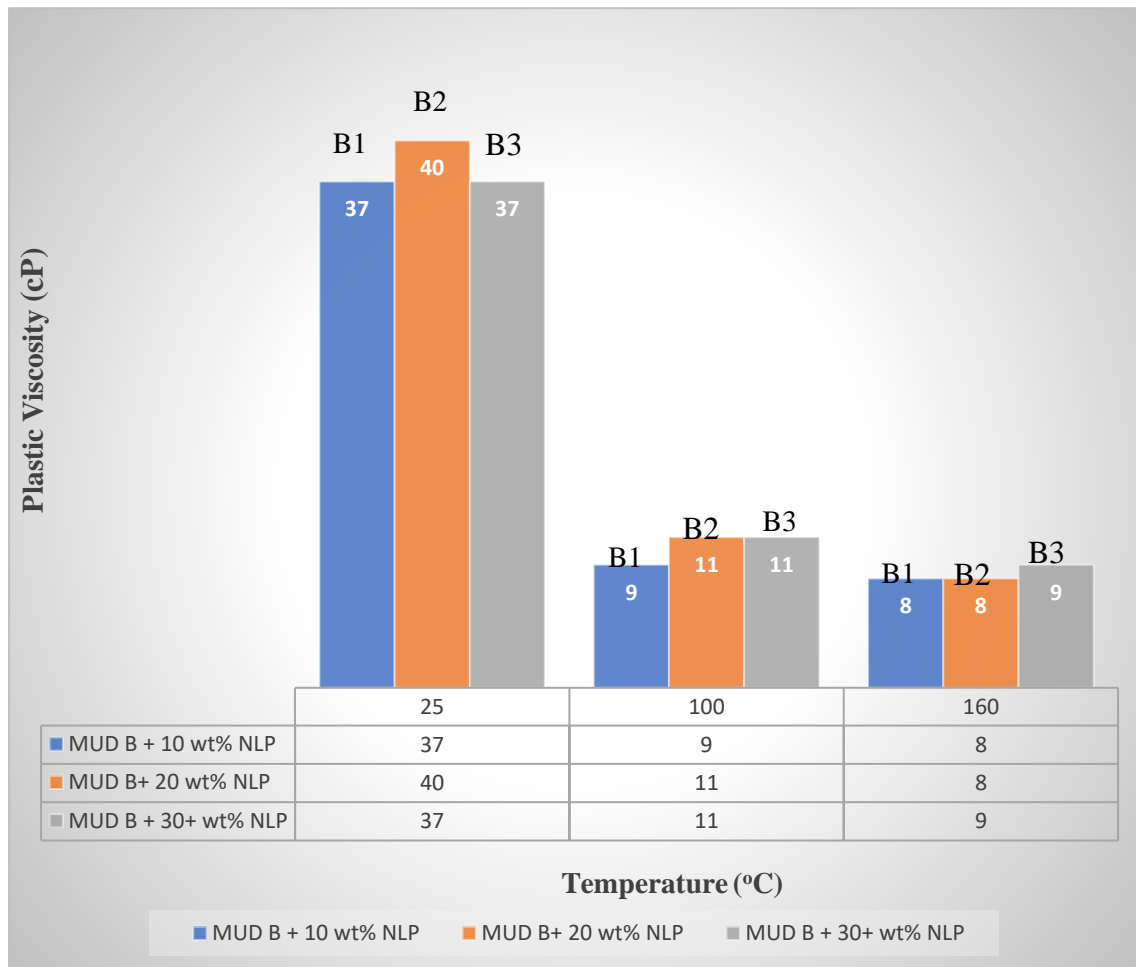


**Figure 4.2E:** The Plastic Viscosity of Modified Commercial Bentonite Clay Muds After 10 hours Hot Rolling at Different Temperatures.

Figure 4.2F, shows the apparent viscosity of muds modified with various concentration of Nigerian nano lignite coal at different temperatures, it was observed that the apparent viscosity decreases as a result of increasing aging temperature but there were more decrease in the apparent viscosity of mud modified with 10 wt% of Nigerian nano lignite coal at different elevated temperatures than the drop in the apparent viscosity of mud modified with other concentrations. However, as the temperature increases from room temperature to 100 °C, the apparent viscosity decreased by 75.0 %, 73.26 % and 72.73 % respectively, and as the temperature was increased to 160 °C, the apparent viscosity decreased by 76.88 %, 75.58 % and 73.86 % respectively with

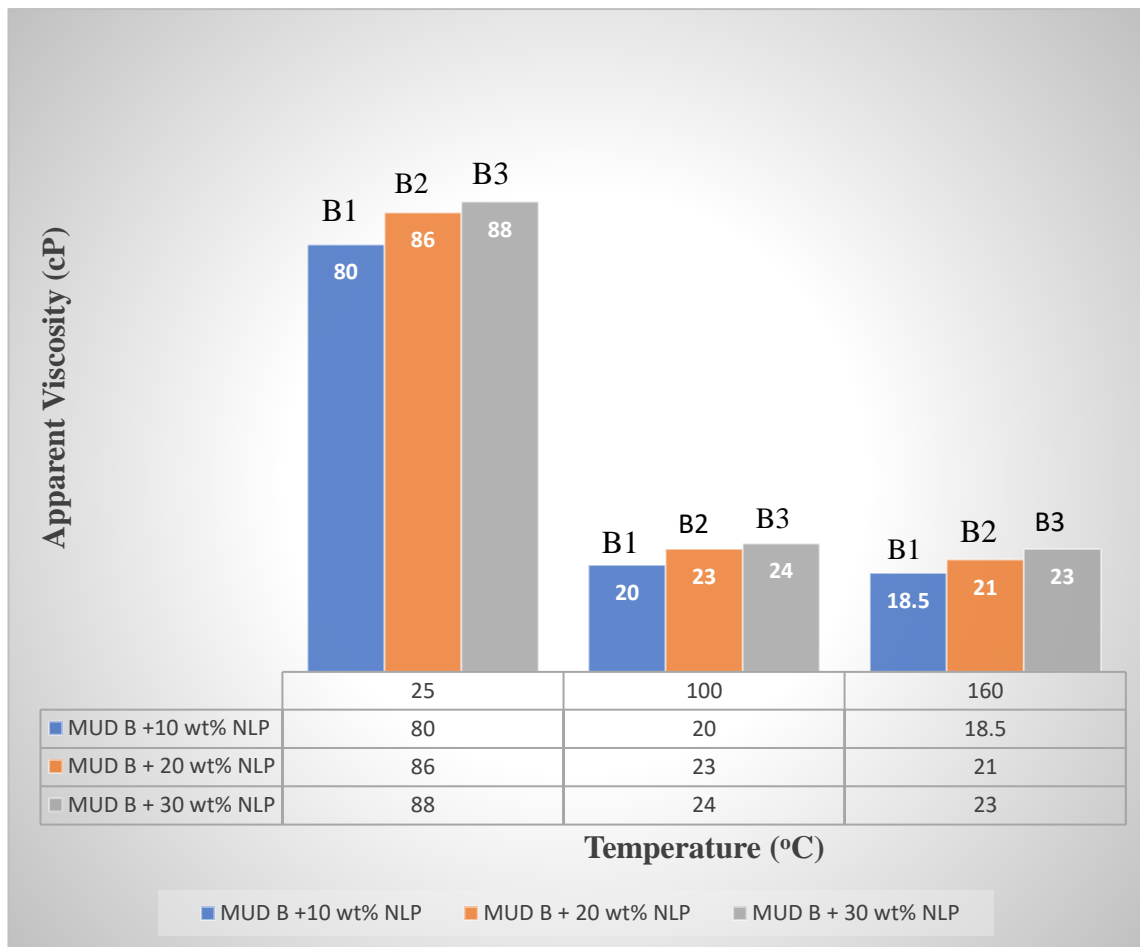


**Figure 4.2F:** The Apparent Viscosity of Modified Commercial Bentonite Clay Muds After 10 hours Hot Rolling at Different Temperatures.

Respect to various concentration of Nigerian nano lignite coal used for modification. More than 23.0 % of their original values were retained at various concentration (from 10 wt% to 30 wt%) of Nigerian nano lignite coal used for modification at elevated temperatures examined.

Figure 4.2G shows the yield point of muds modified with different concentration of Nigerian nano lignite coal at different temperatures. As the concentration of Nigerian nano lignite coal increases, the yield point also increases at each temperature. However, as the temperature increases to 100 °C, yield point decreased by 74.42 %, 74.19 % and 74.51 % respectively, and as the temperature was increased to 160 °C, the yield point decreased by 75.58 %, 72.04 % and 72.55 % respectively. It was observed that more than

24.0 % of their original values were retained at different concentration (from 10 wt% to 30 wt%) of Nigerian nano lignite coal used for modification at elevated temperatures examined.

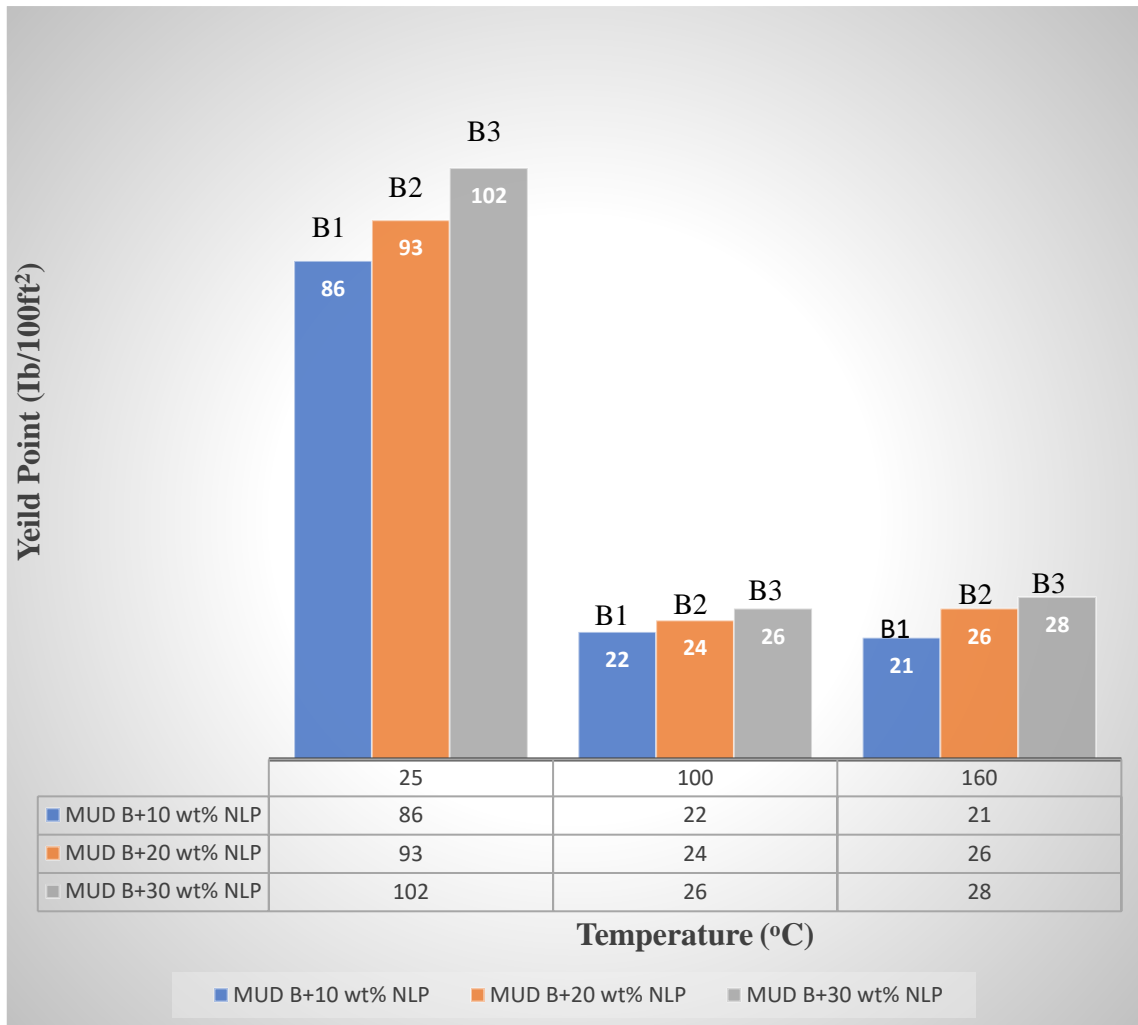


**Figure 4.2G:** The Yield Point of Modified Commercial Bentonite Clay Muds After 10 hours Hot Rolling at Different Temperatures.

Figure 4.2h shows the fluid loss of muds modified with various concentration of Nigerian nano lignite coal at different temperatures. As the concentration of Nigerian nano lignite coal increases, fluid loss decreases at each temperature in similar reduction trend.

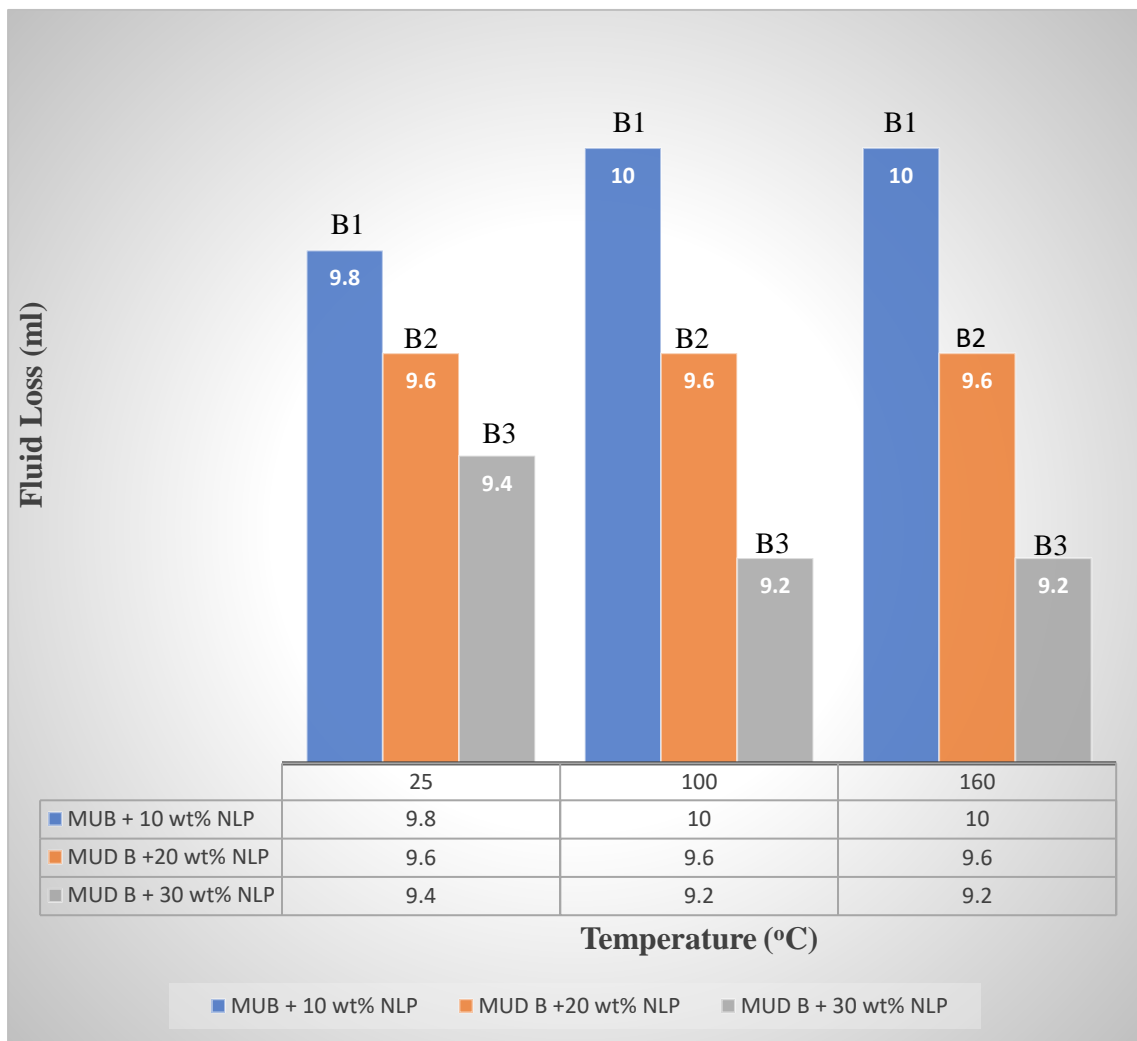


**Figure 4.2H:** The Fluid Loss of Modified Commercial Bentonite Clay Muds After 10 hours Hot Rolling at Different Temperatures.

However, as the temperature increases to 100 °C, fluid loss increased by 2.04 %, 0.0 % and decreased by 2.13 % respectively at different concentration (from 10 wt% to 30 wt%) of Nigerian nano lignite coal and as the temperature was increased to 160 °C, the fluid loss also has the same trend as that at 100 °C. It was observed that at both elevated temperatures examined, the fluid loss of muds has the same trend.

Table 4.2H and Table 4.2I shows the comparisons between both muds (modified with different concentration on Nigerian nano lignite coal from 10 wt% to 30 wt%) in this work and other reported work in literature. However, it was observed that the rheological

and filtration properties deduced may depend on the following factors: the nature of raw material used, types and concentration of modifying additives, operating condition selected for wells and types of well to be drilled (Ebikapaye, 2018 and Mansoor *et al.*, 2018).

**Table 4.2H:** Comparative Rheological and Filtration Properties between this (Local Clay) and previous work.

Samples	Present Work									Previous Work						API
	Temp. (25 °C)			Temp. (100 °C)			Temp. (160 °C)			Temp. (25 °C)		Temp. (120 °C)		Temp. (160 °C)		
	A1	A2	A3	A1	A2	A	A1	A2	A3	X	Y	X	Y	X	Y	
PV (cP)	40	39	40	8	8	9	8	8	11	13	15	7	14	2	11	≥ 8
AV (cP)	80	85	87	18	20.5	2	14.5	18	20	17	23	8	21	2.5	13	≥ 15
YP (Ib/100ft <sup>2</sup> )	80	92	95	18	25	2	13	20	18	14	16	2	14	1	4	
GEL (Ib/100ft <sup>2</sup> )	6	9	9	0	0	0	0	0	0	3	3.5	1.5	3	0.5	1.5	
GEL (Ib/100ft <sup>2</sup> )	6	10	10	1	1	1	0	2	2	4	4.5	2.5	4	1	2	
FL (ml)	9.6	9.4	9.2	7.6	7.2	6	10	9.6	9.2	6.5	4.3	32	4.4	---	93	> 15

**A1, A2 and A3 (present study), X and Y- Valizadeh and Nasiri, (2012). API- Okorie *et al.*, 2016**

Furthermore, Table 4.2H, shows that sample A with different concentration (from 10 wt% to 30 wt%) Nigerian nano lignite coal at room temperature, have high rheological properties than the rheological properties of the previous work while the previous work have reduced fluid loss as compared with sample. Although, at 160 °C temperature, sample A with different concentration (from 10 wt% to 30 wt%) Nigerian nano lignite coal, still have high rheological properties and reduced fluid loss as compared with rheological properties and fluid loss of the previous work, except for the gel strength of both test (10 sec/ 10 min) which were less than or equal to 2 Ib/100ft<sup>2</sup>.

Table 4.2I, shows that sample B with different concentration (from 10 wt% to 30 wt%) Nigerian nano lignite coal at room temperature, have high rheological properties than the

rheological properties of the previous work while the previous work have reduced fluid loss as compared with sample B.

**Table 4.2I:** Comparative Rheological and Filtration Properties between this (Commercial Bentonite Clay) and previous work.

Samples	Present Work									Previous Work						API min.
	Temp. (25 °C)			Temp. (100 °C)			Temp. (160 °C)			Temp. (25 °C)		Temp. (120 °C)		Temp. (160 °C)		
	B1	B2	B3	B1	B2	B3	B1	B2	B3	X	Y	X	Y	X	Y	
PV (cP)	37	40	37	9	11	11	8	8	9	13	15	7	14	2	11	< 8
AV (cP)	80	86.6	88	20	23	24	18.	21	23	17	23	8	21	2.5	13	< 15
YP (lb/100ft <sup>2</sup> )	86	93	102	22	24	26	21	26	28	14	16	2	14	1	4	
GEL (lb/100ft <sup>2</sup> )	12	20	24	3	3	4	2	2	2	3	3.5	1.5	3	0.5	1.5	
GEL (lb/100ft <sup>2</sup> )	15	24	25	4	4	6	4	2	3	4	4.5	2.5	4	1	2	
FL (ml)	9.8	9.6	9.4	10	9.6	9.2	10	9.6	9.2	6.5	4.3	32	4.4	---	93	> 15

**B1, B2 and B3 (present study), X and Y- Valizadeh and Nasiri, (2012). API- Okorie et al., 2016**

This is similar observation with sample A in Table 4.2h, meanwhile at 160 °C temperature, sample B with different concentration (from 10 wt% to 30 wt%) Nigerian nano lignite coal, still have high rheological properties and reduced fluid loss as compared with rheological properties and fluid loss of the previous work. Thus, Nigerian nano lignite coal have proved useful in modifying drilling muds to be used for drilling high temperature wells, geothermal wells, deep wells and shale formation within the set point temperature of 160 °C.

### 4.3 Rheological Model

The estimation of the rheological model parameters for the drilling fluids described by Power Law rheological model is an important task for the economics and the safety of drilling a well. Different statistical methods were considered to evaluate these parameters such as coefficient of determination ( $R^2$ ) and root mean square error

From Table 4.3A, at room temperature, the power law model predicated shear stress values for beneficiated mud from local clay shows higher model predicated shear stress

value than mud from commercial bentonite clay, but both muds prove to be non-Newtonian fluid as the curve fitting of both muds do not pass through the origin as exhibited in figure 4.3a.

**Table 4.3A:** Power Law Model Shear Stress Values of at 25 °C

Shear Rate ( $S^{-1}$ )	Local Clay Shear Stress ( $\tau$ ) (Pa)				Commercial Bentonite Shear Stress ( $\tau$ ) (Pa)			
	A0	A1	A2	A3	B0	B1	B2	B3
1022	78.91	87.07	92.51	95.23	60.96	87.07	94.07	95.77
511	60.95	65.3	71.29	73.47	45.72	66.93	72.37	75.64
341	52.42	55.21	61.23	63.15	38.65	57.41	62.1	65.91
170	40.44	41.35	47.14	48.66	28.95	44.08	47.73	52.01
10.22	14.19	12.87	16.38	16.99	9.01	15.17	16.48	19.97
5.11	10.96	9.65	12.62	13.11	6.76	11.66	12.68	15.77

The power law model predicated shear stress values for modified muds was observed to have increased as the nano lignite coal concentration increases in the muds system from 10 to 30 wt% for muds formulated from local and commercial bentonite clay.

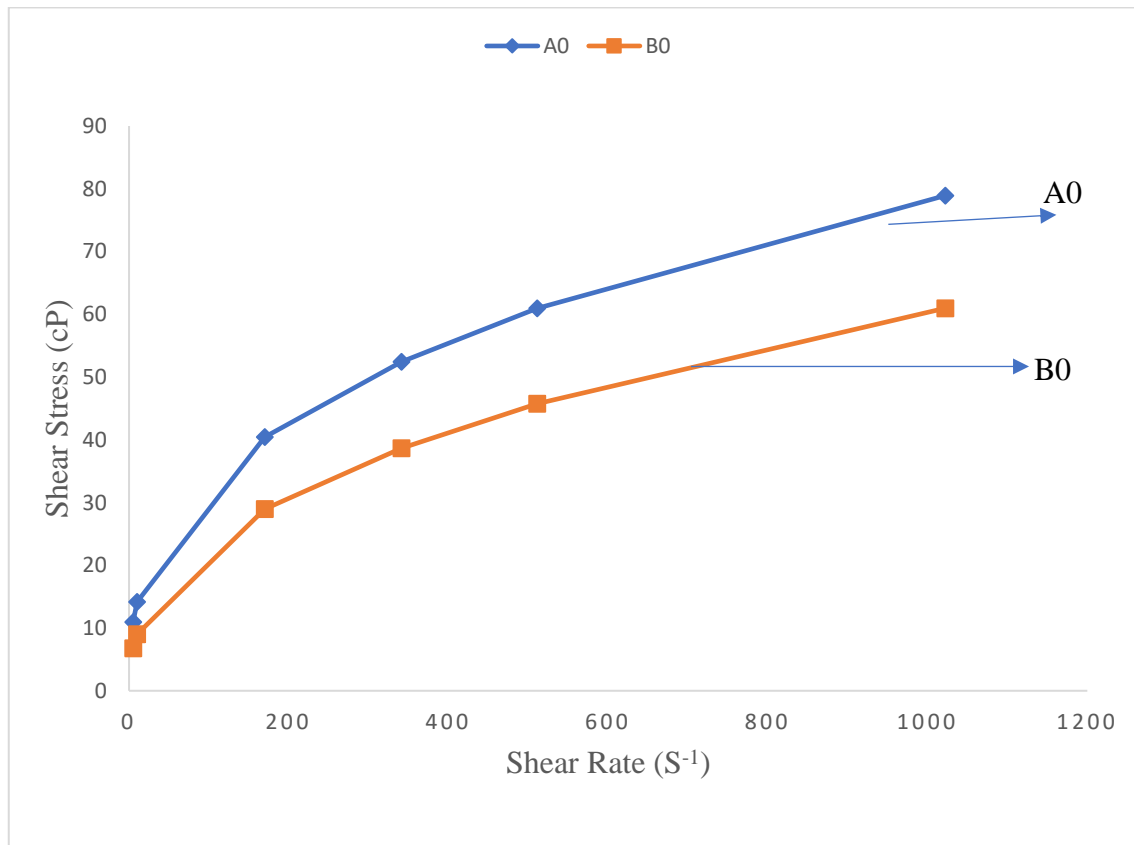


**Figure 4.3A:** Power Law fitting curves of beneficiated mud at room temperature.

However, the modified muds from local and commercial bentonite clay have similar predicated shear stress values, muds formulated with commercial bentonite clay still shows higher model predicated shear stress values as summarized in table 4.3A. All the muds prove to be non-Newtonian fluid as the curve fitting of all muds do not pass through the origin as exhibited in figure 4.3B which is in confirmation with the plot of shear stress against shear rate obtained from (Folayan *et al.*, 2017).

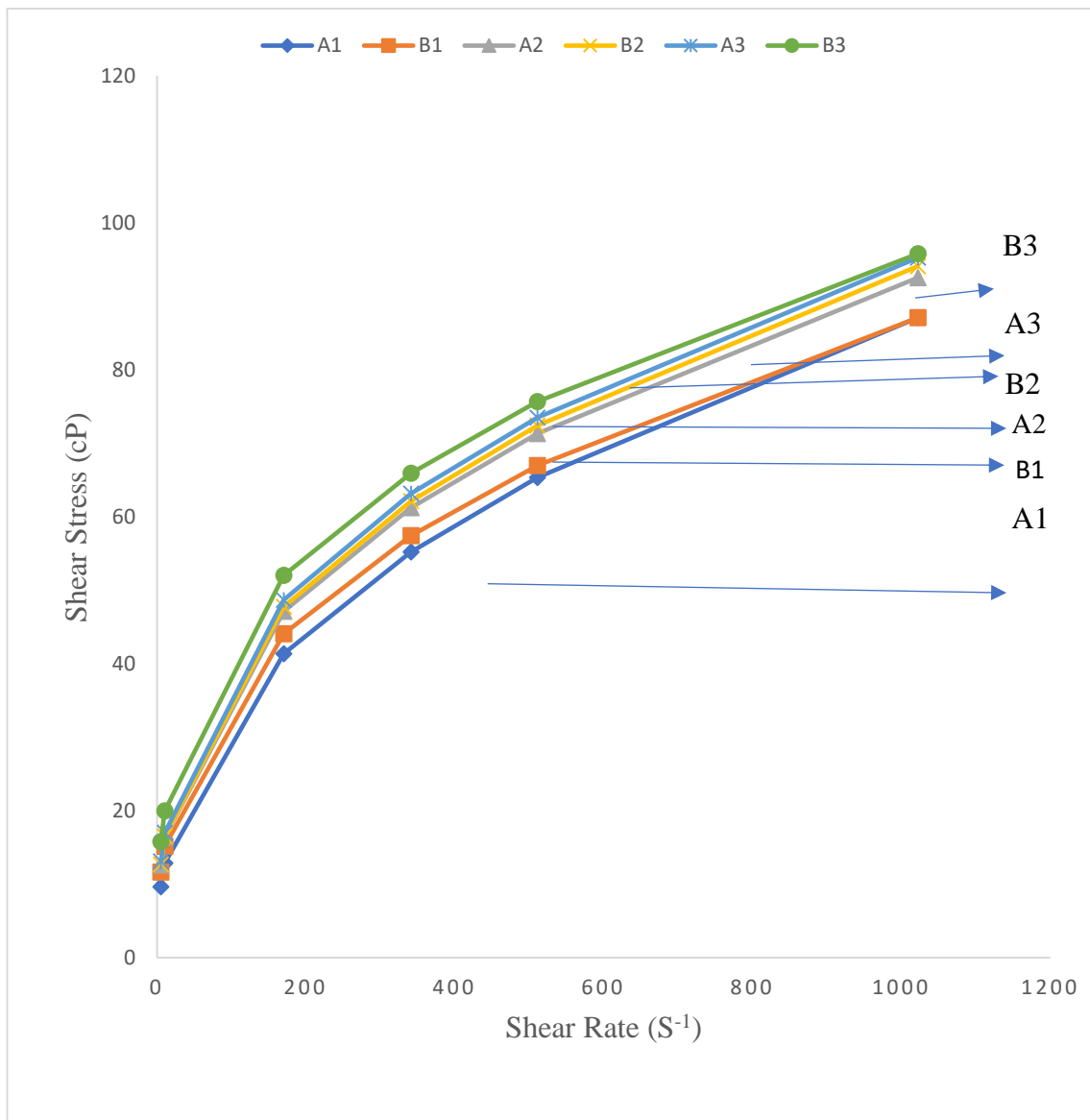


**Figure 4.3B:** Power Law fitting curves of modified mud at room temperature.

From Table 4.3B, it was observed that the power law model predicated shear stress values for modified mud increases as the nano lignite coal concentration increases in the muds system from 10 to 30 wt% for both muds formulated from local and commercial bentonite clay, muds formulated with commercial bentonite clay shows higher model predicated shear stress values than those formulated with local clay mud.

**Table 4.3B:** Power Law Shear Stress Values of at 100 °C

Shear Rate (S <sup>-1</sup> )	local clay Shear Stress ( $\tau$ ) (Pa)			commercial bentonite Shear Stress ( $\tau$ ) (Pa)		
	A1	A2	A3	B1	B2	B3
1022	19.59	22.31	23.94	21.77	25.03	26.12
511	15.23	17.95	19.05	16.87	19.05	20.13
341	13.15	15.81	16.67	14.54	16.24	17.29
170	10.21	12.71	13.25	11.25	12.35	13.31
10.22	3.68	5.26	5.25	3.99	4.08	4.63
5.11	2.86	4.23	4.18	3.1	3.11	3.57

At 100 °C of aging, the muds still proved to be non-Newtonian fluid as the curve fitting of all muds do not pass through the origin as exhibited in figure 2 which is in confirmation with the plot of shear stress against shear rate obtained from (Folayan *et al.*, 2017).

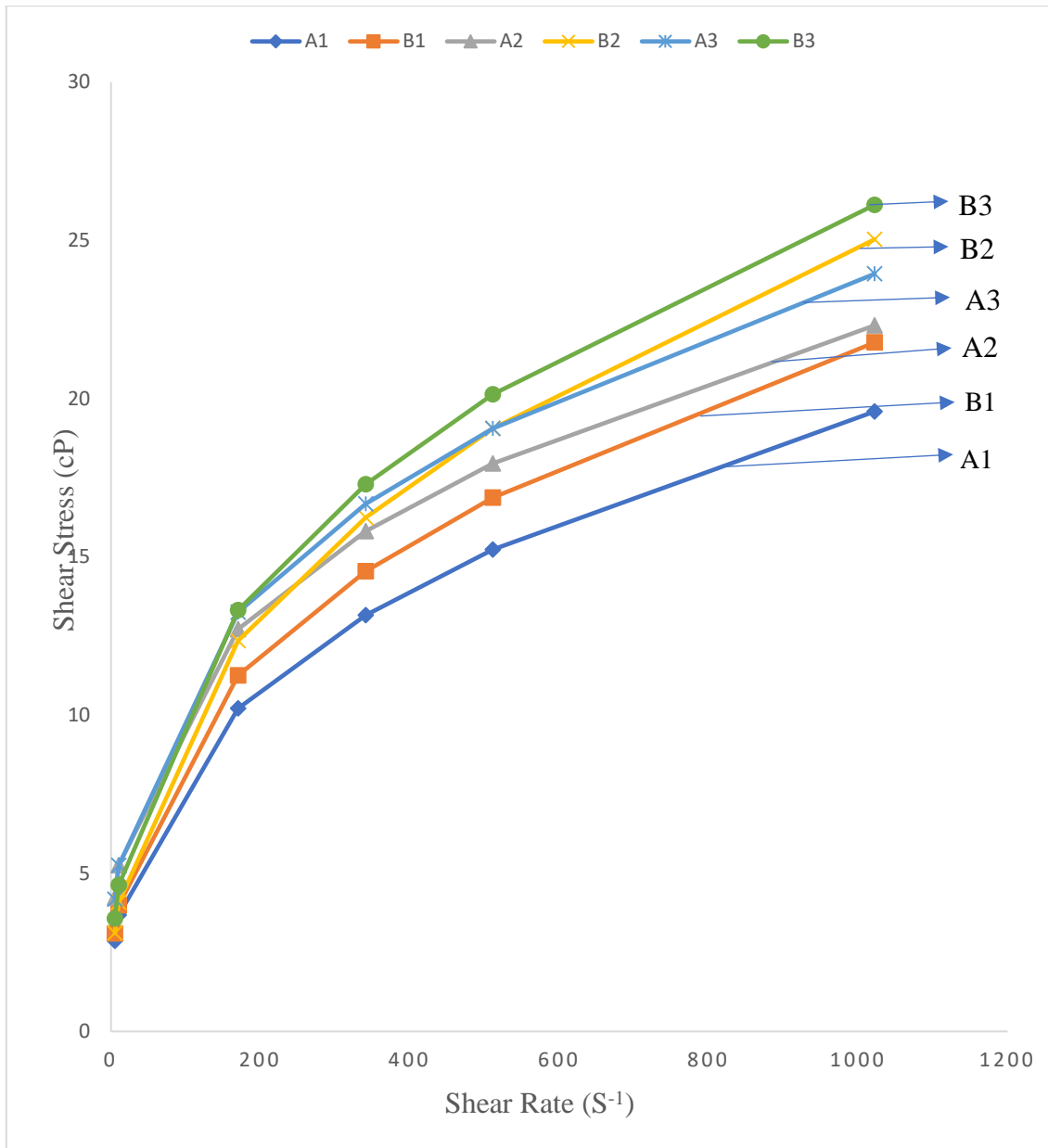


**Figure 4.3C:** Power Law Fitting Curves of Modified Mud at 100 °C Temperature.

From table 4.3C, it was also observed that the power law model predicated shear stress values for modified muds increases as the nano lignite coal concentration increases in the muds system from 10 to 30 wt% for both muds formulated from local and commercial bentonite clay, muds formulated with commercial bentonite clay shows higher model predicated shear stress values than those from local clay mud. At 160 °C, the muds prove to be non-Newtonian fluid as

**Table 4.3C:** Power Law Model Shear Stress Values of at 160 °C

Shear Rate ( $S^{-1}$ )	Local Bentonite Shear Stress ( $\tau$ ) (Pa)			Commercial Bentonite Shear Stress ( $\tau$ ) (Pa)		
	A1	A2	A3	B1	B2	B3
1022	15.78	19.59	21.77	20.13	22.85	24.5
511	11.43	15.24	15.78	15.78	18.5	19.59
341	9.47	13.16	13.08	13.69	16.35	17.19
170	6.85	10.23	9.47	10.72	13.28	13.73
10.22	1.85	3.69	2.57	3.99	5.62	5.54
5.11	1.34	2.87	1.86	3.13	4.55	4.43

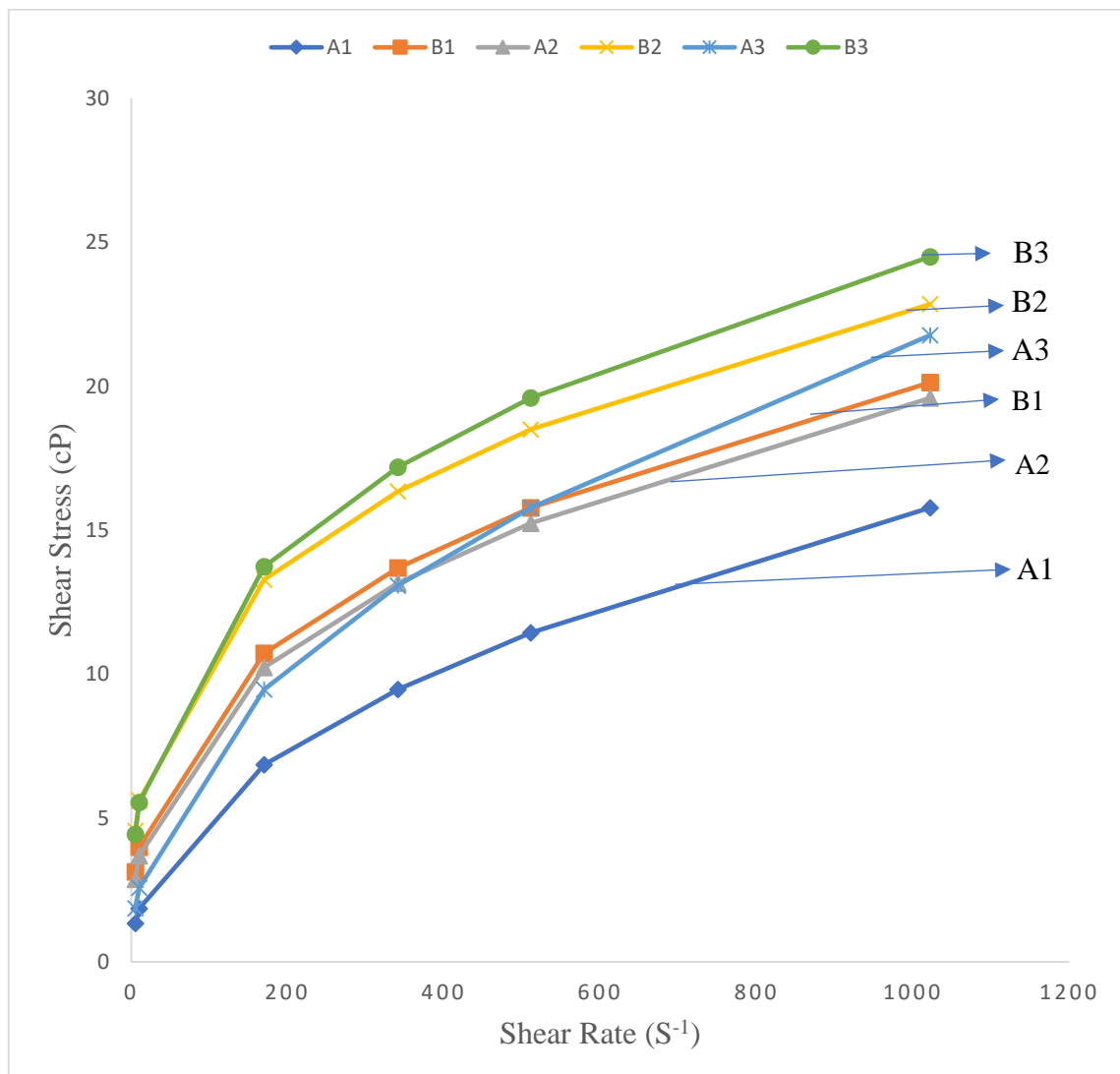


**Figure 4.3D:** Power Law Fitting Curves of Modified Mud at 160 °C Temperature.

The curve fitting of all muds does not pass through the origin as exhibited in Figure 4.3D which is in confirmation with the plot of shear stress against shear rate obtained from (Folayan *et al.*, 2017).

From Table 4.4, Mud A (Local Bentonite) at 25 °C, the flow behaviour index (n) and the fluid consistency coefficient (k) of mud A ranged from 0.3726 to 0.4151 and 4.9051 Pa.s to 7.1176 Pa.s as the nano lignite coal concentrations in the mud system increases from 0 to 30 wt%. The mud containing 10 wt% nano lignite coal concentrations have the highest value of 0.4151 as the flow behaviour index and the mud with 0 wt% nano lignite coal concentrations have the list value of 0.3726 as the flow behaviour index, the mud containing 30 wt% nano lignite coal concentrations have the highest value of 7.1176 Pa.s as the fluid consistency coefficient, while the mud containing 10 wt% nano lignite coal concentrations have the list value of 4.9051 Pa.s as the fluid consistency coefficient. The mud systems exhibited non-Newtonian behaviour and shear thinning, as the values of flow behaviour index were less than unity ( $n < 1$ ). The coefficient of determination ( $R^2$ ) and Root Mean Square Error (RMSE) are ranged from 0.9976 to 0.9990 and 3.5910 Pa to 5.1268 Pa as the nano lignite coal concentrations in the mud system increases from 0 to 30 wt%. The closer the value of  $R^2$  to 1, the better precise the model is in predicting the rheological behaviours of the drilling mud. The mud containing 20 wt% nano lignite coal concentrations have the highest value of 0.9990 as  $R^2$  while the mud containing 10 wt% nano lignite coal concentrations have the list value of 0.9976 as  $R^2$ , the mud containing 30 wt% nano lignite coal concentrations have the highest value of 5.1268 Pa as RMSE, while the mud containing 10 wt% nano lignite coal concentrations have the list value of 3.5910 Pa as RMSE as summarized in Table 4.4. The coefficient of determination ( $R^2$ ) and Root Mean Square Error (RMSE) are the parameters used for evaluating the

goodness of fit of predicted values to experimental values (Wenxi *et al.*, 2020 and Vipulanandan and Mohammed, 2014).

**Table 4.4:** Power Law Rheological Model Fitting Parameters.

Temp. (°C)	LNP (%)	Power Law Model							
		Local Clay Mud (A)				Commercial Bentonite Mud (B)			
		n	k (Pa.s)	R <sup>2</sup>	RMSE (Pa)	n	k (Pa.s)	R <sup>2</sup>	RMSE (Pa)
25	0	0.3726	5.9678	0.9984	4.8324	0.4151	3.4340	0.9997	1.8063
	10	0.4151	4.9051	0.9976	3.5910	0.3795	6.2774	0.9917	3.3793
	20	0.3759	6.8381	0.9990	4.9275	0.3783	6.8387	0.9968	2.1188
100	30	0.3743	7.1176	0.9988	5.1268	0.3404	9.0534	0.9906	3.1336
	10	0.3632	1.5813	0.9516	2.6930	0.3679	1.7009	0.9613	2.8209
	20	0.3137	2.5377	0.9412	3.6496	0.3939	1.9332	0.9947	1.6631
160	30	0.3296	2.4390	0.9643	3.0218	0.3758	1.9321	0.6259	0.9342
	10	0.4653	0.6278	0.8807	2.9271	0.3512	1.7657	0.9211	3.4980
	20	0.3623	1.5911	0.8620	4.4363	0.3047	2.7663	0.9041	4.6169
	30	0.4642	0.8727	0.9023	3.4656	0.3227	2.6183	0.9017	4.7913

For mud B at 25 °C, the flow behaviour index and the fluid consistency coefficient of mud B ranged from 0.3404 to 0.4151 and 3.4340 Pa.s to 9.0534 Pa.s as the nano lignite coal concentrations in the mud system increases from 0 to 30 wt%. It was observed in table 5, as the nano lignite coal concentrations in the mud system increases from 0, to 30 wt%, the fluid consistency coefficient of mud B increase while the flow behaviour index decreases. The mud without nano lignite coal concentrations have the highest values of 0.4151 as the flow behavior index while the mud containing 30 wt% nano lignite coal concentrations have the list values of 0.3404 as flow behavior index, the mud containing 30 wt% nano lignite coal concentrations have the highest value of 9.0534 Pa.s as the fluid consistency coefficient, while the mud without nano lignite coal concentrations have the list value of 3.4340 Pa.s as the fluid consistency coefficient. The mud B also exhibited non-Newtonian behaviour and shear thinning, as the values of flow behaviour index were less than unity ( $n < 1$ ). The coefficient of determination ( $R^2$ ) and Root Mean Square Error (RMSE) are ranged from 0.9906 to 0.9997 and 1.8063 Pa to 3.3793 Pa as the nano lignite

coal concentrations in the mud system increases from 0 to 30 wt%. The mud without nano lignite coal concentrations have the highest value of 0.9997 as  $R^2$  while the mud containing 30 wt% nano lignite coal concentrations have the list value of 0.9906 as  $R^2$ , the mud containing 10 wt% nano lignite coal concentrations have the highest value of 3.3793 Pa as RMSE, while the mud without nano lignite coal concentrations have the list value of 1.8063 Pa as RMSE as seen in Table 4.4. However, mud B have the highest values of  $R^2$  and the list values of RMSE without nano lignite coal concentrations while mud A have the highest values of  $R^2$  containing 20 wt% nano lignite coal concentrations and the list values of RMSE containing 10 wt% nano lignite coal concentrations.

For mud A at 100 °C, the flow behaviour index ( $n$ ) and the fluid consistency coefficient ( $k$ ) of mud A ranged from 0.3137 to 0.3632 and 1.5813 Pa.s to 2.5377 Pa.s as the nano lignite coal concentrations in the mud system increases from 10 to 30 wt%. The mud containing 10 wt% nano lignite coal concentrations have highest flow behaviour index value of 0.3632 while the mud containing 20 wt% nano lignite coal concentrations have list flow behaviour index value of 0.3137, the mud containing 20 wt% nano lignite coal concentrations have highest fluid consistency coefficient value of 2.5377 Pa.s while the mud containing 10 wt% nano lignite coal concentrations have list fluid consistency coefficient value of 1.5813 Pa.s. The mud A at 100 °C also exhibited non-Newtonian behaviour and shear thinning, as the values of flow behaviour index were less than unity ( $n < 1$ ). The coefficient of determination ( $R^2$ ) and Root Mean Square Error (RMSE) are ranged from 0.9412 to 0.9643 and 2.6930 Pa to 3.6496 Pa as the nano lignite coal concentrations in the mud system increases from 10 to 30 wt%. The mud containing 30 wt% nano lignite coal concentrations have the highest  $R^2$  value of 0.9643 while the mud containing 20 wt% nano lignite coal concentrations have the list  $R^2$  value of 0.9412, the mud containing 20 wt% nano lignite coal concentrations have the highest RMSE value of

3.6496 Pa while the mud containing 20 wt% nano lignite coal concentrations have the list RMSE value of 2.6930 Pa. While mud B at 100 °C have the flow behaviour index (n) and the fluid consistency coefficient (k) of mud A ranged from 0.3679 to 0.3939 and 1.7009 Pa.s to 1.9332 Pa.s as the nano lignite coal concentrations in the mud system increases from 10 to 30 wt%. The mud containing 20 wt% nano lignite coal concentrations have highest flow behaviour index value of 0.3939 while the mud containing 10 wt% nano lignite coal concentrations have list flow behaviour index value of 0.3679, the mud containing 20 wt% nano lignite coal concentrations have highest fluid consistency coefficient value of 1.9332 Pa.s while the mud containing 10 wt% nano lignite coal concentrations have list fluid consistency coefficient value of 1.7009 Pa.s. The mud B at 100 °C also exhibited non-Newtonian behaviour and shear thinning, as the values of flow behaviour index were less than unity ( $n < 1$ ). The coefficient of determination ( $R^2$ ) and Root Mean Square Error (RMSE) are ranged from 0.6259 to 0.9947 and 0.9342 Pa to 2.8209 Pa as the nano lignite coal concentrations in the mud system increases from 10 to 30 wt%. The mud containing 20 wt% nano lignite coal concentrations have the highest  $R^2$  value of 0.9947 while the mud containing 30 wt% nano lignite coal concentrations have the list  $R^2$  value of 0.6259, the mud containing 10 wt% nano lignite coal concentrations have the highest RMSE value of 2.8209 Pa while the mud containing 20 wt% nano lignite coal concentrations have the list RMSE value of 0.9342 Pa. However, it was observed that mud B have greater flow behaviour index value than mud A at all the nano lignite coal concentrations and less fluid consistency coefficient values than mud A expect for muds containing 10 wt% nano lignite coal concentrations, mud A have its highest  $R^2$  and RMSE values of 0.9643 and 3.6496 Pa at 20 wt% and 10 wt% nano lignite coal concentrations while mud B have its highest  $R^2$  and RMSE values of 0.9947 and 2.8209 Pa. at 20 wt% and 10 wt% nano lignite coal concentrations.

At 160 °C, the flow behaviour index ( $n$ ) and the fluid consistency coefficient ( $k$ ) of mud A ranged from 0.3623 to 0.4653 and 0.6278 Pa.s to 1.5911 Pa.s as the nano lignite coal concentrations in the mud system increases from 10 to 30 wt%, it was observed that mud A have the highest flow behaviour index value of 0.4653 at 10 wt% nano lignite coal concentrations and the list flow behaviour index value of 0.3623 at 20 wt% nano lignite coal concentrations, the highest fluid consistency coefficient value of 1.5911 Pa.s at 20 wt% nano lignite coal concentrations and the list fluid consistency coefficient value of 0.6278 Pa.s at 10 wt% nano lignite coal concentrations, mud A at 160 °C also exhibited non-Newtonian behaviour and shear thinning, as the values of flow behaviour index were less than unity ( $n < 1$ ). The coefficient of determination ( $R^2$ ) and Root Mean Square Error (RMSE) are ranged from 0.8620 to 0.9023 and 2.9271 Pa to 4.4363 Pa as the nano lignite coal concentrations in the mud system increases from 10 to 30 wt%. The mud containing 30 wt% nano lignite coal concentrations have the highest  $R^2$  value of 0.9023 while the mud containing 20 wt% nano lignite coal concentrations have the list  $R^2$  value of 0.8620, the mud containing 20 wt% nano lignite coal concentrations have the highest RMSE value of 4.4363 Pa while the mud containing 10 wt% nano lignite coal concentrations have the list RMSE value of 2.9271 Pa. While mud B at 160 °C have the flow behaviour index ( $n$ ) and the fluid consistency coefficient ( $k$ ) ranged from 0.3047 to 0.3512 and 1.7657 Pa.s to 2.7663 Pa.s as the nano lignite coal concentrations in the mud system increases from 10 to 30 wt%. It was observed that mud B have the highest flow behaviour index value of 0.3512 at 10 wt% nano lignite coal concentrations and the list flow behaviour index value of 0.3047 at 20 wt% nano lignite coal concentrations, the highest fluid consistency coefficient value of 2.7663 Pa.s at 20 wt% nano lignite coal concentrations and the list fluid consistency coefficient value of 1.7657 Pa.s at 10 wt% nano lignite coal concentrations, mud B at 160 °C also exhibited non-Newtonian behaviour and shear

thinning, as the values of flow behaviour index were less than unity ( $n < 1$ ). The coefficient of determination ( $R^2$ ) and Root Mean Square Error (RMSE) are ranged from 0.9017 to 0.9211 and 3.4980 Pa to 4.7913 Pa as the nano lignite coal concentrations in the mud system increases from 10 to 30 wt%. The mud containing 10 wt% nano lignite coal concentrations have the highest  $R^2$  value of 0.9211 while the mud containing 30 wt% nano lignite coal concentrations have the list  $R^2$  value of 0.9017, the mud containing 30 wt% nano lignite coal concentrations have the highest RMSE value of 4.7913 Pa while the mud containing 10 wt% nano lignite coal concentrations have the list RMSE value of 3.4980 Pa. Generally, it was observed that as the temperature increases, the coefficient of determination ( $R^2$ ) of both mud A and B decreases, it means that the coefficient of determination is inversely proportional to temperature as summarized in Table 4.4.

## CHAPTER FIVE

### 5.0 CONCLUSIONS AND RECOMMENDATIONS

#### 5.1 Conclusions

The experiment carried out was based on the modification of rheological and filtration properties of water-based drilling mud using lignite nanoparticles as additive, the spud muds prepared from the local and commercial bentonites were harnessed and the following conclusions are summarized.

The pretreatment with soda ash, enhanced the swelling capacities of the bentonites and easy dispersion when mixed with water. The characterizations carried out shows that the bentonites were crystalline in nature while lignite nanoparticles were semi crystalline, their internal structure were like spherical in shape.

The results of the spud water-based drilling muds obtained shows that the values were below API rheological properties standard ( $\geq 8$  cP for plastic viscosity and  $\geq 15$  cP for apparent viscosity) and above API filtration properties standard ( $\leq 15$  ml for fluid loss).

It can be deduced that the rheological and filtration properties of water-based drilling muds modified with lignite nanoparticles were improved by more than 100 % and the lignite nanoparticles offers stability to the water-based drilling muds with aging temperature up to 160 °C.

Based on the API standard for drilling mud, the laboratory results obtained shows that the lignite nanoparticles has improved effect on rheological and filtration properties of water-based drilling mud.

#### 5.2 Recommendations

- i. The use of micro size lignite particles is recommended in order to justify the effectiveness of nanoparticles for modification of drilling mud properties.

- ii. Chemical substance (metallic oxide) such as nano  $\text{Fe}_2\text{O}_3$ ,  $\text{TiO}_2$ ,  $\text{Al}_2\text{O}_3$ ,  $\text{CuO}$  and  $\text{SiO}$  extract from plants and solid waste combined with lignite nanoparticles for modification of rheological and filtration properties of drilling muds are recommended.
- iii. Because of the availability of local raw materials, it is recommended that drilling industries should patronize muds prepared from locally sourced additive in order to replace or reduced the importation of materials used in drilling Industry.

### **5.3 Contribution to Knowledge**

The lignite coal nanoparticles were found friendly to the environment and equipment due to its low percentage values of 0.10 % and 0.799 % for nitrogen and Sulphur content obtained from physicochemical analysis which may cause little or no environmental pollution and corrosion to the equipment.

The local bentonite used for formulation of drilling muds have substandard rheological properties such as 1.0 cP, 1.0 Ib/100ft<sup>2</sup> and 0 Ib/100ft<sup>2</sup> for plastic viscosity, yield point and gel strength respectively and when properly harnessed, the rheological properties drastically improved to 33.0 cP, 79.0 Ib/100ft<sup>2</sup> and 7.0 Ib/100ft<sup>2</sup> for plastic viscosity, yield point and gel strength respectively at room temperature.

The use of lignite nanoparticles for modification of water-based drilling muds shows drastic improvement on both rheological and filtration properties which were within the API bench marks standard such as plastic viscosity greater than equal to 8.0 cP, yield point 18.0 Ib/100ft<sup>2</sup>, gel strength 2.0 Ib/100ft<sup>2</sup> and the fluid loss less than equal to 15.0 mL at all the modifier concentration and the examined temperatures of 100 and 160 °C.

## REFERENCES

- Abdullahi, S. L. and Audu, A. A. (2017). Comparative Analysis on Chemical Composition of Bentonite Clays Obtained from Ashaka and Tango Deposits in Gombe State, Nigeria. *Chemical Search Journal*. 8(2): 35 – 40.
- Aboyade, A. O., Gorgens, J. F., Carrier, M., Meyer, E. L. and Knoetze, J. H. (2013). “Thermogravimetric study of the pyrolysis characteristics and kinetics of coal blends with corn and sugarcane residues.” *Fuel Processing Technology*. 106: 310–320.
- Adesina, F., Anthony, A., Gbadegesin, A., Eseoghene, O. and Oyakhire, A., (2012), “Environmental Impact Evaluation of a Safe Drilling Mud”, SPE 152865.
- Agarwal, S., Tran, P., Soong, Y., Martello, D. and Gupta, R. K. (2011). Flow Behavior of Nanoparticle Stabilized Drilling Fluids and Effect of High Temperature Aging. *AADE National Technical Conference and Exhibition*, 12–14, Houston, USA.
- Ahmed, S. M. (2016). Effect Of Temperature on the Rheological Properties with Shear Stress Limit of Iron Oxide Nanoparticle Modified Bentonite Drilling Muds. *Egyptian Journal of Petroleum*. <http://dx.doi.org/10.1016/j.ejpe>.
- Ali, E. B., Peyman, J. M., Ali, P., and Roozbeh, R. (2018). Experimental investigation of rheological and filtration properties of water- based drilling fluids in presence of various nanoparticles. *Department of Petroleum Engineering, Faculty of Petroleum and Chemical Engineering, Science and Research Branch, Islamic Azad University (IAU), Tehran, Iran*.
- Amani, M., Al-Jubouri, M. and Shadravan, A. (2012). Comparative Study of Using Oil-Based Mud Versus Water-Based Mud in HPHT Fields. *Advances in Petroleum Exploration and Development*, 4(2): 18-27 DOI: <http://dx.doi.org/10.3968/j.aped.1925543820120402.987>.
- Amanullah, M., Al-Arfaj, K. M, and Al-Abdullatif, Z, (2011). “Preliminary Test Results of Nano-based Drilling Fluids for Oil and Gas Field Application”, *SPE/AIDC 139534*, 1-9.
- Aminu, A., Lilian, A. O. and Gideon, M. A. (2013). Rheological and Filtration Properties of Kaolinite Based Drilling Mud. *International Journal of Scientific and Engineering Research*, 4(1): 2229-5518.
- Angaji, M. T., Amir, Z. Z. and Nader T. Q. (2013); Study of Physical, Chemical and Morphological Alterations of Smectite Clay upon Activation and Functionalization via the Acid Treatment. *World Journal of Nano Science and Engineering*. 3(1): 161-168.
- Annudeep, S. D. (2012). Rheological Properties and Corrosion Characteristics of Drilling Mud Additives. M.Eng. Thesis published. Dalhousie University.

- Apaleke, A. S., Al-Majed, A. A. and Hossain, M. E., (2012), “State of the Art and Future Trend of Drilling Fluid: An Experimental Study”, *SPE 153676. Arabia*.
- Aroke, U. O., Abdulkarim, A. and Ogubunka, R. O. (2013). Fourier-Transform Infrared Characterization of Kaolin, Granite, Bentonite and Barite. *ATBU Journal of Environmental Technology* 6(1): 42-53.
- Bageri, B., Al-Mutairi, S. and Mahmoud, M. (2013). Different Techniques for Characterizing the Filter Cake, *SPE Middle East Unconventional Gas Conference and Exhibition, Society of Petroleum Engineers, Muscat, Sultanate of Oman*.
- Bhattacharya, S. S. and Mandot, A. (2014). Studies on Preparation and Analysis of Organoclay Nano Particles. *Research Journal of Engineering Sciences*. 3(3), 10-16.
- Bizualem, W. and Busha A (2017). Physicochemical Characterization of Coal and its alternative as a Source of Energy (in case of Yayo Coal Mining). *Journal of Environmental Science, Toxicology and Food Technol.* 11(5): 44-50.
- Bodude, M. A., Ayoola, W. A., Oyetunji, A., Baba, Y.D., Odukoya, A. L., Onifade, O. A. and Olugbile, O. O. (2018). Proximate, Ultimate Analysis and Industrial Application of Some Nigerian Coals. *Journal of Engineering Research and Development*. 2(1): 20-25
- Caenn, R., Darley, H. C. H. and Gray, G.R. (2011). Composition and Properties of Drilling and Completion Fluids, The Filtration Properties of Drilling Fluids, sixth ed., Gulf Professional Publishing, Kidlington, Oxford.
- Chenevert, M.E., and Sharma, M. M. (2009). “Maintaining shale stability by pore plugging,” U S Patent 0314549.
- Dantas, A. P. T., Leite, R. S., Nascimento, R. C. A. M., And Amorim, L. V. (2014). The Influence of Chemical Additives in Filtration Control of Inhibited Drilling Fluids. *Brazilian Journal of Petroleum and Gas*. 8 (3): 097-108.
- Dardira, M. M., Ibrahimeia, S., Solimanb, M., Desoukya, S. D. and Hafiza, A. A. (2014). “Preparation and Evaluation of some Esteramides as Synthetic Based Drilling Fluids,” *Egypt Journal of Petroleum*. 23(1): 35–43.
- Deepark, K. (2014). Investigation of Flow Characteristics of Coal Water Slurry. M.Eng. Thesis published.
- Deng, Z., Livanec, P. W. and Deville, J. P. (2015). Novel Water-Based Fluids for oil-Sands Drilling. *SPE Canada Heavy Oil Technical Conference, Calgary, Alberta, Canada*. <http://dx.doi.org/10.2118/174420-MS>.
- Dina, K., Robiah, Y., Rozita, O., Suraya, A. R., and Badrul M. J. (2015). A review of biolubricants in drilling fluids: Recent research, performance, and applications. *Journal of Petroleum Science and Engineering*. 13(5): 177–184.

- Dutta, A. and Singh, N. (2014); Surfactant-Modified Bentonite Clays: Preparation, Characterization, and Atrazine Removal. *Environ Sci Pollut Res; Published online*.
- Ebikapaye, J. P. (2018). Effects of Temperature on the Density of Water Based Drilling Mud. *Journal of Applied Science and Environmental Management*. 22(3): 406–408. DOI: <https://dx.doi.org/10.4314/jasem.v22i3.20>
- Emine, A. and Bayram, A. M. (2019). The Rheology and Performance of Geothermal Spring Water-Based Drilling Fluids. *Hindawi Geofluids*.  
<https://doi.org/10.1155/2019/3786293>
- Ewy, R.T. and Morton, E.K. (2009). Wellbore-Stability performance of water-based mud additives, *SPE Drilling Completion*. 24 (3): 390–397.
- Ezquerro, C. S., Gemma, I. R., Cristina, C. M., Javier, S. B. (2015). Characterization of Montmorillonites Modified with Organic Divalent Phosphonium Cations. *Applied Clay Science*. 11(1): 1–9.
- Folayan, J. A., Anawe, P. L., Abioye, P. O. and Elehinafe, F. B. (2017). Selecting the Most Appropriate Model for Rheological Characterization of Synthetic Based Drilling Mud. *International Journal of Applied Engineering Research*. 12(18): 7614-7629.
- Francis, D. U. and Okon, A. (2012). Formulation of Water-Based Drilling Fluid Using Local Material. *Asian Journal of Microbiology Biotechnology and Environment Science*. 14 (2): 167-174.
- Gana, I. N., Ohageria, V. U., Akpan, U.G and Ani, I. J. (2019). Synthesis and Characterization of Bio-Synthesized Need-Based Zinc Oxide (ZnO) Photocatalyst. *Proceedings of the 49<sup>th</sup> Nigerian Society of Chemical Engineers (NSChE) Annual Conference KADA*: 479-488.
- Ghosn, R., Mihelic, F., Hochepped, J.F. and Dalmazzone, D. (2017). Silica Nanoparticles for the Stabilization of W/O Emulsions at HTHP Conditions for Unconventional Reserves Drilling Operations. *Oil Gas Science Technology* 72 (4): 21-27.
- Hanyi, Z., Peng, Y., Zhengsong, Q., Junbin, J. and Xiaodong, X. (2018). Mitigation of Lost Circulation in Oil-Based Drilling Fluids Using Oil Absorbent Polymers. *Journal of Petroleum Science and Engineering*. 16(3): 611–615.
- He, W., Jimbi, E., Chamberlin, M. and Zakaria, A. (2016). Invasion and Movement of Fluids in Shale Formations and Wellbore Stability. *In Proceedings of the SPE 178766, IADC/SPE Drilling Conference and Exhibition, Fort Worth, TX, USA*.
- Hoelscher, K. P., Stefano, G., Riley, M. and Young, S. (2012). Application of Nanotechnology in Drilling Fluids. *SPE International Oilfield Nanotechnology Conference* :1–7. Noordwijk: Society of Petroleum Engineers.

- Hossain, M. E. and Al-Majeed, A. A. (2012) ‘Fundamentals of Sustainable Drilling Engineering’ John Wiley and Sons and Scrivener Publishing Company, Austin, TX 78702, in press.
- Husein, M. M. and Nassar, N. N. (2008). “Nanoparticles Preparation using the single microemulsion scheme, “*Current Nanoscience*.4(1): 370-380,
- Idris, M. N. and Ahmed, Z. D. (2019) Qualitative Characterization of Coal Minerals Selected From 5 Different Locations in Nigeria For Possible Studies on Gasification Technology. *International Journal of Engineering and Modern Technology* E-ISSN 2504-8848 P-ISSN 2695-2149, 5 (2): 55-69. [www.iiardpub.org](http://www.iiardpub.org)
- Jeffrey, O. O., Afeez, O. G., Adebayo, O. and Oluwagbenga, O. O. (2018). Transports of Different Cuttings Sizes in A Wellbore using Henna and Lignite Materials. *ABUAD Journal of Engineering Research and Development*. 1 (3): 351-365.
- Jung, C. M., Zhang, R., Chenevert, M. and Sharma, M. (2013). High Performance Water-Based Mud using Nanoparticles for Shale Reservoirs. *Unconventional Resources Technology Conference*: 1–7. Denver, CO: Society of Petroleum Engineers.
- Kania, D., Yunus, R. Omar, R., Abdulrashid, S. and Mohamad, B. J. (2015) “A Review of Biolubricants in Drilling Fluids: Recent research, performance, and applications.” *Journal of Petroleum Science and Engineering*. 135(9): 177–184.
- Li, F. X., Jiang, G. C., Wang, Z. K. and Cui, M. R., (2014), “Drilling Fluid from Natural Vegetable Gum”. *Petroleum Science and Technology*., 32 (6): 738-744.
- Liang, L. He, S., Zeng, Y., Ding, Y., Lin, Y. and Liu, X. (2016). The Influence of Water-Based Drilling Fluid on Mechanical Property of Shale and the Wellbore Stability. *Journal of Petroleum*. 2 (1): 61– 66.
- Mahmoud, O., Nasr El-Din, H., Vryzas, Z., & Kelessidis, V. (2016). Nanoparticle Based Drilling Fluids for Minimizing Formation Damage in HP/HT applications. *SPE International Conference and Exhibition on Formation Damage and Control*: 1–26. Lafayette, LA: Society of Petroleum Engineers.
- Mansoor, A. K., Hikmat, S. A., Leila, N. A. (2018). Development of High Temperature High Pressure (HTHP) Water Based Drilling Mud using Synthetic Polymers, and Nanoparticles. *Journal of Advanced Research in Fluid Mechanics and Thermal Sciences*. 45 (1): 99-108.
- Mehaysen A. M. and Shakhathreh K. S. (2012) Evaluation of Jordanian Bentonite Performance for Drilling Fluid Applications. *Contemporary Engineering Sciences*. 5(3):149-170.
- Mehran, H., Moshfiqu, R. and Rajender, G. (2015). Kinetic Study and Thermal Decomposition Behavior of Lignite Coal. *International Journal of Chemical Engineering*. <http://dx.doi.org/10.1155/2015/481739>

- Mohammad, F. Z. (2013). Nanoparticle-based Drilling Fluids with Improved Characteristics. Phd Thesis. University of Calgary.
- Mohamed, K., Malika, K. S., Jean, P. C., Nathalie, C., and Faïza, B. (2010). Drilling Fluid Technology: Performances and Environmental Considerations. *Journal of Applied Clay Science*. 49 (4): 383-393.
- Noah, A. Z., El Semary, M. A., Youssef, A. M. and El-Safty, M.A. (2017). Enhancement of Yield Point at High Pressure High Temperature Wells by using Polymer Nanocomposites Based on ZnO and CaCO<sub>3</sub> Nanoparticles. *Egypt Journal of Petroleum*. 26 (1): 33–40.
- Nwaoboli, A. (2014). Investigation of Additives on Drilling Mud Performance With “Tønder Geothermal Drilling” as a Case Study. Master Thesis Published by Aalborg University Denmark.
- Nweke, O. M., Igwe, E. O. and Nnabo, P. N. (2015). Comparative Evaluation of Clays from Abakaliki Formation with Commercial Bentonite Clays for use as Drilling Mud. *Africa Journal of Environmental Science and Technology*. 9(6): 508-518.
- Ogbeide, P. O. and Igbinere, S. A. (2016). The Effect of Additives on Rheological Properties of Drilling Fluid in Highly Deviated Wells. *FUTO Journal Series*. 2 (2): 68 - 82.
- Okorie, E. A., Anietie, N. O. and Francis, D. U. (2014). A Comparative Study of Diesel Oil and Soybean Oil as Oil-Based Drilling Mud. *Journal of Petroleum Engineering*. DOI: <http://dx.doi.org/10.1155/2015/828451>.
- Okorie, E. A., Anietie, N. O. and Offiong, I. A. (2016). Activation of Local Bentonitic Clays for Use as Viscosifiers in Water-based Drilling Fluids. *Journal of Scientific Research and Reports*. 12(2): 1-11.
- Omer, A. A. M., Mutasim, H. A. A., Mutasim, A. K. A. and Mohammed, F. M. (2016). Evaluation of Local Bentonite for Utilization as Oil Well Drilling Mud. Bachelor of Science Thesis Published by Sudan University of Science and Technology.
- Omole, O., James, O. A., Olugbenga, F., Malomo, S. and Oyedeji, O. A. (2013). Investigation into the Rheological and Filtration Properties of Drilling Mud Formulated with Clays from Northern Nigeria. *Journal of Petroleum and Gas Engineering*. 4(1): 1-13.
- Pavel, A. B., and Mikhail, V. D. (2018). Rheological and Filtration Parameters of the Polymer Salt Drilling Fluids Based on Xanthan Gum. Department of Borehole Drilling. *Journal of Engineering and Applied Sciences*. 13(14): 5661-5664.
- Piroozian, A., Ismail, I., Yaacob, Z., Babakhani, P. and Ismail, A. S. I. (2012). Impact of Drilling Fluid Viscosity, Velocity and Hole Inclination on Cuttings Transport in

- Horizontal and Highly Deviated Wells. *Journal of Petroleum Exploration and Production Technology*. 2 (3): 149–156.
- Putri Y., Sonny, I. and Dina K. (2016). Optimization of Water-Based Drilling Fluid using Non-ionic and Anionic Surfactant Additives. *4th International Conference on Process Engineering and Advanced Materials*. 148(4): 1184-1190.
- Rasheed, M. A., Srinivasa Rao, P. L., Annapurna, B., Syed, Z. H., Arpit, P. V. and Velani, K. P. (2015). Geochemical Characterization of Coals Using Proximate and Ultimate Analysis of Tadkeshwar Coals, Gujarat. *Geosciences*. 5(4): 113-119 DOI:10.5923/j.geo.20150504.01
- Rezaee, R., Saeedi, A. and Clennell, B. (2012). “Tight Gas Sands Permeability Estimation from Mercury Injection Capillary Pressure and Nuclear Magnetic Resonance Data”. *Journal of Petroleum Science and Engineering*. 88(89): 92-99.
- Richard, O. A, Oyinkepreye, D. O. and Vincent, E. E. (2016). Properties and Application of Nigerian Bentonite Clay Deposits for Drilling Mud Formulation. <http://dx.doi.org/10.1016/j.clay.2017.03.009>
- Sadeghalvaad, M. and Sabbaghi, S. (2015). The Effect of the TiO<sub>2</sub> Polyacrylamide Nanocomposite on Water-Based Drilling Fluid Properties. *Powder Technology*. 272(7): 113–119. <http://dx.doi.org/10.1016/j.powtec.2014.11.032>
- Sahni, A., Saraswati, P. K., Rana, R. S., Kumar, K., Singh, H., Alimohammadian, H., Sahni, N., Rose, Kd, Singh, L. and Smith, T. (2013). Palynostratigraphy and Depositional Environment of Vastan Lignite Mine Gujarat, Western India. *Journal of Earth System Science*. 122(1): 289-307.
- Sedaghatzadeh, M., Khodadadi, A. A. and Tahmasebi Birgani, M. R. (2012). An Improvement in Thermal and Rheological Properties of Water-based Drilling Fluids Using Multiwall Carbon Nanotube (MWCNT). *Iranian Journal of Oil and Gas Science and Technology*. 1 (1): 55-65.
- Sehly, K., Chiew, H. L., Li, H., Song, A., Leong, Y. and Huang, W. (2015). Stability and Ageing Behaviour and the Formulation of Potassium-Based Drilling Muds. *Journal of Applied Clay Science*. 104(2): 309–317.
- Sensoy, T., Chenevert, M. E. and Sharma, M. M. (2009) “Minimizing water invasion in shale using nanoparticles”, PE 124429 presented at the 2009 PE Annual Technical Conference and Exhibition, New Orleans, LA.
- Skalle, P., (2010). Drilling Fluid Engineering. Bookboon.
- Solomon, A. R. and Aliyu, J. (2013). Proximate analysis, rheological properties and technological applications of some Nigerian coals. *Ryemshak and Jauro International Journal of Industrial Chemistry*. 4(7): 1-7.

- Speight, J. G. (2013). *The Chemistry and Technology of Coal*. 3rd Ed. Boca Raton: CRC Press, 2013. ISBN 978-14398-3648-4.
- Toka, B. and Toka, N. (2015). Preparing Drilling Fluid Compositions for Geothermal Reservoirs.
- Toyese, O. (2013). Optimization of Rheological and Filtration Properties of Nigeria Clay Using Factorial Design. *International Journal of Innovative Scientific and Engineering Technologies Research*. 1(1): 25-36.
- Valizadeh, M. and Nasiri, A. R. (2012). Improving Thermal Stability of Starch in Formate Fluids for Drilling High Temperature Shales. *Journal of Petroleum Science and Technology*. 2(1): 61-64.
- Vipulanandan, C and Mohammed, A. (2014). Hyperbolic Rheological Model with Shear Stress Limit for Acrylamide Polymer Modified Bentonite Drilling Muds. *Journal of Petroleum Science and Engineering*.  
DOI: <http://dx.doi.org/10.1016/j.petrol.2014.08.004>
- Wenxi, Z., Xiuhua, Z. and Zeng, L. (2020). Improvement of CMC on the Performance of CGA Drilling Fluids for Geothermal Drilling. *Proceedings World Geothermal Congress*. Reykjavik, Iceland.
- Yao, R., Jiang, G., Li, W., Deng, T. and Zhang, H. (2013). Effect of Water-Based Drilling fluid Components on Filter Cake Structure. *Journal of Petroleum Technology*. 23(19): 1193-1201.
- Zakaria, M. F., Husein, M. and Hareland, G. (2012). Novel Nanoparticle-Based Drilling Fluid with Improved Characteristics. *SPE International Oil field Nanotechnology Conference*: 1–6. Noordwijk: Society of Petroleum Engineers.
- Zisis, V., Omar, M., Hisham, N., Vassilis, Z. and Vassilios, C. K. (2016). Incorporation of Fe<sub>3</sub>O<sub>4</sub> Nanoparticles as Drilling Fluid Additives for Improved Drilling Operations. *Proceedings of the 35<sup>th</sup> International Conference on Ocean, Offshore and Arctic Engineering Busan, South Korea*.

## Appendix A

The equipment's used in the laboratory



Plate A-1: Fann 35A Viscometer



Plate A-2: Mud balance



Plate A-3 Aging cell



Plate A-4 Aging cell assembly



Plate A-5 Roller oven



Plate A-6 Roller Oven in operation



Plate A-7 Fluid loss setup



Plate A-8 Prepared drilling mud and their cake thickness

## Appendix B

### Characterization of samples

#### Size Distribution Report by Volume

v2.2



##### Sample Details

Sample Name: Lignite Coal  
 SOP Name: Test.sop  
 General Notes: Average result created from record number(s): 200 202

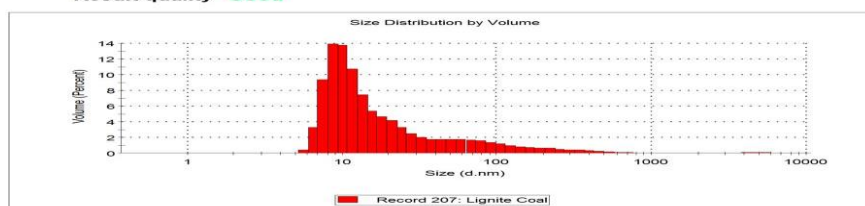
File Name: D S L.dts	Dispersant Name: Water
Record Number: 207	Dispersant RI: 1.330
Material RI: 1.59	Viscosity (cP): 0.8872
Material Absorbtion: 0.010	Measurement Date and Time: 14 February 2020 19:47:59

##### System

Temperature (°C): 25.0	Duration Used (s): 70
Count Rate (kcps): 184.7	Measurement Position (mm): 4.65
Cell Description: Disposable sizing cuvette	Attenuator: 10

##### Results

Z-Average (d.nm): 101.4	Peak 1: 129.8	Size (d.nm): 129.8	% Volume: 16.8	St Dev (d.nm): 114.6
Pdl: 0.289	Peak 2: 14.15	Size (d.nm): 14.15	% Volume: 82.9	St Dev (d.nm): 8.168
Intercept: 0.950	Peak 3: 4984	Size (d.nm): 4984	% Volume: 0.3	St Dev (d.nm): 889.2
Result quality: <b>Good</b>				



Malvern Instruments Ltd  
www.malvern.com

Zetasizer Ver. 7.01  
Serial Number: N/A

File name: D S L  
Record Number: 207  
14 Feb 2020 19:49:11

#### Size Distribution Report by Intensity

v2.2



##### Sample Details

Sample Name: Lignite Coal  
 SOP Name: Test.sop  
 General Notes: Average result created from record number(s): 200 202

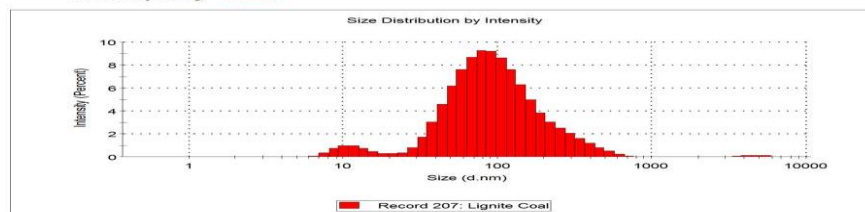
File Name: D S L.dts	Dispersant Name: Water
Record Number: 207	Dispersant RI: 1.330
Material RI: 1.59	Viscosity (cP): 0.8872
Material Absorbtion: 0.010	Measurement Date and Time: 14 February 2020 19:47:59

##### System

Temperature (°C): 25.0	Duration Used (s): 70
Count Rate (kcps): 184.7	Measurement Position (mm): 4.65
Cell Description: Disposable sizing cuvette	Attenuator: 10

##### Results

Z-Average (d.nm): 101.4	Peak 1: 119.8	Size (d.nm): 119.8	% Intensity: 94.8	St Dev (d.nm): 90.95
Pdl: 0.289	Peak 2: 12.21	Size (d.nm): 12.21	% Intensity: 4.7	St Dev (d.nm): 3.541
Intercept: 0.950	Peak 3: 4647	Size (d.nm): 4647	% Intensity: 0.4	St Dev (d.nm): 809.3
Result quality: <b>Good</b>				



Malvern Instruments Ltd  
www.malvern.com

Zetasizer Ver. 7.01  
Serial Number: N/A

File name: D S L  
Record Number: 207  
14 Feb 2020 19:49:31

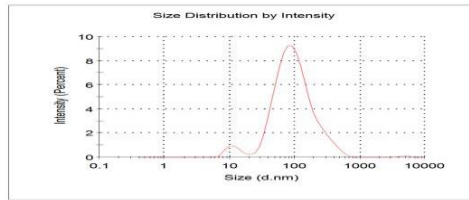
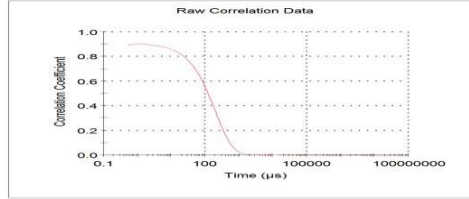
**Size Quality Report**  
v2.0

Malvern Instruments Ltd - © Copyright 2008



**Sample Name:** Lignite Coal  
**SOP Name:** Test.sop  
**File Name:** D S L.dts  
**Record Number:** 207  
**Measurement Date and Time:** 14 February 2020 19:47:59  
**Temperature (°C):** 25.0

**RESULT MEETS QUALITY CRITERIA**



Malvern Instruments Ltd  
www.malvern.com

Zetasizer Ver. 7.01  
Serial Number : N/A

File name: D S L  
Record Number: 207  
14 Feb 2020 19:49:42

# Correlogram Report

v2.0

Malvern Instruments Ltd - © Copyright 2008



## Sample Details

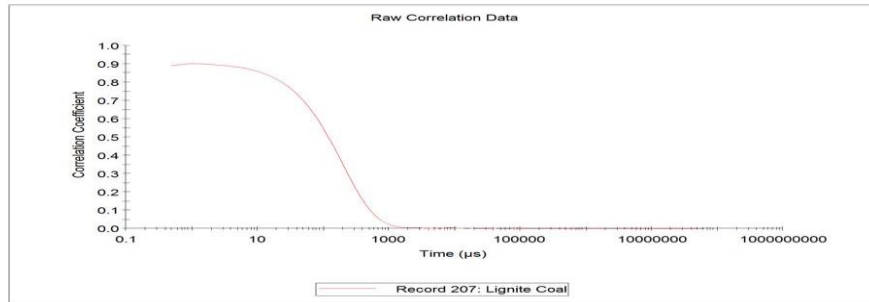
**Sample Name:** Lignite Coal  
**SOP Name:** Test.sop  
**General Notes:** Average result created from record number(s): 200 202

<b>File Name:</b> D S L.dts	<b>Dispersant Name:</b> Water
<b>Record Number:</b> 207	<b>Dispersant RI:</b> 1.330
<b>Material RI:</b> 1.59	<b>Viscosity (cP):</b> 0.8872
<b>Material Absorbtion:</b> 0.010	<b>Measurement Date and Time:</b> 14 February 2020 19:47:59

## System

<b>Temperature (°C):</b> 25.0	<b>Duration Used (s):</b> 70
<b>Count Rate (kcps):</b> 184.7	<b>Measurement Position (mm):</b> 4.65
<b>Cell Description:</b> Disposable sizing cuvette	<b>Attenuator:</b> 10

## Results



Malvern Instruments Ltd  
www.malvern.com

Zetasizer Ver. 7.01  
Serial Number : N/A

File name: D S L  
Record Number: 207  
14 Feb 2020 19:49:54

# Cumulants Fit Report

v2.0

Malvern Instruments Ltd - © Copyright 2008



## Sample Details

**Sample Name:** Lignite Coal  
**SOP Name:** Test.sop  
**General Notes:** Average result created from record number(s): 200 202

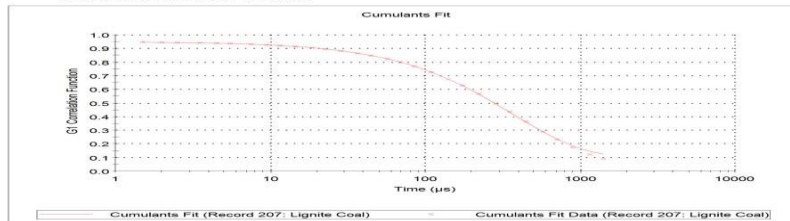
<b>File Name:</b> D S L.dts	<b>Dispersant Name:</b> Water
<b>Record Number:</b> 207	<b>Dispersant RI:</b> 1.330
<b>Material RI:</b> 1.59	<b>Viscosity (cP):</b> 0.8872
<b>Material Absorbtion:</b> 0.010	<b>Measurement Date:</b> 14 February 2020 19:...

## System

<b>Temperature (°C):</b> 25.0	<b>Duration Used (s):</b> 70
<b>Count Rate (kcps):</b> 184.7	<b>Measurement Position (mm):</b> 4.65
<b>Derived Count Rate (kcps):</b> 657.1	<b>Attenuator:</b> 10
<b>Cell Description:</b> Disposable sizing cuvette	

## Results

**Cumulants Fit Error:** 0.00196



Malvern Instruments Ltd  
www.malvern.com

Zetasizer Ver. 7.01  
Serial Number : N/A

File name: D S L  
Record Number: 207  
14 Feb 2020 19:50:07

## Distribution Fit Report

v2.0



Malvern Instruments Ltd - © Copyright 2008

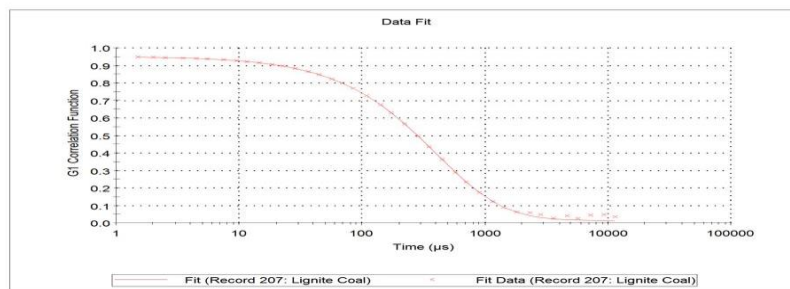
### Sample Details

<b>Sample Name:</b>	Lignite Coal	<b>Dispersant Name:</b>	Water
<b>SOP Name:</b>	Test.sop	<b>Dispersant RI:</b>	1.330
<b>General Notes:</b>	Average result created from record number(s): 200 202		
<b>File Name:</b>	D S L.dts	<b>Viscosity (cP):</b>	0.8872
<b>Record Number:</b>	207	<b>Measurement Date and Time:</b>	14 February 2020 19:4...
<b>Material RI:</b>	1.59		
<b>Material Absorbtion:</b>	0.010		

### System

<b>Temperature (°C):</b>	25.0	<b>Duration Used (s):</b>	70
<b>Count Rate (kcps):</b>	184.7	<b>Measurement Position (mm):</b>	4.65
<b>Derived Count Rate (kcps):</b>	657.1	<b>Attenuator:</b>	10
<b>Cell Description:</b>	Disposable sizing cuvette		

### Results



Malvern Instruments Ltd  
www.malvern.com

Zetasizer Ver: 7.01  
Serial Number: N/A

File name: D S L  
Record Number: 207  
14 Feb 2020 19:50:18

Figure B-1: Nano Size Distribution of Lignite Coal



# SPECTRAL LABORATORY SERVICES

[YOUR ONE STOP LAB FOR ANALYSES]

SPECIALISE IN LABORATORY ANALYSIS SUCH AS:

WATER ANALYSIS, PROXIMATE & ULTIMATE ANALYSIS, PHYSICO-CHEMICAL PARAMETERS, TGA, FTIR, SEM, AAS, GAS ANALYSIS, MICROBIAL ANALYSIS, ETC.

15<sup>th</sup> February, 2020

Dear Client: Mr. Aliyu

Below is the result of the proximate analysis on the sample. Thank you for the patronage.

SPECTRAL LABORATORY  
SERVICES  
SIGN \_\_\_\_\_  
DATE \_\_\_\_\_

Sign:

Engr. Tech. Wahidat Ibrahim

Lab. Technologist

Table B-1: Proximate Analyses of Nano Lignite Coal

S/N	PARAMETERS	UNIT	Trial 1	Trial 2	Trial 3
1	MOISTURE CONTENT	%	1.79	1.30	1.45
2	ASH CONTENT	%	1.825	1.825	1.775
3	VOLATILE MATTER	%	15.085	15.475	15.48
4	FIXED CARBON	%	81.3	81.4	81.3

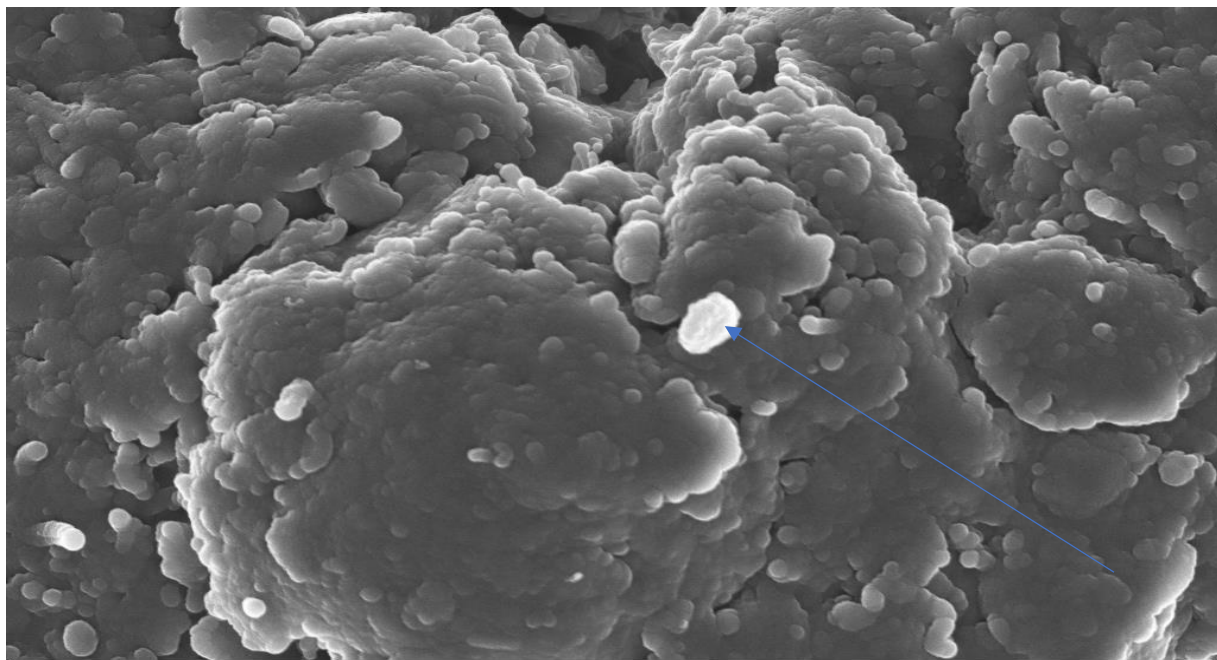
Table B-2: Proximate Analyses of Nano Lignite Coal

S/N	PARAMETERS	UNIT	VALUE
1	CARBON	%	90.0
2	HYDROGEN	%	8.38
3	NITROGEN	%	0.16
4	SULPHUR	%	0.79
5	OXYGEN	%	0.67

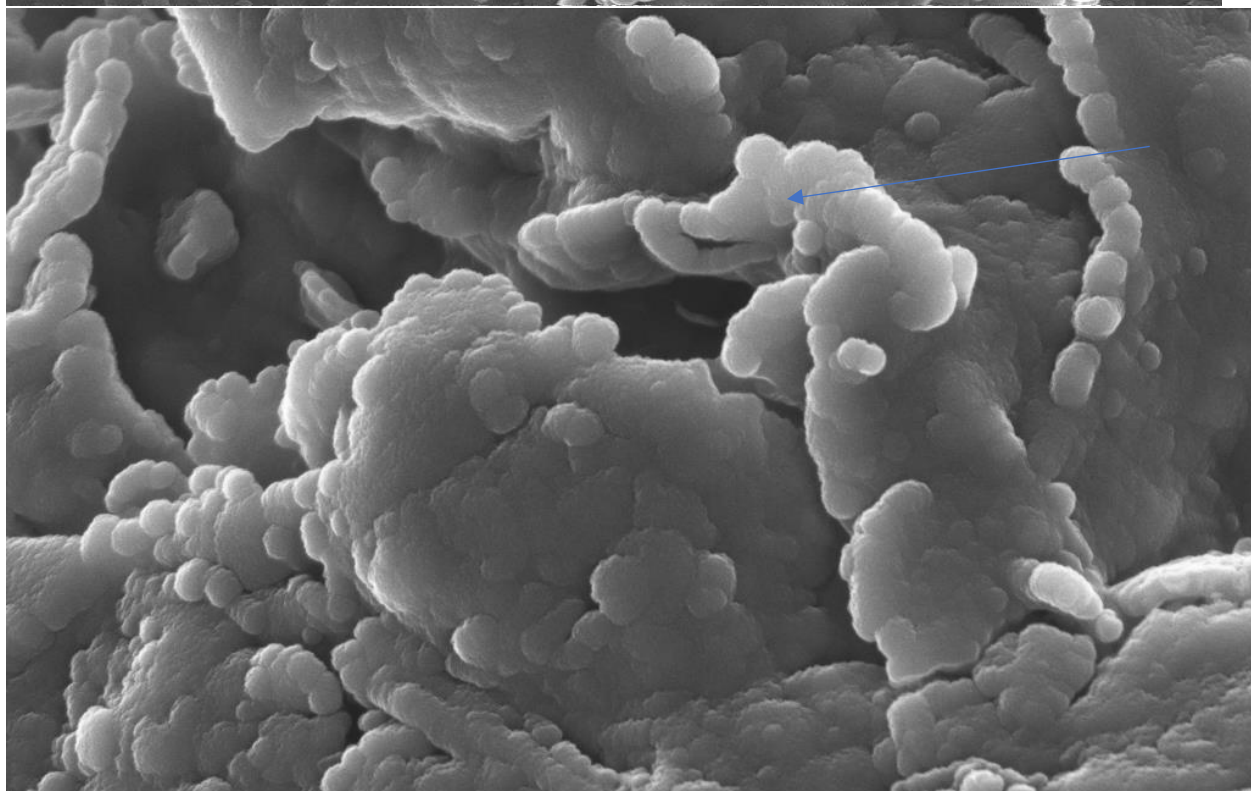
Consultant :  
LAWAL, KABIR, ENGR. TECH.  
COREN/REG/R3879ET  
NATE: 6183

14. FORTE OIL STATION POLYTECHNIC ROAD, KADUNA SOUTH, KADUNA STATE.

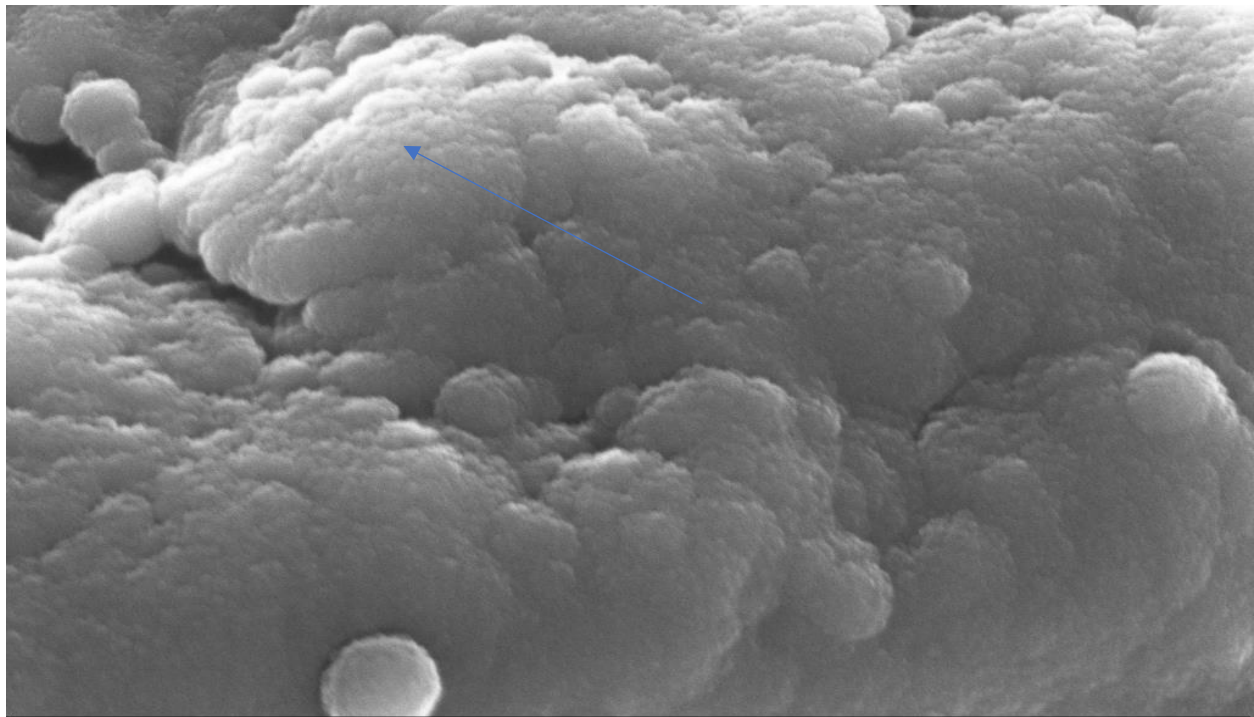
+234(0)703 134 4626, 0816 631 3988 Fax: +234-8025-472-083 wahidatibrahim@gmail.com



1  $\mu\text{m}$  | EHT = 5.00 kV | Signal A = InLens | Date :4 Mar 2020  
WD = 4.5 mm | Mag = 10.00 K X | Pixel Size = 11.16 nm | ZEISS



300 nm | EHT = 5.00 kV | Signal A = InLens | Date :4 Mar 2020  
WD = 4.5 mm | Mag = 20.00 K X | Pixel Size = 5.582 nm | ZEISS

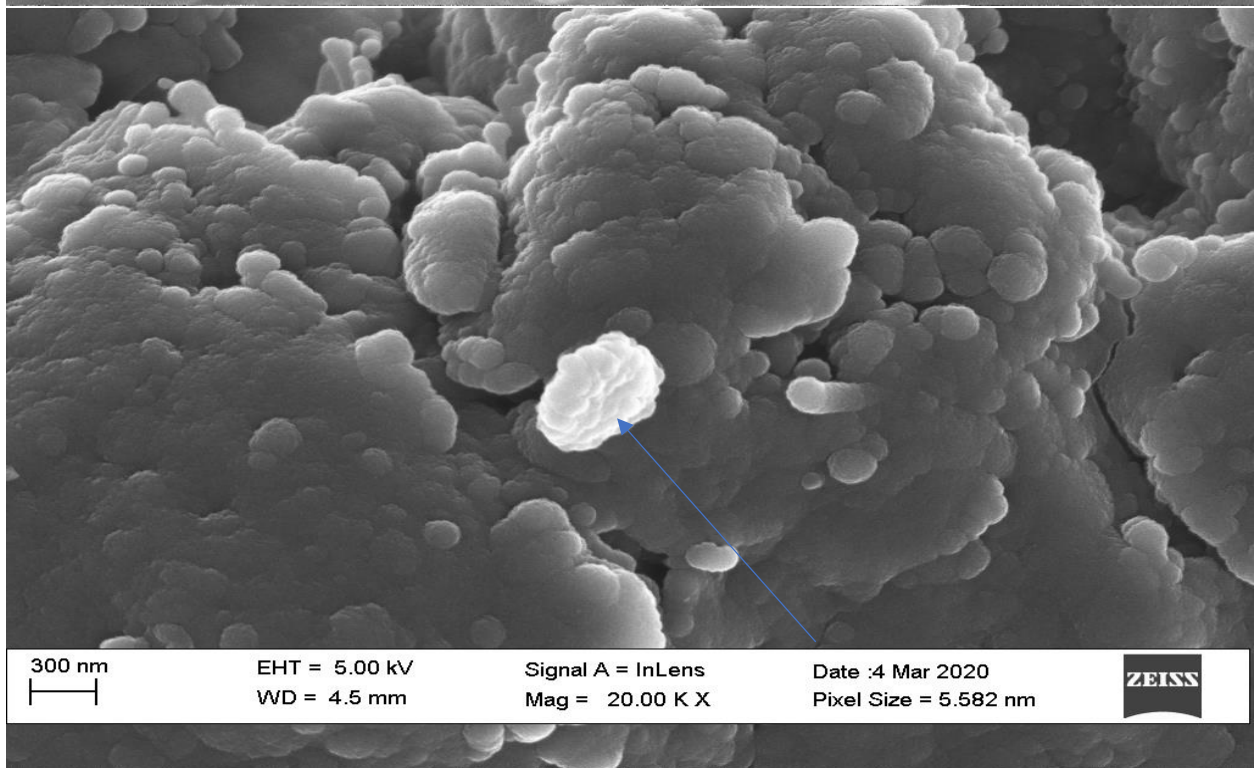


100 nm  
|—|

EHT = 5.00 kV  
WD = 4.5 mm

Signal A = InLens  
Mag = 50.00 K X

Date :4 Mar 2020  
Pixel Size = 2.233 nm



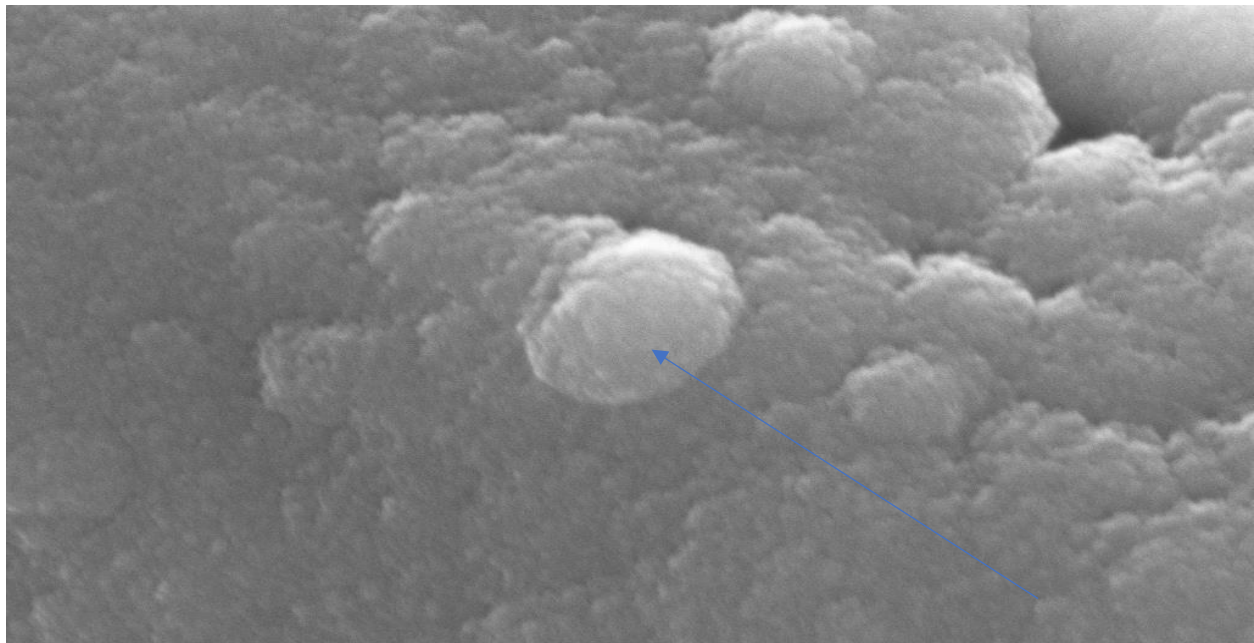
300 nm  
|—|

EHT = 5.00 kV  
WD = 4.5 mm

Signal A = InLens  
Mag = 20.00 K X

Date :4 Mar 2020  
Pixel Size = 5.582 nm





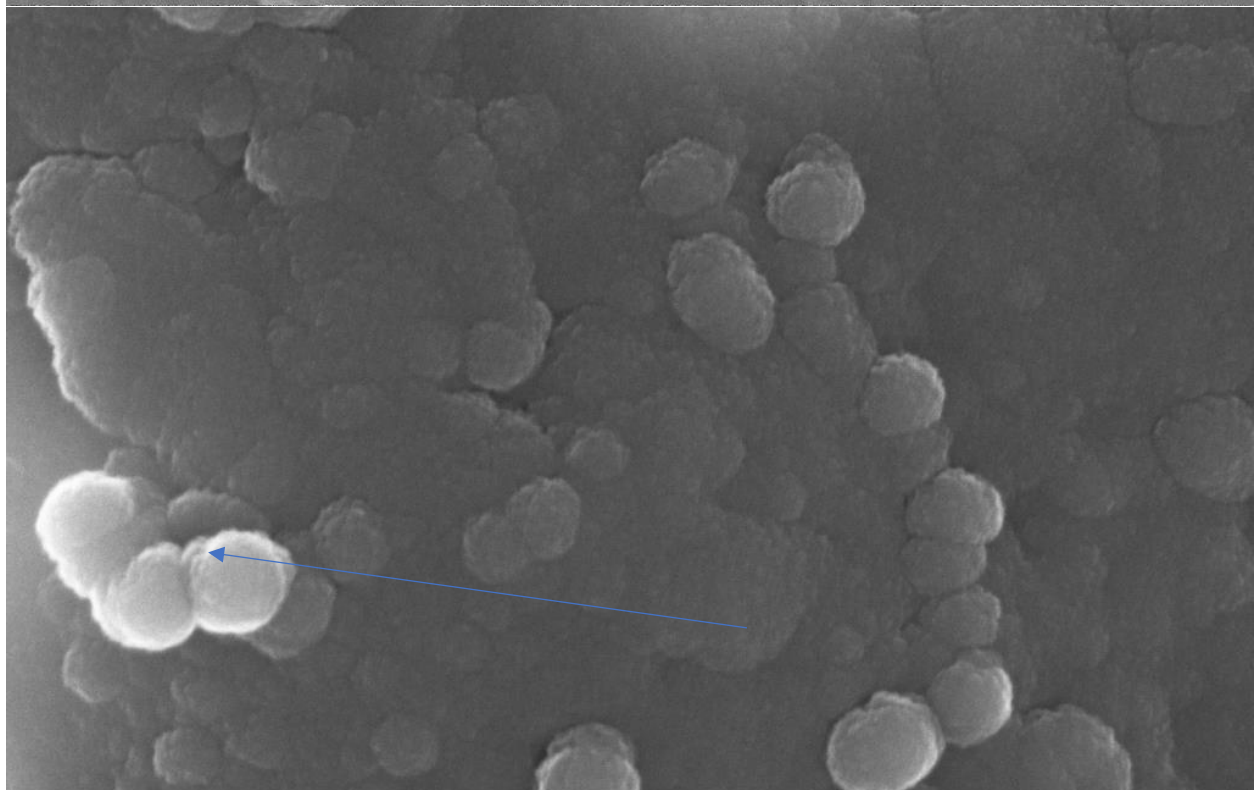
100 nm



EHT = 5.00 kV  
WD = 4.5 mm

Signal A = InLens  
Mag = 100.00 K X

Date :4 Mar 2020  
Pixel Size = 1.116 nm



200 nm



EHT = 5.00 kV  
WD = 4.5 mm

Signal A = InLens  
Mag = 50.00 K X

Date :4 Mar 2020  
Pixel Size = 2.233 nm



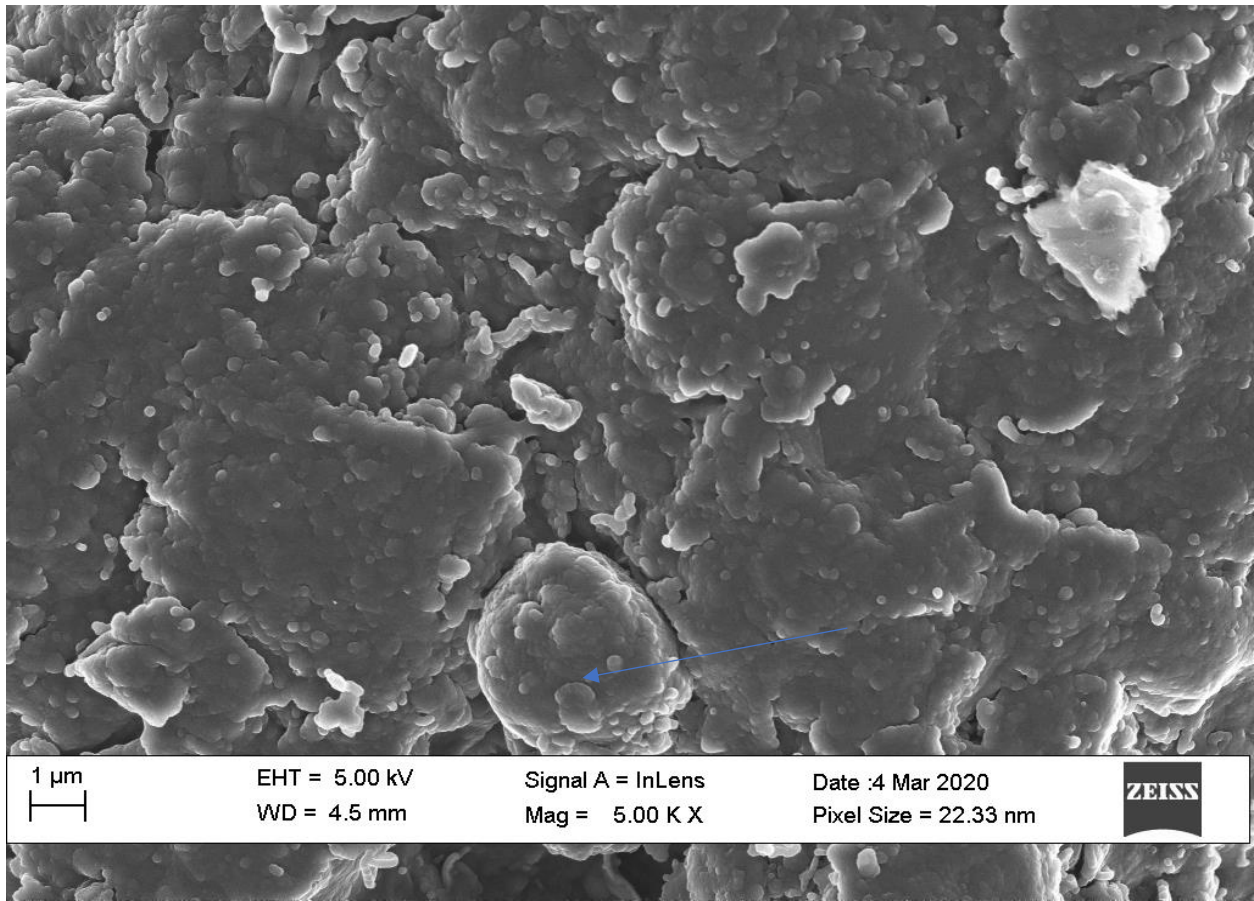
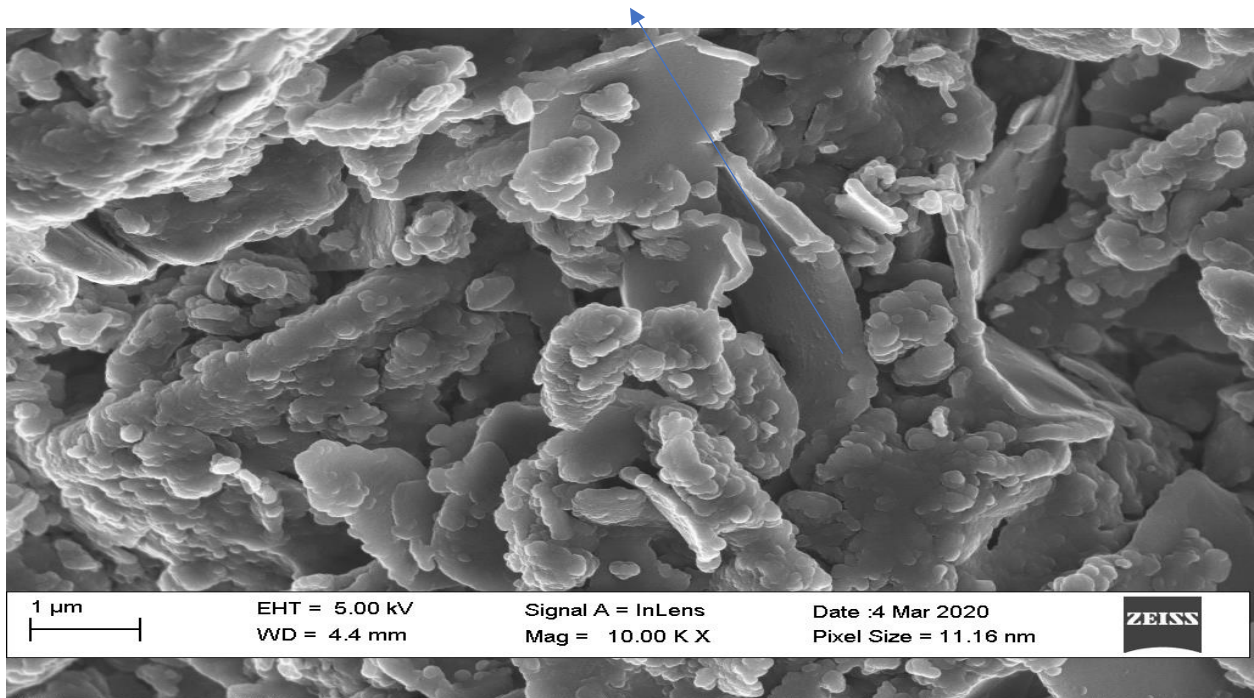
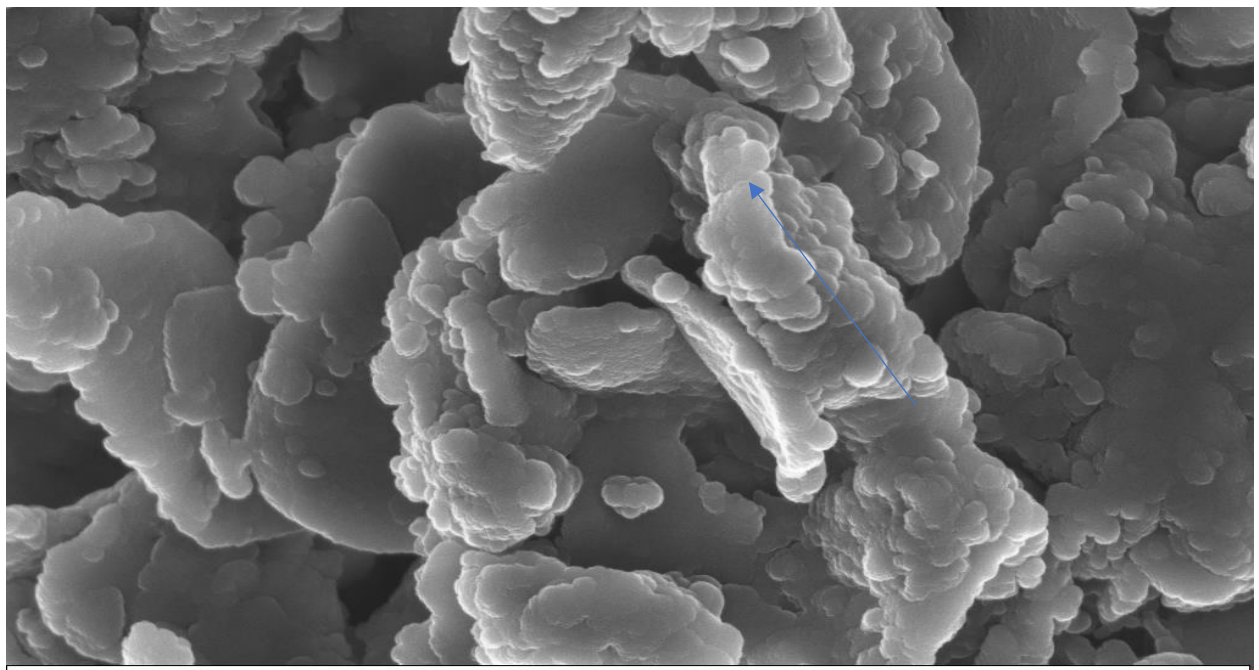
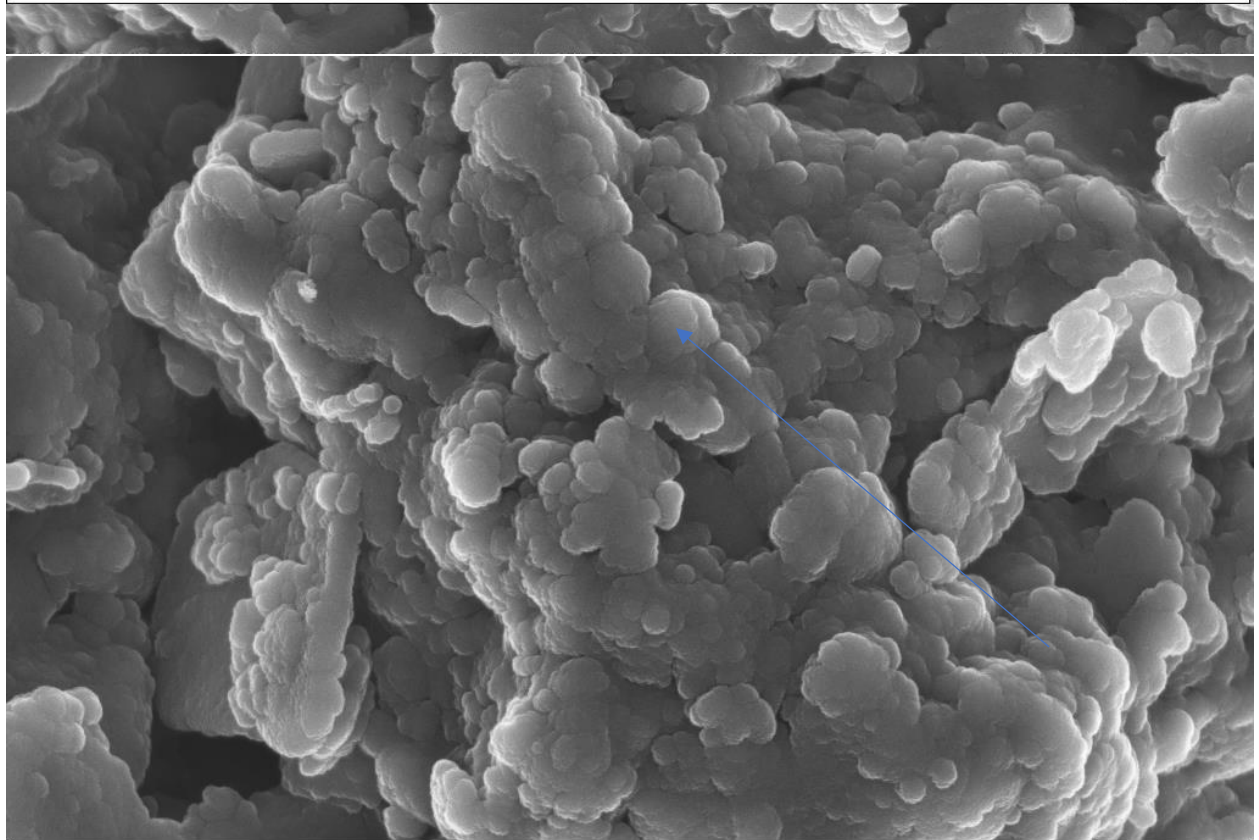


Figure B-2: SEM Image of Commercial Bentonite Clay

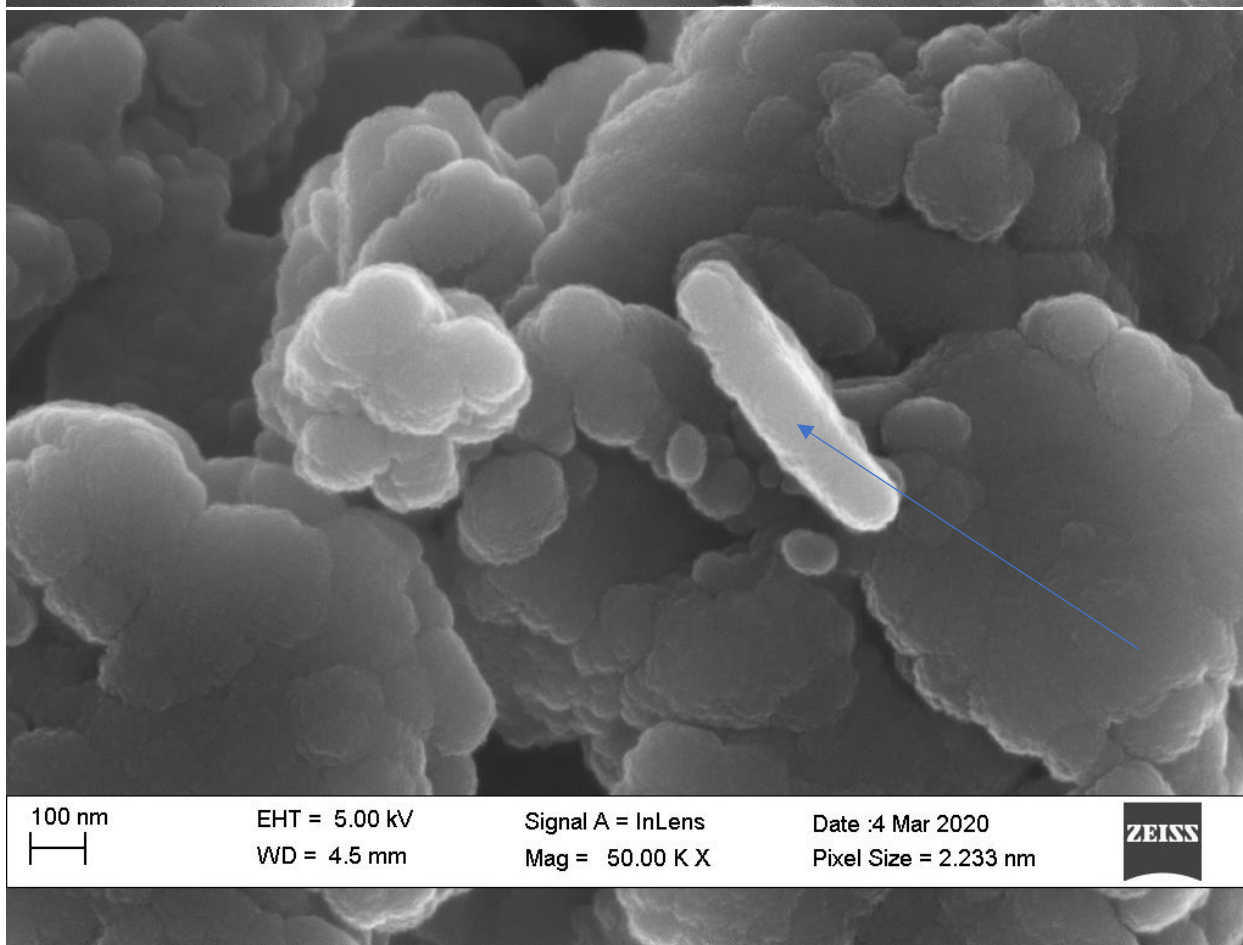
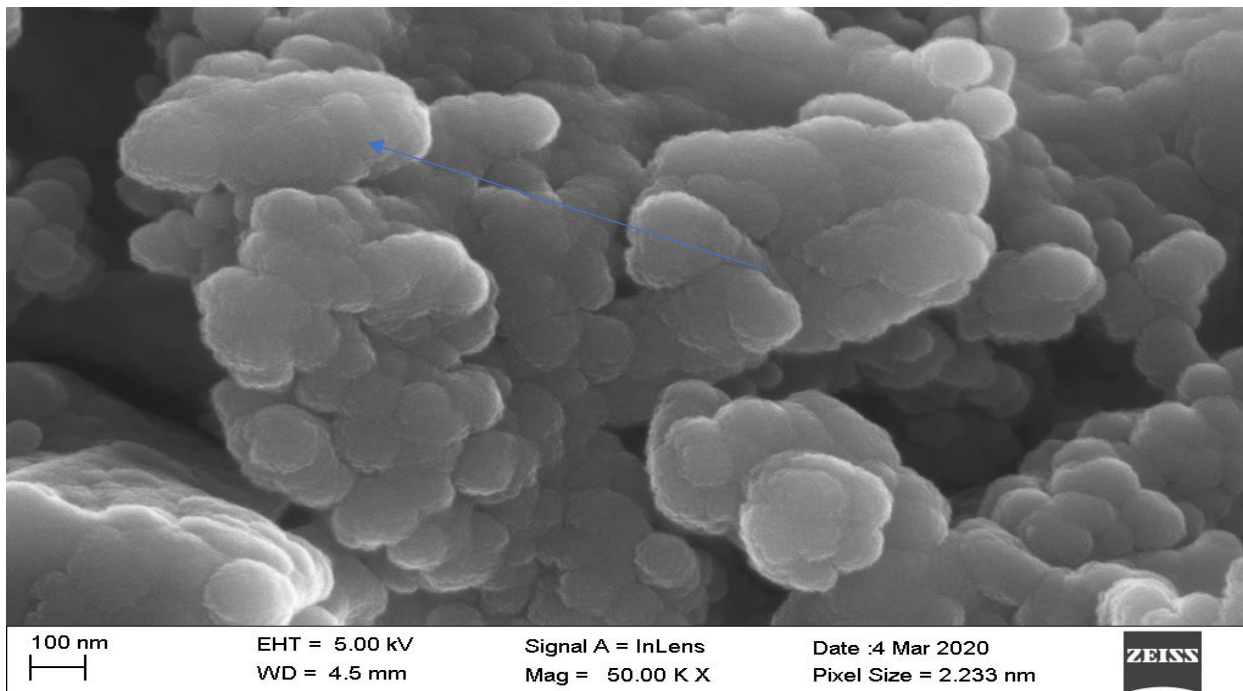




200 nm EHT = 5.00 kV Signal A = InLens Date :4 Mar 2020  
WD = 4.4 mm Mag = 20.00 K X Pixel Size = 5.582 nm ZEISS



200 nm EHT = 5.00 kV Signal A = InLens Date :4 Mar 2020  
WD = 4.5 mm Mag = 20.00 K X Pixel Size = 5.582 nm ZEISS



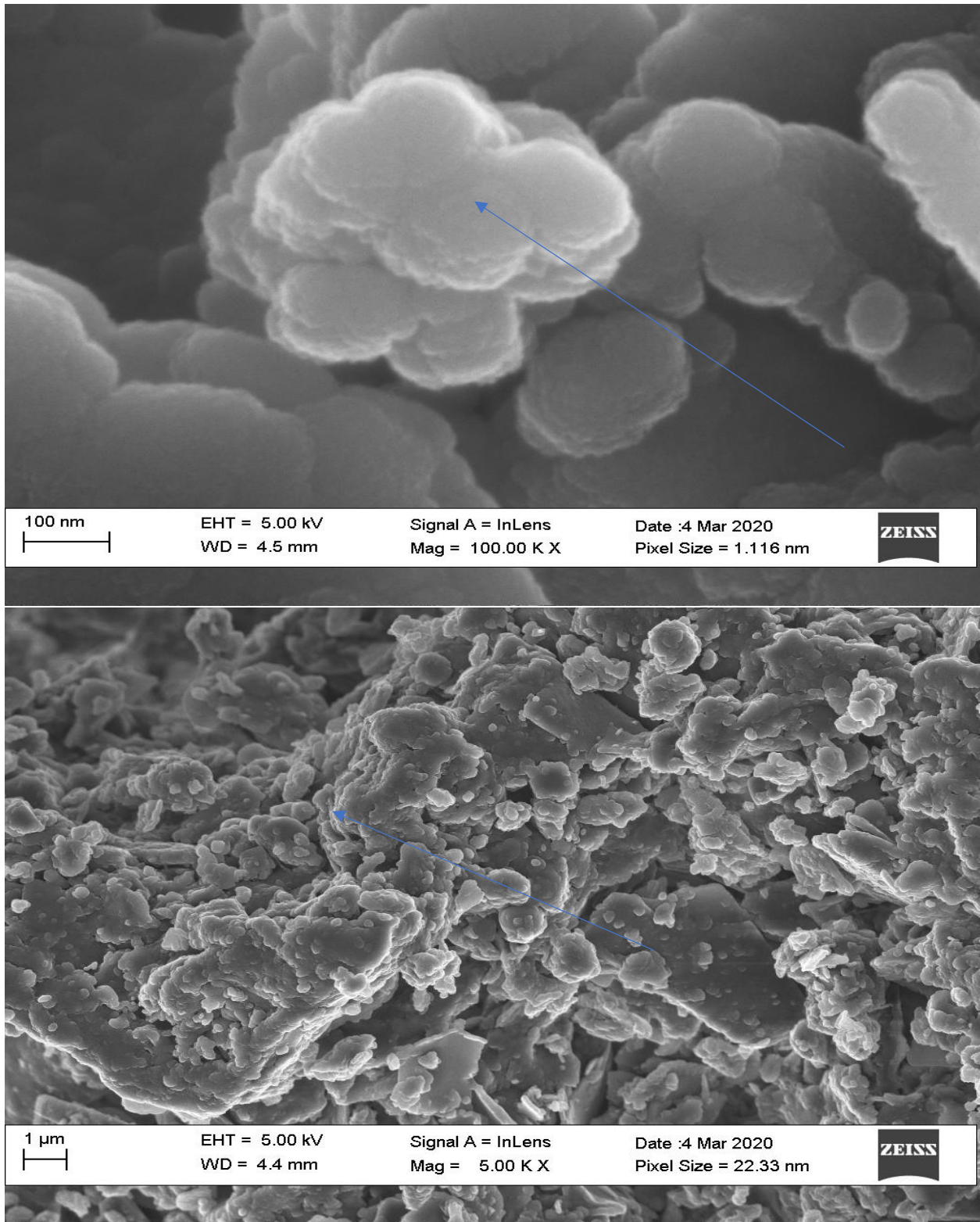
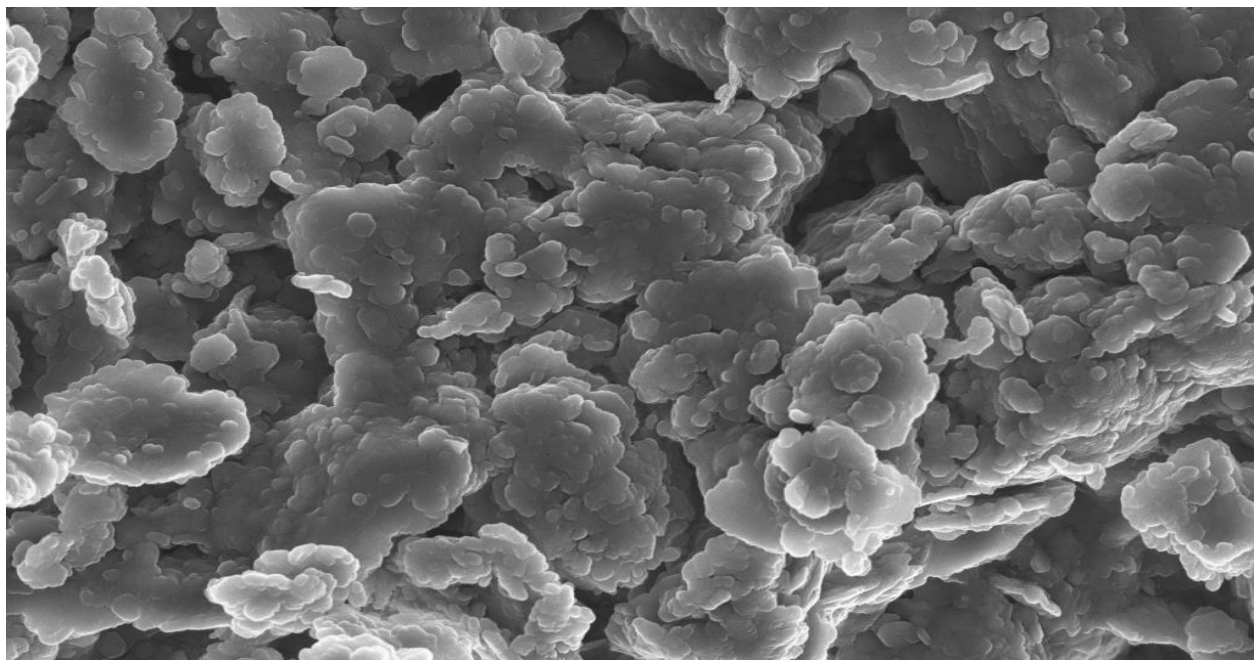
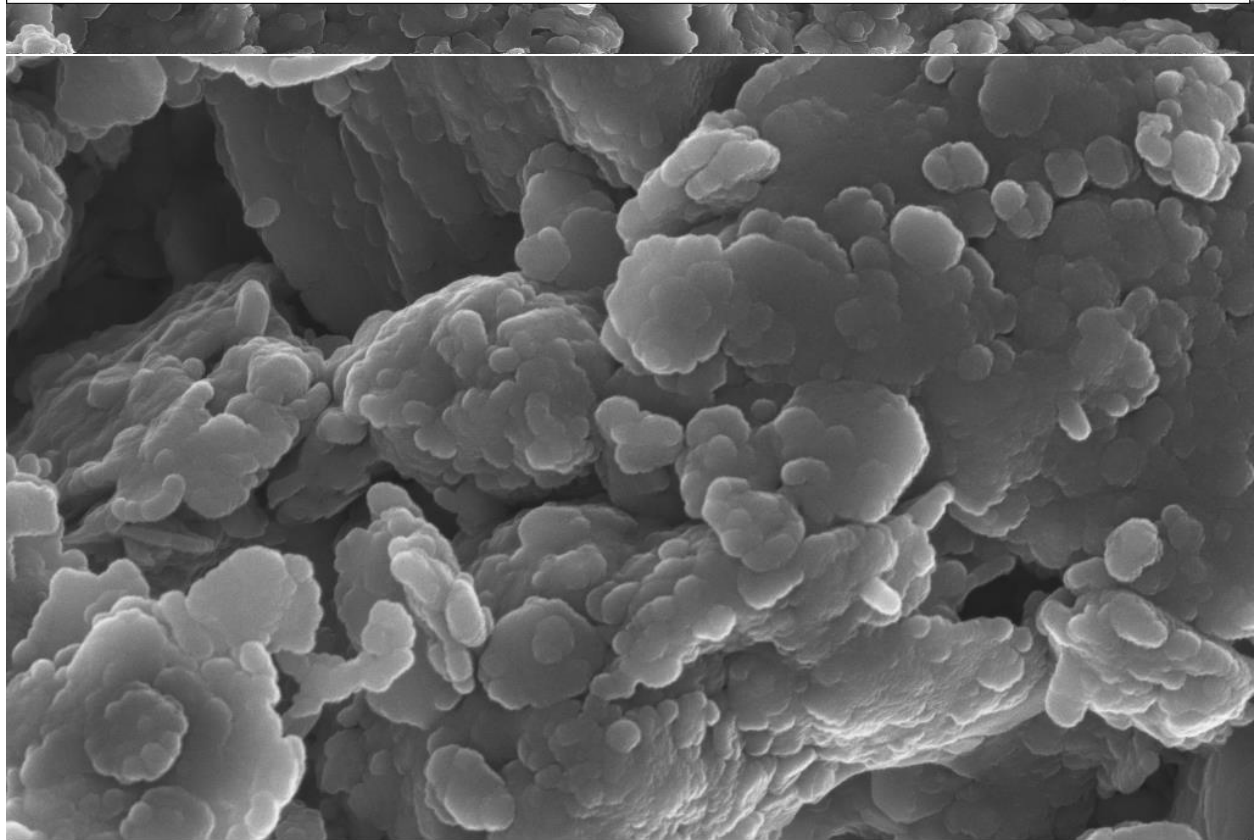


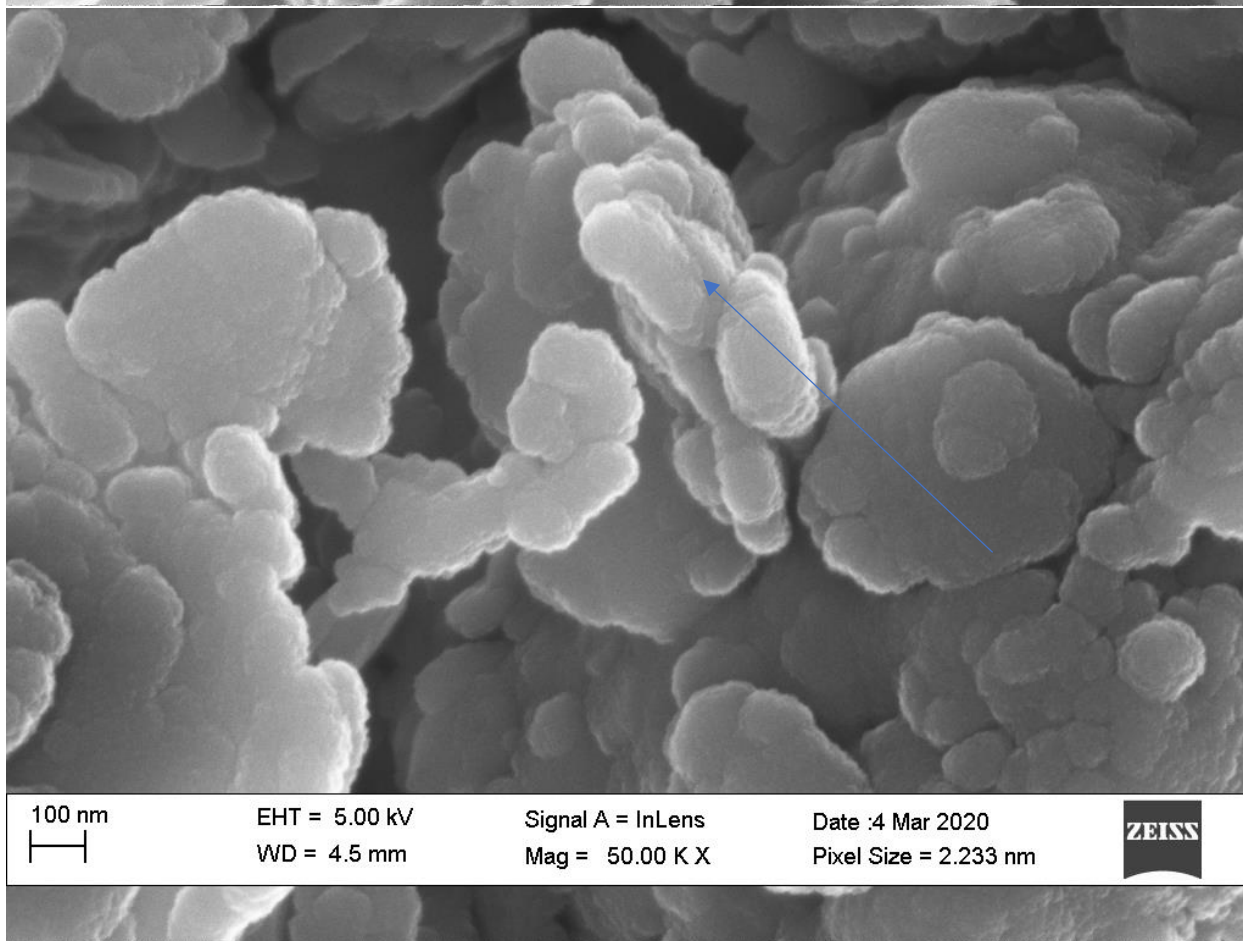
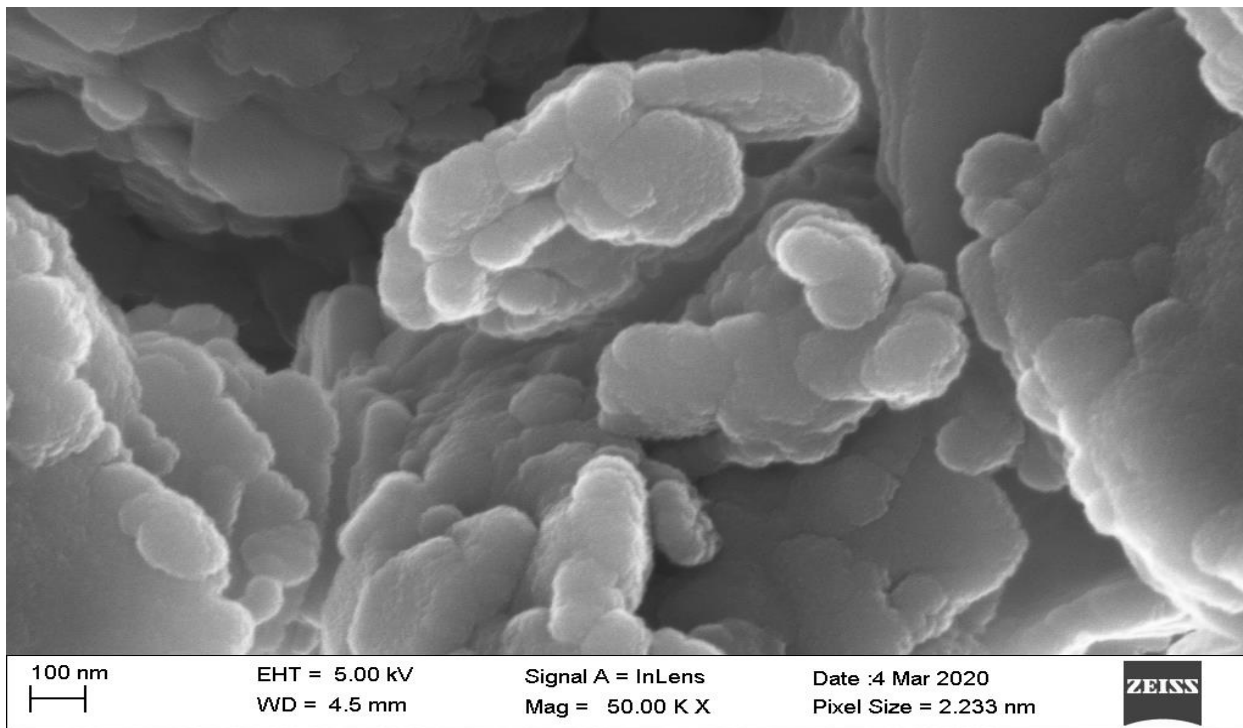
Figure B-3: SEM Image of Local Clay



1  $\mu$ m  
EHT = 5.00 kV  
WD = 4.5 mm  
Signal A = InLens  
Mag = 10.00 K X  
Date :4 Mar 2020  
Pixel Size = 11.16 nm  
ZEISS



200 nm  
EHT = 5.00 kV  
WD = 4.5 mm  
Signal A = InLens  
Mag = 20.00 K X  
Date :4 Mar 2020  
Pixel Size = 5.582 nm  
ZEISS



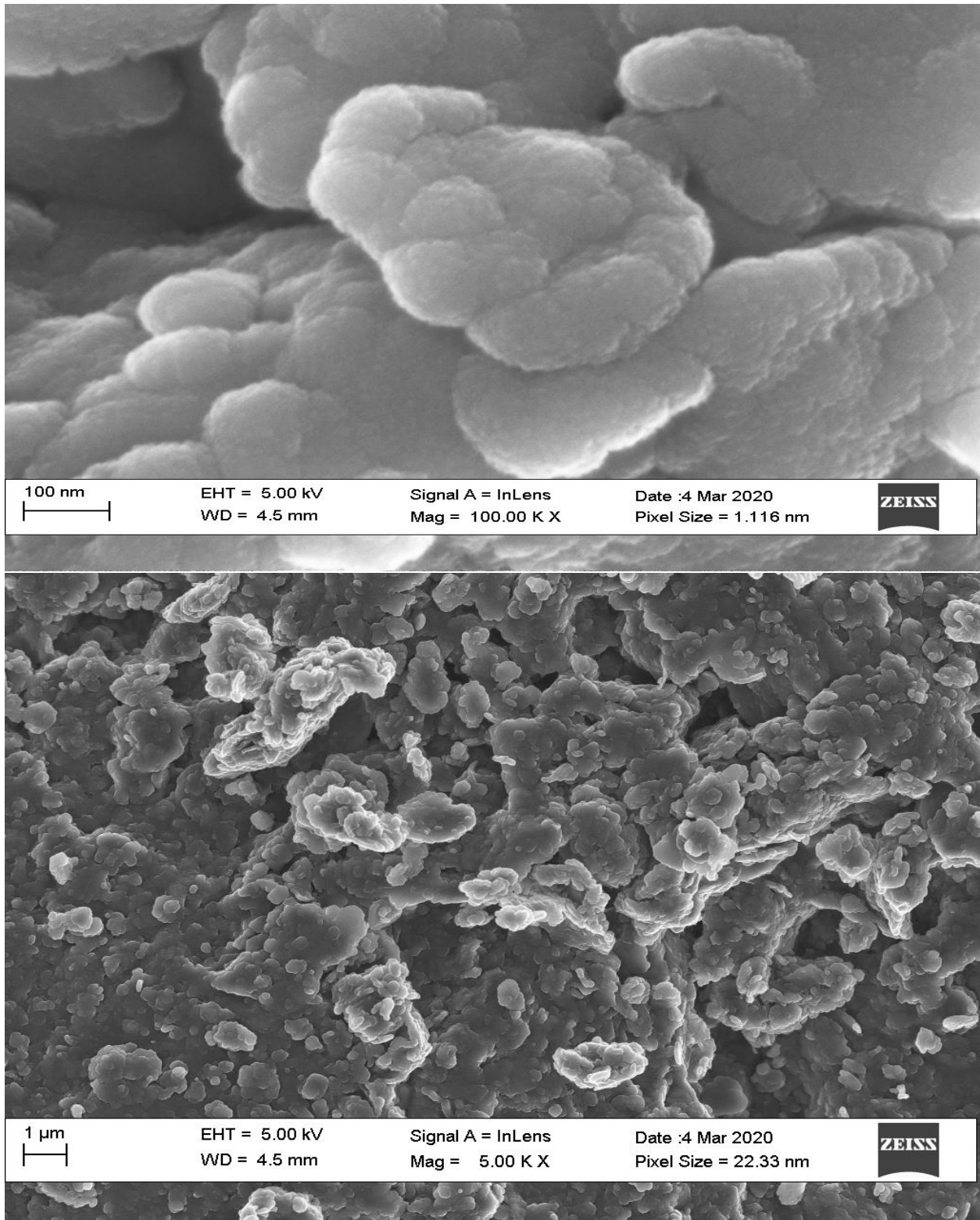


Figure B-4: SEM Image of Nano Lignite Coal

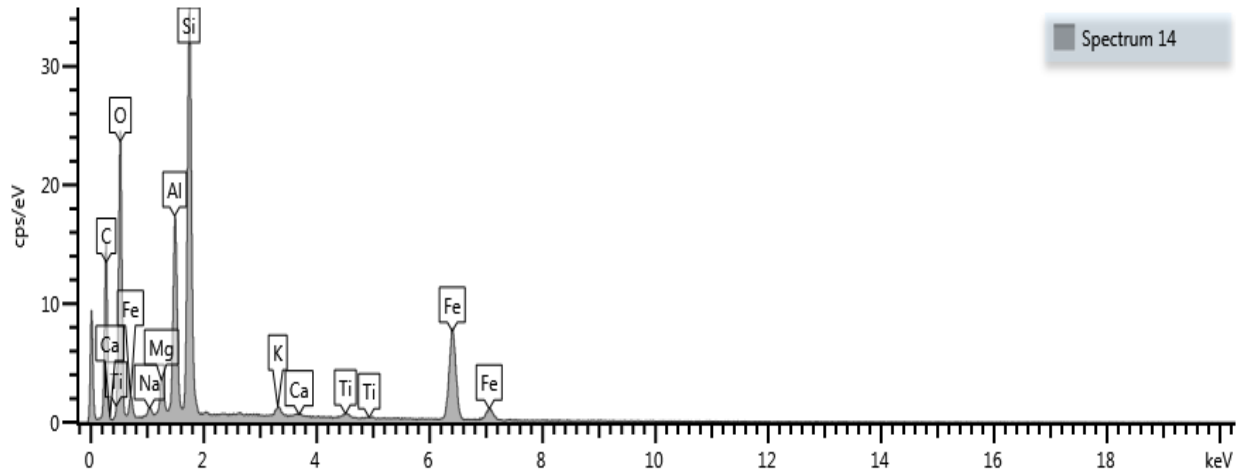


Figure B-5: EDX Spectra of Commercial Bentonite Clay

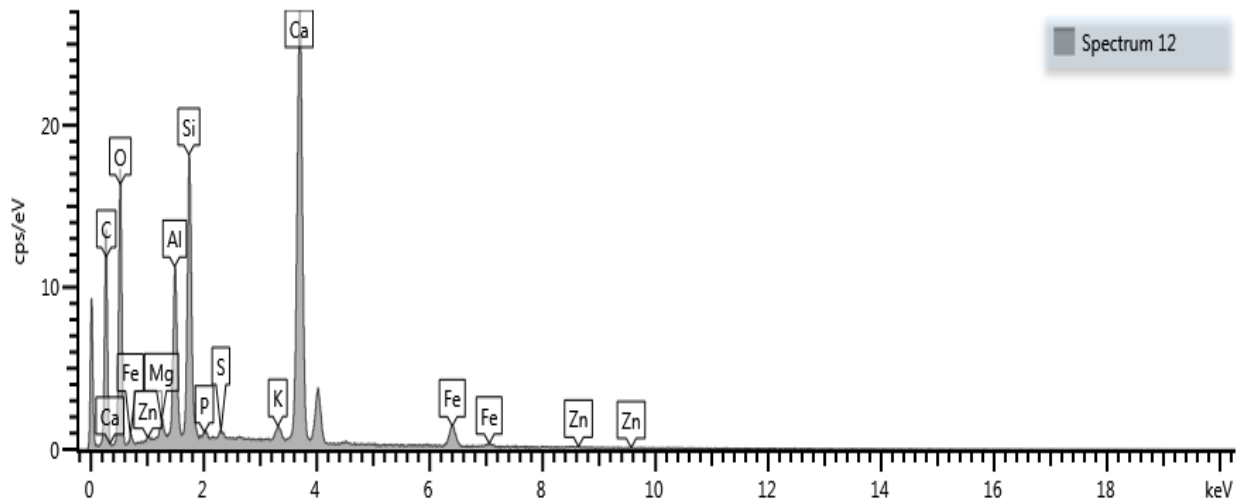


Figure B-6: EDX Spectra of Local Clay

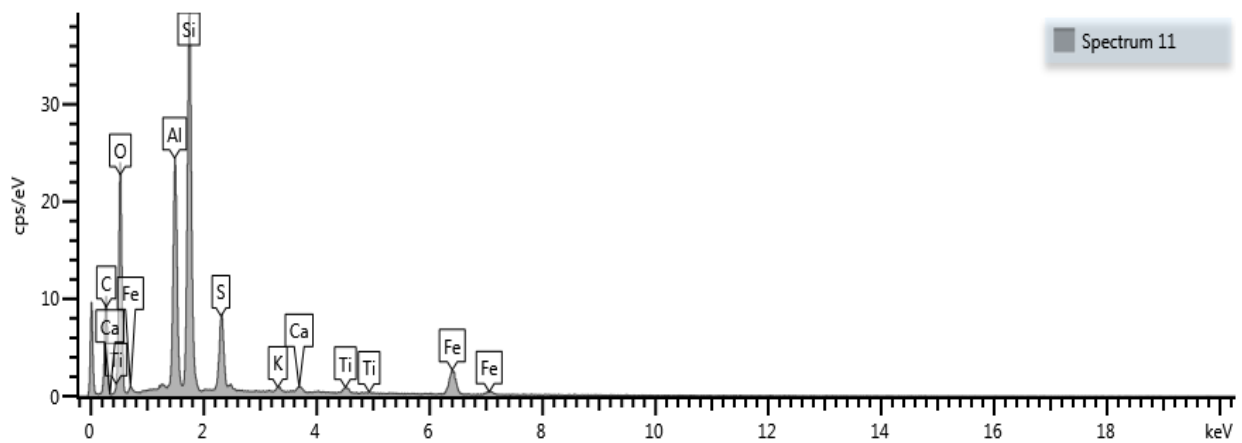


Figure B-7: EDX Spectra of Nano Lignite Coal

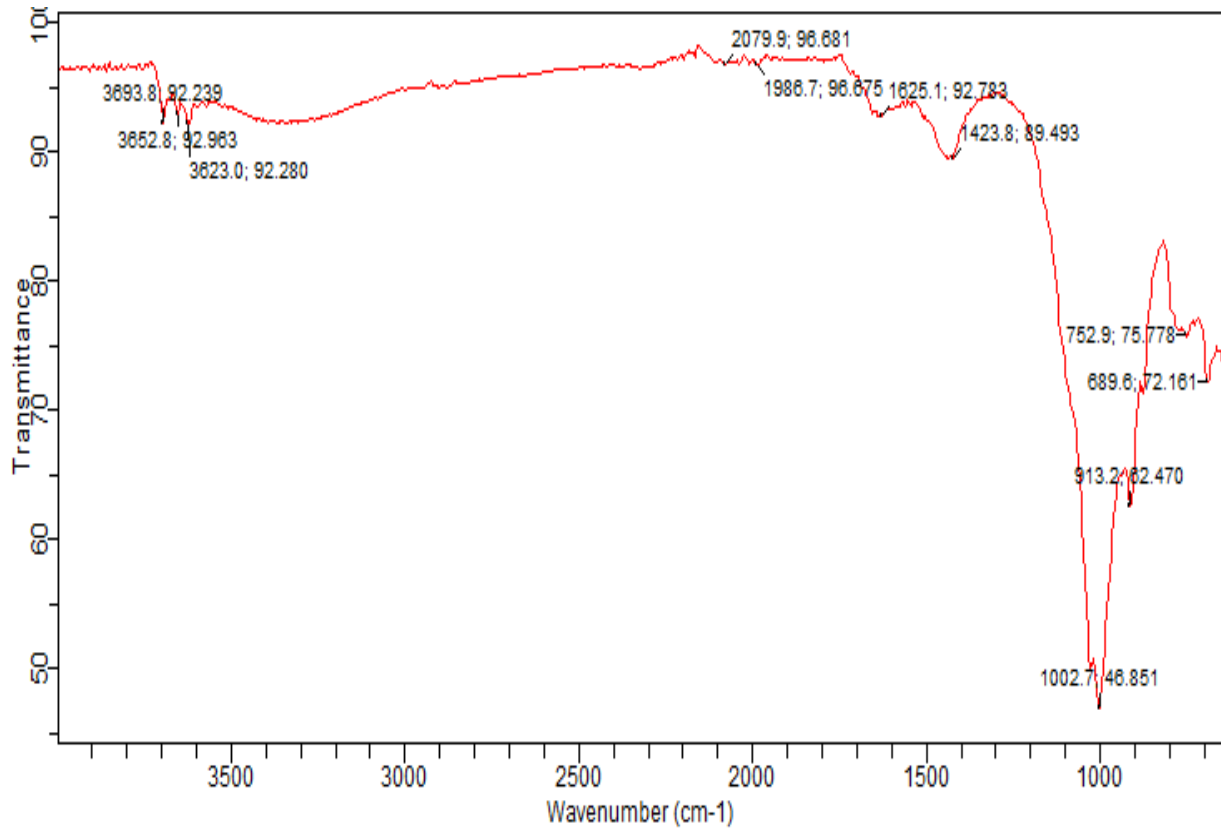


Figure B-8: FTIR Spectra of Local Clay

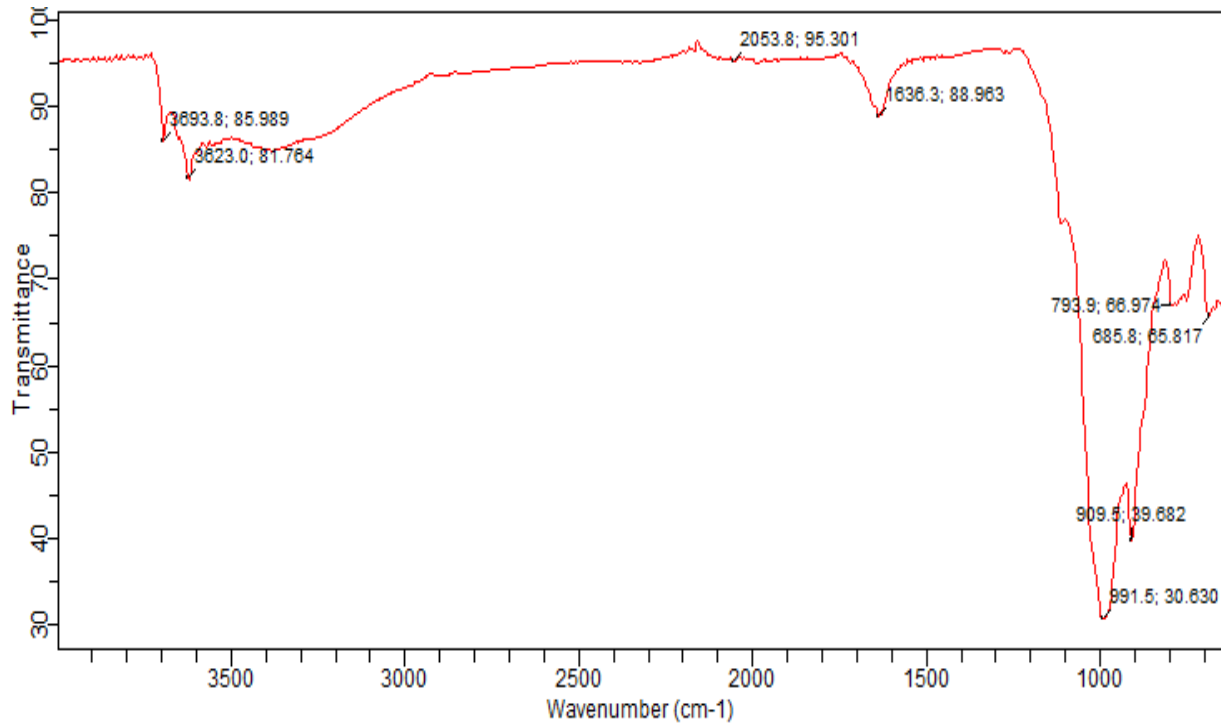


Figure B-9: FTIR Spectra of Commercial Bentonite Clay

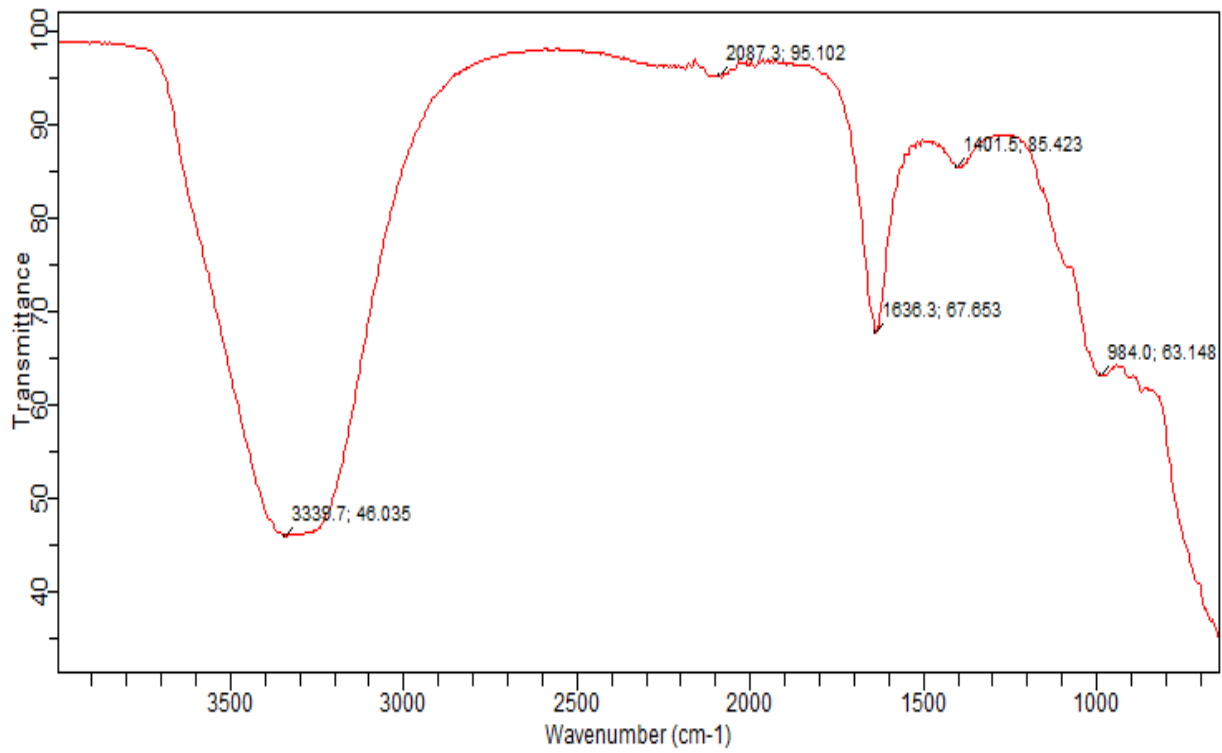


Figure B-10: FTIR Spectra of Beneficiated Local Clay Mud

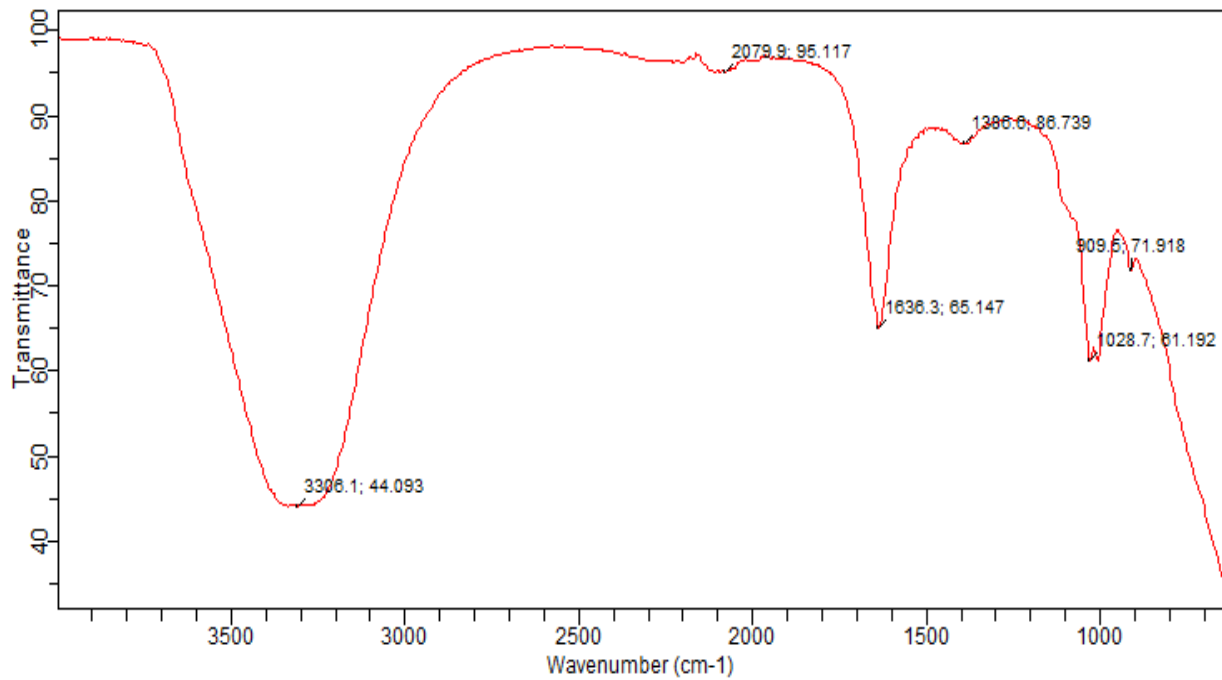


Figure B-11: FTIR Spectra of Beneficiated Commercial Bentonite Clay Mud

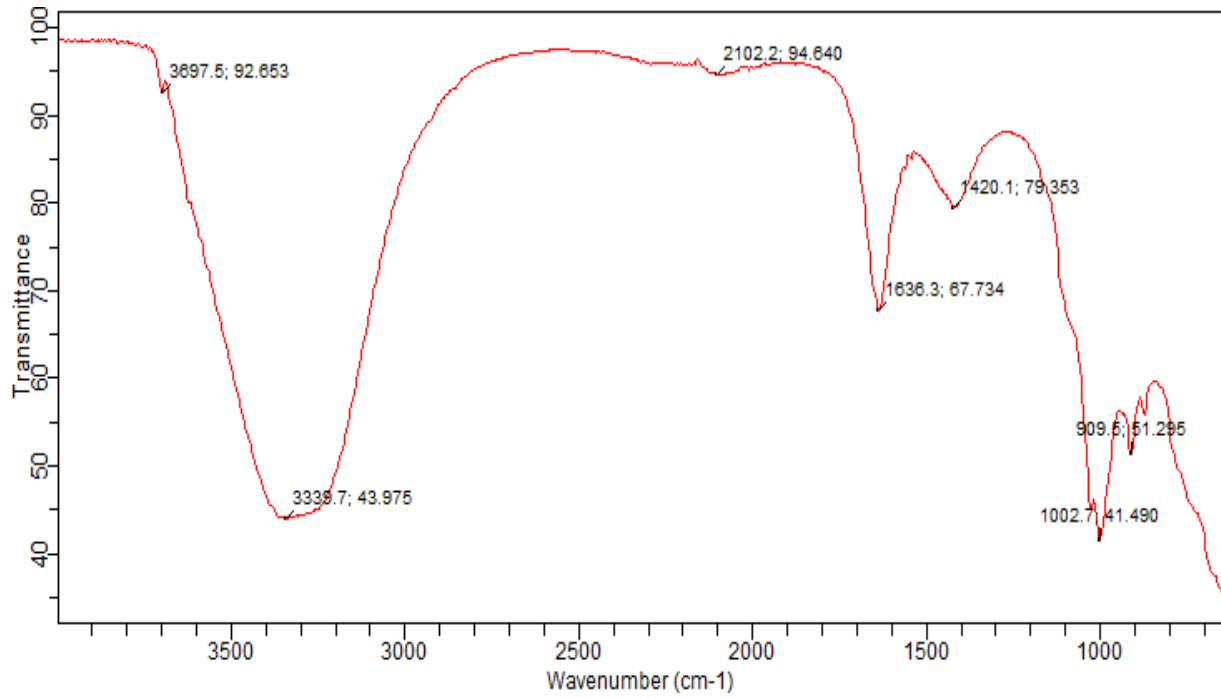


Figure B-12: FTIR Spectra of Modified Local Clay Mud (30 wt%)

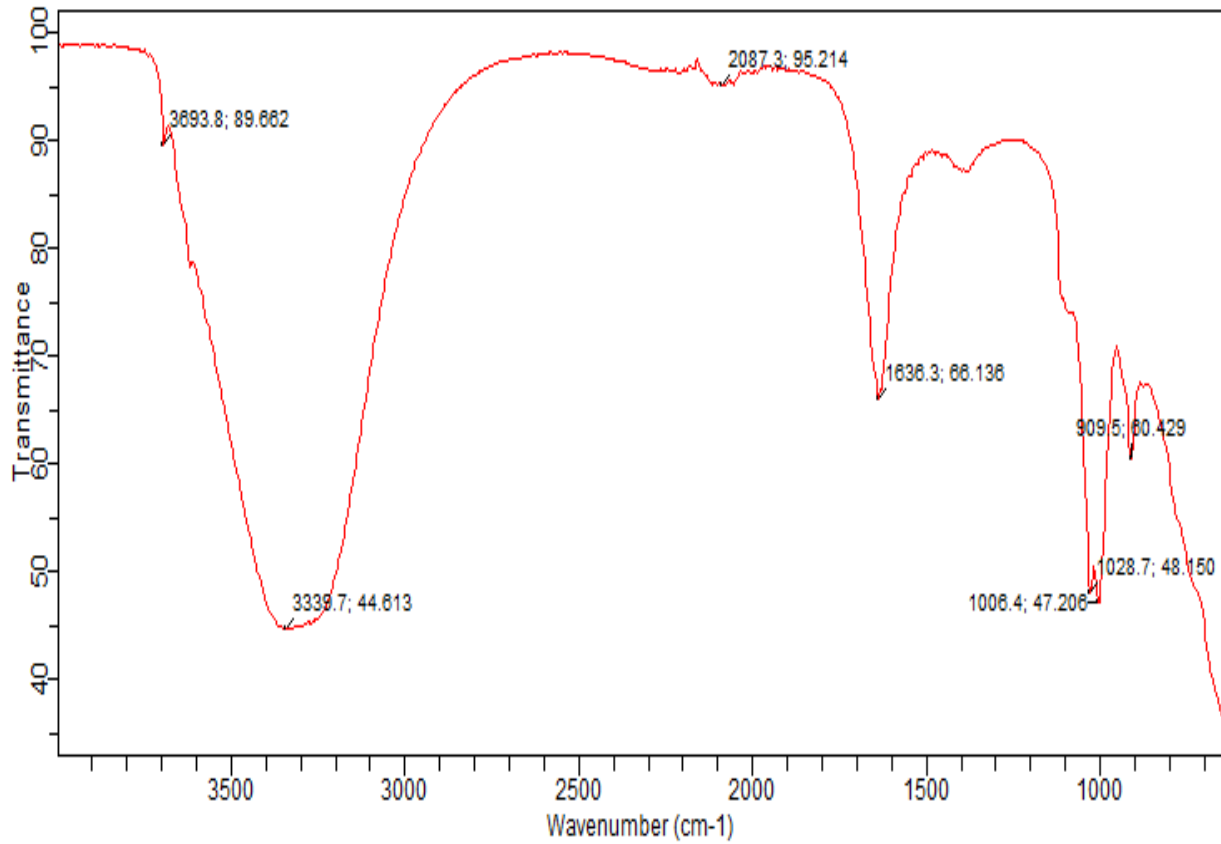


Figure B-13: FTIR Spectra of Modified Commercial Bentonite Clay Mud (30 wt%)

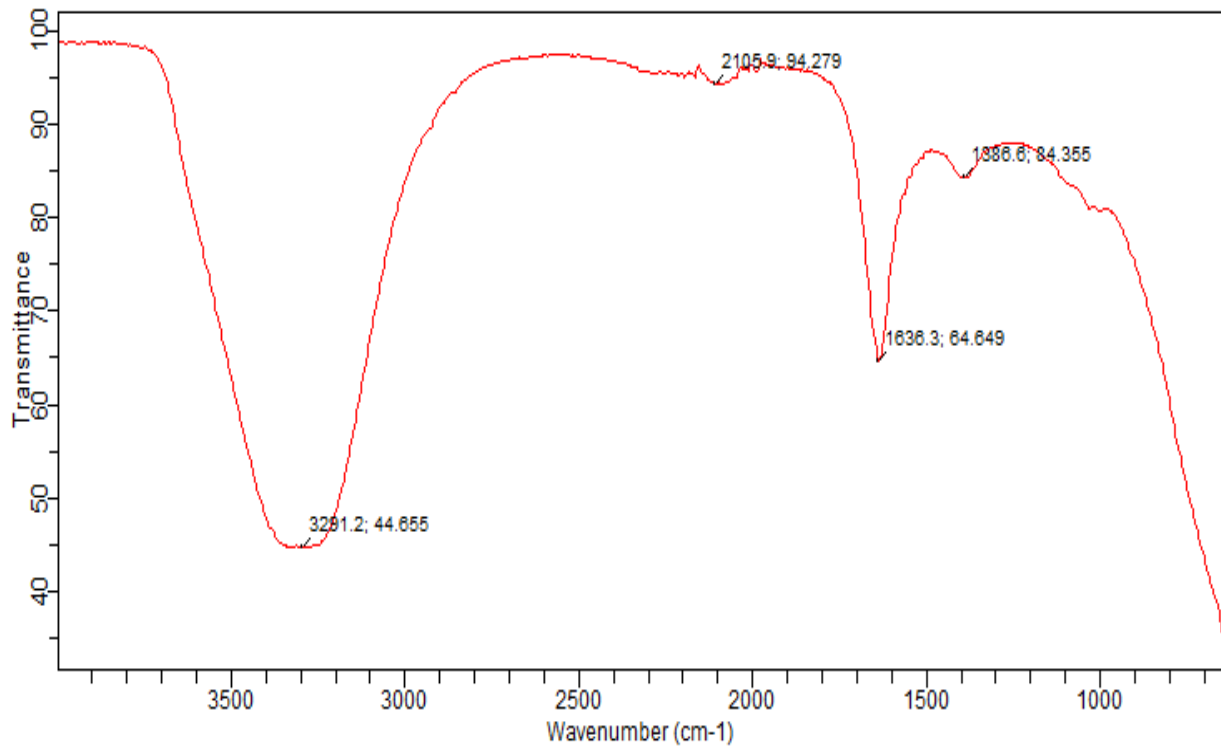


Figure B-14: FTIR Spectra of Modified Local Clay Mud (30 wt%) aged at 100 °C

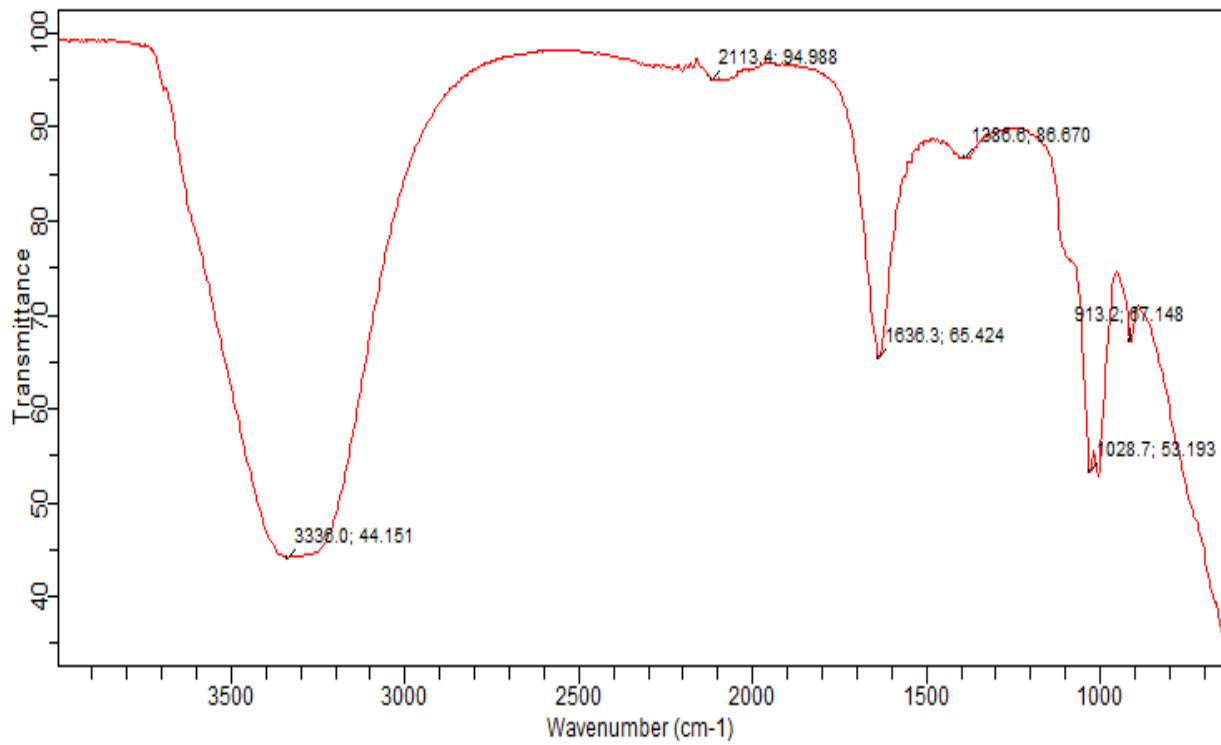


Figure B-15: FTIR Spectra of Modified Commercial Bentonite Clay Mud (30 wt%) aged at 100 °C

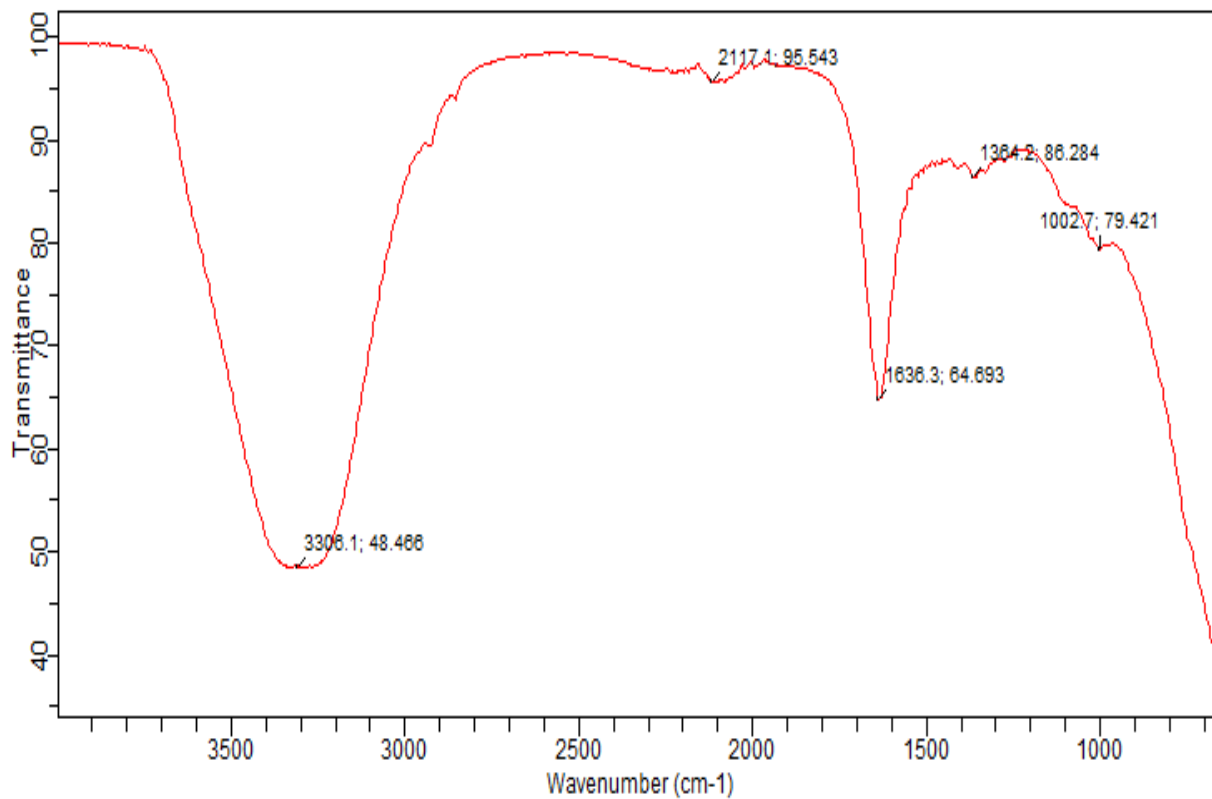


Figure B-16: FTIR Spectra of Modified Local Clay Mud (30 wt%) aged at 160 °C

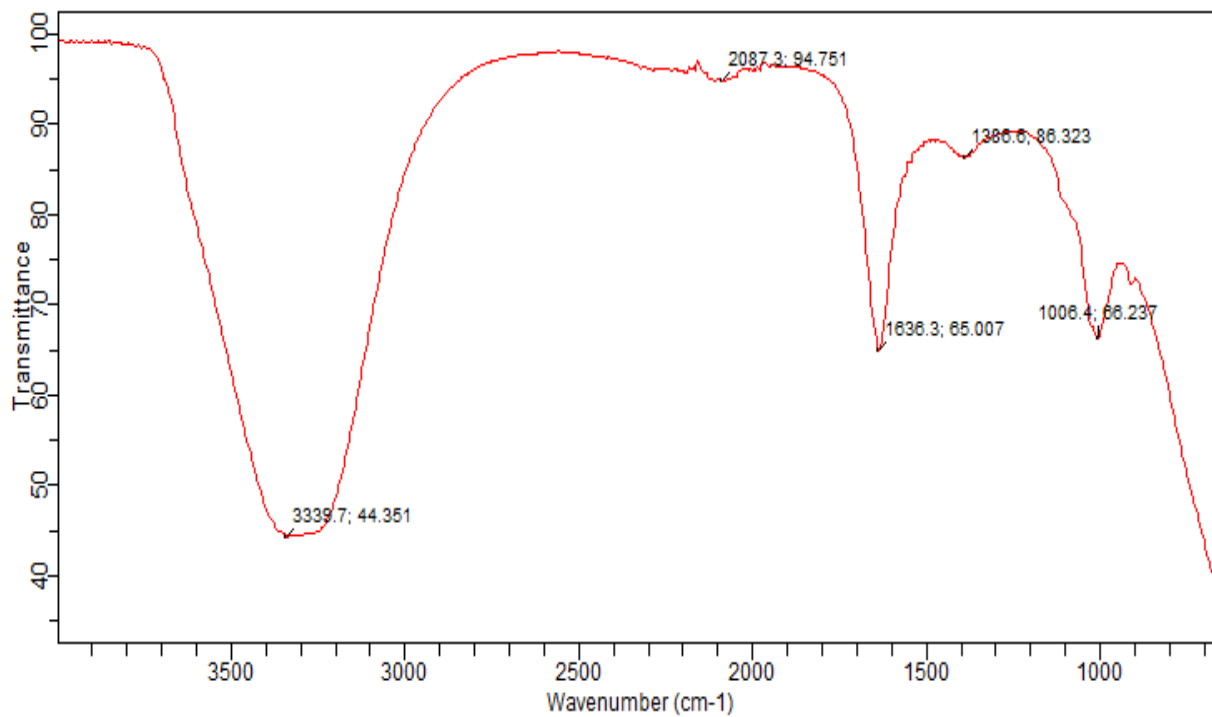


Figure B-15: FTIR Spectra of Modified Commercial Bentonite Clay Mud (30 wt%) aged at 100 °C

Table B-3: Absorption bands on the FTIR spectrum (de Oliveira *et al.*, 2016)

Wavenumber (cm <sup>-1</sup> )	Intensity	Attribution
3698	m	O-H stretching
3622		O-H asymmetric stretching
3441	s, broad	O-H symmetric stretching
1638	m	H-O-H bending
1113	s	Si-O stretching
1041	s	Si-O stretching
912	m-s	Octahedral sheet
794	m	Octahedral sheet
693	w	Si-O-Al bending
535	w	Si-O bending
472	w	Si-O-Si bending

## Appendix C

Experimental Result of Muds Formulated using both Local and Commercial Bentonite Clay with Nigerian Nano Lignite Coal as Additive.

Table C-1: Control Sample (Spud Mud) at Room Temperature.

Sample	A	B
θ600 (cP)	3	10
θ300 (cP)	2	5
θ200 (cP)	1	4
θ100 (cP)	0	3
θ6 (cP)	0	0
θ3 (cP)	0	0
10 sec. Gel (Ib/100 ft <sup>2</sup> )	0	0
10 min. Gel (Ib/100 ft <sup>2</sup> )	0	0
Fluid loss (mL)	248	20
Cake thickness (mm)	1.8	0.6
Density (ppg)	8.3	8.45
pH	8.0	9.0

Table C-2: Beneficiated Mud Samples at Room Temperature.

Sample	A	B
θ600 (cP)	145	112
θ300 (cP)	112	84
θ200 (cP)	95	70
θ100 (cP)	68	51
θ6 (cP)	10	11
θ3 (cP)	7	7
10 sec. Gel (Ib/100 ft <sup>2</sup> )	7	6
10 min. Gel (Ib/100 ft <sup>2</sup> )	10	9
Fluid loss (mL)	12.40	14.2
Cake thickness (mm)	0.35	0.45
Density (ppg)	8.3	8.2
pH	11.0	12.0

Table C-3: Modified Mud Samples with Various Concentration of Nigerian Lignite Nanoparticles aged at Room temperature.

Sample	A1	A2	A3	B1	B2	B3
θ600 (cP)	160	170	175	160	173	176
θ300 (cP)	120	131	135	123	133	136
θ200 (cP)	104	111	115	116	118	124
θ100 (cP)	74	81	83	83	96	109
θ6 (cP)	12	15	15	20	33	38
θ3 (cP)	7	8	9	14	23	26
10 sec. Gel (Ib/100 ft <sup>2</sup> )	6	9	9	12	20	24
10 min. Gel (Ib/100 ft <sup>2</sup> )	6	10	10	15	24	25
Fluid loss (mL)	9.6	9.4	9.2	9.2	10	10
Cake thickness (mm)	0.8	0.4	0.5	0.4	0.9	0.6
Density (ppg)	8.4	8.3	8.3	8.2	8.2	8.2
pH	12.0	12.0	12.0	13.0	13.0	13.0

Table C-4: Modified Mud Samples with Various Concentration of Nigerian Lignite Nanoparticles aged At Elevated temperature (100 °C).

Sample	A1	A2	A3	B1	B2	B3
θ600 (cP)	36	41	44	40	46	48
θ300 (cP)	28	33	35	31	35	37
θ200 (cP)	18	21	24	20	27	31
θ100 (cP)	10	12	15	12	18	23
θ6 (cP)	3	4	5	3	4	7
θ3 (cP)	1	1	2	1	2	3
10 sec. Gel (Ib/100 ft <sup>2</sup> )	0	0	0	3	3	4
10 min. Gel (Ib/100 ft <sup>2</sup> )	1	1	1	4	4	6
Fluid loss (mL)	7.6	7.2	6.8	10	9.6	9.2
Cake thickness (mm)	1.3	0.8	0.5	1.0	1.0	0.8
Density (ppg)	8.2	8.2	8.2	8.2	8.2	8.2
pH	12.0	12.0	12.0	13	13.0	13.0

Table C-5: Modified Mud Samples with Various Concentration of Nigerian Lignite Nanoparticles aged At Elevated temperature (160 °C).

Sample	A1	A2	A3	B1	B2	B3
θ600 (cP)	29	36	40	37	42	45
θ300 (cP)	21	28	29	29	34	36
θ200 (cP)	8	11	13	15	17	17
θ100 (cP)	4	6	7	10	12	13
θ6 (cP)	1	1	2	2	3	3
θ3 (cP)	0	0	1	1	1	1
10 sec. Gel (Ib/100 ft <sup>2</sup> )	0	2	0	2	2	2
10 min. Gel (Ib/100 ft <sup>2</sup> )	0	2	2	3	3	4
Fluid loss (mL)	10	9.6	9.2	10	9.6	9.2
Cake thickness (mm)	0.7	0.7	0.5	0.9	0.9	0.8
Density (ppg)	8.2	8.2	8.2	8.2	8.2	8.2
pH	12.0	12.0	12.0	13.0	13.0	13.0

$$PV(cP) = (\theta 600 \text{ rpm} - \theta 300 \text{ rpm}) \quad \text{C-1}$$

$$AV (cP) = \left( \frac{\theta 600 \text{ rpm}}{2} \right) \quad \text{C-2}$$

$$YP (\text{lb}/100 \text{ ft}^2) = (\theta 300 \text{ rpm} - PV) \quad \text{C-3}$$

$$\tau = k * \Upsilon^n \quad \text{C-4}$$

$$\Upsilon = 1.703\gamma \quad \text{C-5}$$

$$n = 3.32 \log\left(\frac{\theta 600}{\theta 300}\right) \quad \text{C-6}$$

$$k = \left( \frac{\tau}{\Upsilon^n} \right) = \left( \frac{\theta 600}{1022^n} \right) \quad \text{C-7}$$

$$R^2 = \left( \frac{\sum_i (X_i - \bar{x})(Y_i - \bar{y})}{\sqrt{\sum_i (X_i - \bar{x})^2 * \sum_i (Y_i - \bar{y})^2}} \right) \quad \text{C-8}$$

$$\text{RMSE} = \sqrt{\frac{\sum_{i=1}^n (Y_i - X_i)^2}{N}} \quad \text{C-9}$$

$$\text{MC (\%)} = \left( \frac{\text{Wet Weight} - \text{Dry Weight}}{\text{Wet Weight}} \right) \times 100 \% \quad \text{C-10}$$

$$\text{AC (\%)} = \left( \frac{\text{Weight of Residue}}{\text{Weight of Sample}} \right) \times 100 \% \quad \text{C-11}$$

$$\text{VM (\%)} = \left( \frac{B-C}{B} \right) \times 100 \% \quad \text{C-12}$$

$$\text{FC} = 100 \% - (\text{MC} + \text{AC} + \text{VM}) \quad \text{C-13}$$